European Society
ESGAR
Gastrointestinal and Abdominal Radiology

Insights into Imaging

Education and strategies in European radiology

ESGAR 2013 Book of Abstracts / Volume 4, 2013 / Supplement 2 / June 2013

ESGAR 2013 / June 4 – 7 / Barcelona, Spain
24th Annual Meeting and Postgraduate Course

ESR
European Society of Radiology

European Society
ESGAR
Gastrointestinal and Abdominal Radiology

JUNE 4-7

ESGAR 2013

BARCELONA
SPAIN

European
Society
of Gastrointestinal
and Abdominal
Radiology

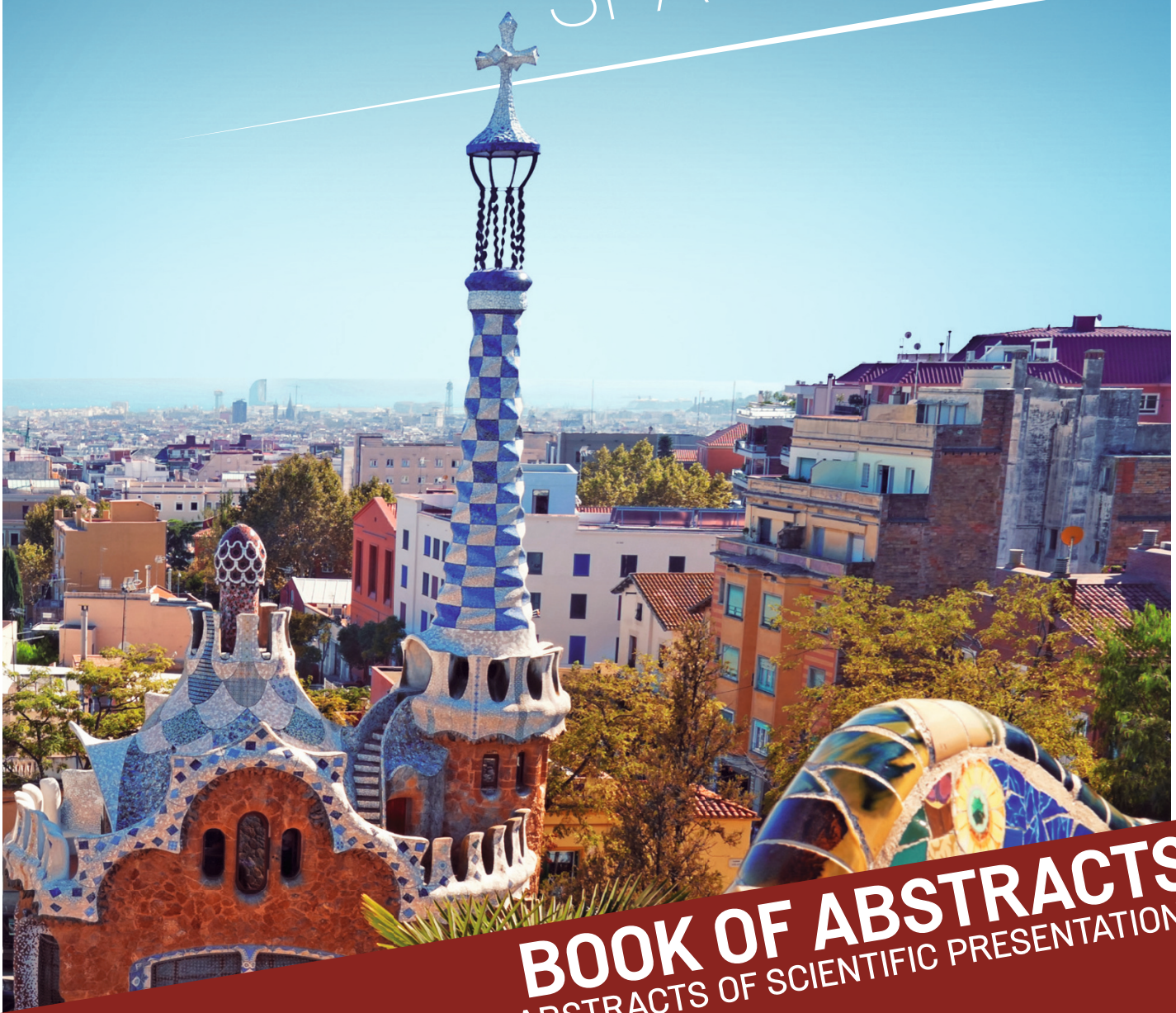

BOOK OF ABSTRACTS

INCLUDES ABSTRACTS OF SCIENTIFIC PRESENTATIONS

IMPORTANT ADDRESSES

ORGANISING SECRETARIAT
Central ESGAR Office
Neutorgasse 9
AT – 1010 Vienna, Austria
Phone: +43 1 535 89 27
Fax: +43 1 535 70 37
E-Mail: office@esgar.org

EXECUTIVE DIRECTOR
Ms. Brigitte Lindlbauer
E-Mail: blindlbauer@esgar.org

WEBSITE
www.esgar.org

EXHIBITION MANAGEMENT
MAW – Medizinische Ausstellungsgesellschaft
Freyung 6
AT – 1010 Vienna, Austria
Phone: +43 1 536 63 35 or -34
Fax: +43 1 535 60 16
E-Mail: maw@media.co.at

CONFERENCE VENUE
Palau de Congressos de Catalunya
Av. Diagonal, 661-671
ES – 08028 Barcelona, Spain

PATRONAGE

SEDIA
(Sociedad Española de
Diagnóstico por Imagen del Abdomen)

SEDIA
SOCIEDAD ESPAÑOLA DE DIAGNÓSTICO POR IMAGEN DEL ABDOMEN

Date of publishing: May 2013

CME

The 'ESGAR' (or) 'ESGAR 2013 - the 24th ESGAR Annual Meeting' is accredited by the European Accreditation Council for Continuing Medical Education (EACCME) to provide the following CME activity for medical specialists. The EACCME is an institution of the European Union of Medical Specialists (UEMS), www.uems.net.

The 'ESGAR 2013 - the 24th ESGAR Annual Meeting' is designated for a maximum of (or 'for up to') 24 hours of European external CME credits. Each medical specialist should claim only those hours of credit that he/she actually spent in the educational activity.

SPONSORS

ESGAR wishes to gratefully acknowledge the support of its Corporate Members:

Bayer HealthCare
BRACCO LIFE FROM INSIDE
GE Healthcare
Guerbet Contrast for Life
PHILIPS sense and simplicity

The Final Programme of ESGAR 2013 is available on the ESGAR website www.esgar.org

TABLE OF CONTENTS

ESGAR MEETING PRESIDENT

Prof. Carmen Ayuso
University of Barcelona
Hospital Clinic
Department of Radiology
Villaroel 170
ES – 08036 Barcelona, Spain

ESGAR EXECUTIVE COMMITTEE

PRESIDENT
F. Caseiro Alves (Coimbra/PT)

PRESIDENT-ELECT
L. Martí-Bonmatí (Valencia/ES)

VICE PRESIDENT
C. Matos (Brussels/BE)

SECRETARY
A. Palkó (Szeged/HU)

TREASURER
S. Jackson (Plymouth/UK)

PAST PRESIDENT &
PROGRAMME COMMITTEE CHAIRMAN
Y. Menu (Paris/FR)

BY-LAWS COMMITTEE
P. Prassopoulos (Alexandroupolis/GR)

EDUCATION COMMITTEE
H. Fenlon (Dublin/IE)

MEMBERSHIP COMMITTEE
R.G.H. Beets-Tan (Maastricht/NL)

WORKSHOP COMMITTEE
A. Laghi (Latina/IT)

MEETING PRESIDENT
C. Ayuso (Barcelona/ES)

PRE-MEETING PRESIDENT
G.H. Mostbeck (Vienna/AT)

PRE-PRE-MEETING PRESIDENT
Y. Menu (Paris/FR)

FELLOWS REPRESENTATIVES
T. Helmberger (Munich/DE)

ESGAR 2013 PROGRAMME COMMITTEE

CHAIRMAN

Y. Menu (Paris/FR)

MEMBERS

C. Ayuso (Barcelona/ES)
R.G.H. Beets-Tan (Maastricht/NL)
F. Caseiro Alves (Coimbra/PT)
H. Fenlon (Dublin/IE)
N. Gourtsoyiannis (Athens/GR)
S. Halligan (London/UK)
T. Helmberger (Munich/DE)
S. Jackson (Plymouth/UK)
A. Laghi (Latina/IT)
L. Martí-Bonmatí (Valencia/ES)
C. Matos (Brussels/BE)
G.H. Mostbeck (Vienna/AT)
A. Palkó (Szeged/HU)
P. Prassopoulos (Alexandroupolis/GR)

LOCAL ORGANISING COMMITTEE

R. Bouzas (Vigo/ES)
L. Donoso (Barcelona/ES)
E. Fraile (Madrid/ES)
J.L. Lopez-Moreno (Barcelona/ES)
L. Martí-Bonmatí (Valencia/ES)
R. Méndez (Madrid/ES)
C. Pérez (Barcelona/ES)
B. Vargas (Sevilla/ES)

This edition of the ESGAR 2013 Book of Abstracts was language edited by:

ABSTRACT EDITOR

S. Jackson (Plymouth/UK)

ABSTRACT REVIEWING PANEL

D. Akata (Ankara/TR)
O. Akhan (Ankara/TR)
C. Ayuso (Barcelona/ES)
M.A. Bali (Brussels/BE)
R.G.H. Beets-Tan (Maastricht/NL)
P. Boraschi (Pisa/IT)
R. Bouzas (Vigo/ES)
G. Brancatelli (Palermo/IT)
D.J. Breen (Southampton/UK)
C. Bru (Barcelona/ES)
F. Caseiro Alves (Coimbra/PT)
C. Catalano (Rome/IT)
J. Cazejust (Paris/FR)
N. Courcoutsakis (Alexandroupolis/GR)
E. Delabrousse (Besançon/FR)
M.C. Della Pina (Pisa/IT)
R.F. Dondelinger (Liège/BE)
M. D'Onofrio (Verona/IT)
N. Elmas (Izmir/TR)
H. Fenlon (Dublin/IE)
B. Fox (Plymouth/UK)
A.H. Freeman (Cambridge/UK)
A. Furlan (Pittsburgh, PA/US)
A. Gillams (London/UK)
S. Gourtsoyianni (London/UK)
L. Guimaraes (Porto/PT)
J.A. Guthrie (Leeds/UK)
T. Helmberger (Munich/DE)
P. Huppert (Darmstadt/DE)
F. Iafrate (Rome/IT)
S. Jackson (Plymouth/UK)
M. Karcaaltincaba (Ankara/TR)
C. Kay (Bradford/UK)
S.H. Kim (Busan/KR)
H.-U. Laasch (Manchester/UK)
A. Laghi (Latina/IT)
J.S. Lameris (Amsterdam/NL)
P. Lefere (Roeselare/BE)
M. Lewin (Villejuif/FR)
J.H. Lim (Seoul/KR)
D.J. Lomas (Cambridge/UK)
O. Lucidarme (Paris/FR)
M. Maas (Maastricht/NL)
F. Maccioni (Rome/IT)
M. Maher (Wilton, Cork/IE)
D.E. Malone (Dublin/IE)
R. Manfredi (Verona/IT)
T. Mang (Vienna/AT)
D. Marin (Durham, NC/US)
B. Marincek (Cleveland, OH/US)
L. Martí-Bonmatí (Valencia/ES)
D.F. Martin (Manchester/UK)
G.F. Maskell (Truro/UK)
C. Matos (Brussels/BE)
R.M. Mendelson (Perth, WA/AU)
Y. Menu (Paris/FR)
G. Morana (Treviso/IT)
M. Morrin (Dublin/IE)
G.H. Mostbeck (Vienna/AT)
E. Neri (Pisa/IT)
B. Op De Beeck (Edegem/BE)
A. Palkó (Szeged/HU)
P.L. Pereira (Heilbronn/DE)
P. Pokieser (Vienna/AT)
P. Prassopoulos (Alexandroupolis/GR)
M. Puckett (Torquay/UK)
J. Puig Domingo (Sabadell/ES)
C. Ridereau-Zins (Angers/FR)
G.A. Rollandi (Genova/IT)
S. Romano (Naples/IT)
L.H. Ros Mendoza (Zaragoza/ES)
A. Ruiz (Paris/FR)
E.J. Rummeny (Munich/DE)
W. Schima (Vienna/AT)
S. Schmidt Kobbe (Lausanne/CH)
O. Seror (Bondy/FR)
P. Sidhu (London/UK)
S. Skehan (Dublin/IE)
S. Somers (Dundas, ON/CA)
M. Staunton (Cork/IE)
J. Stoker (Amsterdam/NL)
C. Stoupis (Maennedorf/CH)
Z. Tarjan (Budapest/HU)
S.A. Taylor (London/UK)
C. Triantopoulou (Athens/GR)
V. Valek (Brno-Bohunice/CZ)
D. Vanbeckevoort (Leuven/BE)
V. Vilgrain (Clichy/FR)
M.-P. Vullierme (Clichy/FR)
D. Weishaupt (Zurich/CH)
S.D. Yarmenitis (Heraklion/GR)
C.J. Zech (Basel/CH)
M. Zins (Paris/FR)

E-POSTER JURY

D. Akata (Ankara/TR)
O. Akhan (Ankara/TR)
A.J. Aschoff (Kempten/DE)
C. Ayuso (Barcelona/ES)
M.A. Bali (Brussels/BE)
R.G.H. Beets-Tan (Maastricht/NL)
P. Boraschi (Pisa/IT)
R. Bouzas (Vigo/ES)
G. Brancatelli (Palermo/IT)
D.J. Breen (Southampton/UK)
F. Caseiro Alves (Coimbra/PT)
C. Catalano (Rome/IT)
J. Cazejust (Paris/FR)
N. Courcoutsakis (Alexandroupolis/GR)
L. Crocetti (Pisa/IT)
E. Delabrousse (Besançon/FR)
R.F. Dondelinger (Liège/BE)
M. D'Onofrio (Verona/IT)
N. Elmas (Izmir/TR)
H. Fenlon (Dublin/IE)
B. Fox (Plymouth/UK)
A.H. Freeman (Cambridge/UK)
A. Furlan (Pittsburgh/US)
S. Gourtsoyianni (London/UK)
L. Guimaraes (Viseu/PT)
J.A. Guthrie (Leeds/UK)
T. Helmberger (Munich/DE)
P. Huppert (Darmstadt/DE)
F. Iafrate (Rome/IT)
S. Jackson (Plymouth/UK)
M. Karcaaltincaba (Ankara/TR)
C. Kay (Bradford/UK)
S.H. Kim (Busan/KR)
H.-U. Laasch (Manchester/UK)
A. Laghi (Latina/IT)
J.S. Lameris (Amsterdam/NL)
T. Lauenstein (Essen/DE)
P. Lefere (Roeselare/BE)
M. Lewin (Paris/FR)
D.J. Lomas (Cambridge/UK)
O. Lucidarme (Paris/FR)
M. Maas (Maastricht/NL)
A. Madureira (Porto/PT)
M. Maher (Wilton, Cork/IE)
D. E. Malone (Dublin/IE)
R. Manfredi (Verona/IT)
T. Mang (Vienna/AT)
D. Marin (Durham, NC/US)
B. Marincek (Cleveland, OH/US)
L. Martí-Bonmatí (Valencia/ES)
D.F. Martin (Manchester/UK)
G.F. Maskell (Truro/UK)
C. Matos (Brussels/BE)
R.M. Mendelson (Perth, WA/AU)
Y. Menu (Paris/FR)
G. Morana (Treviso/IT)
M. Morrin (Dublin /IE)
G.H. Mostbeck (Vienna/AT)
E. Neri (Pisa/IT)
B. Op de Beeck (Edegem/BE)
A. Palkó (Szeged/HU)
N. Papanikolaou (Heraklion/GR)
P.L. Pereira (Heilbronn/DE)
P. Pokieser (Vienna/AT)
P. Prassopoulos (Alexandroupolis/GR)
M. Puckett (Torquay/UK)
J. Puig Domingo (Sabadell/ES)
C. Ridereau-Zins (Angers/FR)
G.A. Rollandi (Genova/IT)
S. Romano (Naples/IT)
L.H. Ros Mendoza (Zaragoza/ES)
A. Ruiz (Paris/FR)
E.J. Rummeny (Munich/DE)
W. Schima (Vienna/AT)
S. Schmidt Kobbe (Lausanne/CH)
O. Seror (Bondy/FR)
P. Sidhu (London/UK)
S. Skehan (Dublin/IE)
S. Somers (Dundas, ON/CA)
M. Staunton (Cork/IE)
J. Stoker (Amsterdam/NL)
C. Stoupis (Maennedorf/CH)
Z. Tarjan (Budapest/HU)
S.A. Taylor (London/UK)
C. Triantopoulou (Athens/GR)
V. Valek (Brno-Bohunice/CZ)
D. Vanbeckevoort (Leuven/BE)
J. Venancio (Lisbon/PT)
V. Vilgrain (Clichy/FR)
M.-P. Vullierme (Clichy/FR)
D. Weishaupt (Zurich/CH)
S.D. Yarmenitis (Heraklion/GR)
C.J. Zech (Basel/CH)
M. Zins (Paris/FR)


European Society
ESGAR
Gastrointestinal and Abdominal Radiology

11:00 - 12:30 **Auditorium**

Scientific Session 1
Bilio-pancreatic imaging

SS 1.01
Does Electroencephalography Bispectral Index monitoring allow interventional nurses to administer conscious sedation safely and effectively?
J.H. Chuah, P. Puro, S. Vasileuskaya, N. Kibriya, D. Mullan, J.A. Lawrance, S.M. Stivaros, H. Laasch; Manchester/UK

Purpose: UK guidelines suggest that the interventionist should not be the person administering sedation for interventional procedures. The aim of this study was to review whether sedo-analgesia can be administered by nursing staff guided by an Electroencephalography (EEG) Bispectral Index monitor (BIS Vista, Aspect Medical Systems, Leiden, The Netherlands).
Material and Methods: 103 patients requiring sedo-analgesia for a variety of radiological procedures were evaluated. All patients received increments of fentanyl and midazolam to maintain a BIS level of 80-85. Full cardio-respiratory monitoring and nasal oxygen were given routinely. Data evaluated were Ramsay Sedation Score (RSS), tolerance, duration of the procedure and oxygen saturation.
Results: Median procedure duration was 30 min (range 7-150 min). The median BIS score was 84 (range 73-97), with a median RSS of 2 (=drowsy and anxiety free; range 1-3). In 15 of 103 patients, the BIS monitor could not record a reading. The median tolerance level was 1 (no discomfort/pain, range 1-2), median oxygen saturation was 100% (range 90-100%), none of the patients needed airway management or reversal of sedation. Median drug doses administered were 3 mg Midazolam (1-15 mg) and 50 µg Fentanyl (25-300 µg). Doses were correlated strongly with length of procedure (Pearson's correlation coefficient +0.82).
Conclusion: EEG BIS monitoring is a simple tool to allow very accurate and safe administration of conscious sedation by nursing staff, but readings can be difficult to obtain in up to 15% of patients.

SS 1.02
Is CT-assessed sarcopenia predictive of post-Whipple complications?
E. Kasatkina, V. Lyadov, V. Sinitsyn; Moscow/RU

Purpose: To find if CT-assessed sarcopenia (muscle depletion) is predictive of postoperative complications and mortality in patients with pancreatic cancer (PC).
Material and Methods: CT-images/clinical history of 51 patients with resectable PC who undergone Whipple-procedure in 2009-2012 (25 male/26 female) were selected from hospital-database. Mean age of patients was 64.5±10.2 years, mean value of BMI was 25.1±3.9 kg/m^2. Body composition was analyzed using commercially available software (Silce-O-Matic). For sarcopenia evaluation, single CT-scan on level of L3 was used to measure cross-sectional area of skeletal muscle (cm^2). Values were normalized for stature to get L3-skeletal-muscle index (cm^2/m^2). We used sarcopenia thresholds of 52.4 cm^2/m^2 for male and 38,5 cm^2/m^2 for female defined elsewhere (Prado et al.). Surgical complications were stratified using Clavien-Dindo-Classification.
Results: There were 34/51 patients diagnosed with sarcopenia (66.7%), 20/25 male and 14/26 female. Mean value of L3 SMI was 46.7±6.9 cm^2/m^2 for male and 38.3±6.1 cm^2/m^2 for female. 43.1% of patients had severe post-operative complications. Grade V complications (death of a patient) were found only in sarcopenic patients: 6 cases – 11.7% of total and of 17.6% sarcopenic patients. Relationship between sarcopenia and fatal outcomes was revealed (p=0.065, chi-square test (X^2)). No correlation was found between IIIA-IVB complications and sarcopenia. Mean time spent for body composition assessment was 3.7±1.4min.
Conclusion: Pre-operative CT-assessment of sarcopenia can be used as additional prognostic factor in patients with resectable PC. It does not add much time to study and these results can be used in metabolic disorders research in oncologic patients.

SS 1.03
Differential diagnosis of cystic pancreatic lesions: usefulness of diffusion-weighted 3T MR imaging with b-multiple SE-EPI
P. Boraschi, F. Donati, R. Gigoni, G. Gherarducci, F. Pacciardi, U. Boggi, F. Falaschi, C. Bartolozzi; Pisa/IT

Purpose: To evaluate the usefulness of diffusion-weighted 3T MR imaging with b-multiple SE-EPI in providing an objective value for the differentiation of cystic pancreatic lesions.
Material and Methods: A series of 103 patients with cystic pancreatic lesions of at least 1 cm in size identified at US and/or CT and 20 normal subjects underwent MR imaging at 3T-device (GE DISCOVERY MR750; GE Healthcare). After the acquisition of axial T1w and T2w sequences and coronal MRCP, diffusion-weighted MRI was performed using an axial respiratory-triggered spin-echo echo-planar sequence with multiple b values (150, 500, 1000, 1500 s/mm^2) in all diffusion directions. ADC value was calculated by using a dedicated software fitting the curve obtained from the corresponding ADC for each b value. Fitted ADC values were calculated by two observers in conference for each cystic pancreatic lesion and for normal pancreatic parenchyma. Imaging results were correlated with surgery, ERCP, and/or imaging follow up.
Results: Final diagnoses included intraductal papillary mucinous tumor (IPMT) (n=70), serous cystoadenoma (n=21), and mucinous cystoadenoma (n=12). Fitted ADC value was 1.33x10^{-3} mm^2/s for normal pancreatic parenchyma, 3.11x10^{-3} mm^2/s for IPMT, 2.55x10^{-3} mm^2/s for serous cystoadenoma, 2.95x10^{-3} mm^2/s for mucinous cystoadenoma. Fitted ADC values were significantly higher in mucinous neoplasms than in serous cystoadenomas ($p<0.05$).
Conclusion: Our results suggest that diffusion-weighted 3T MR imaging with b-multiple SE-EPI may be helpful to differentiate mucinous from serous cystic pancreatic lesions.

SS 1.04
Prediction of benign neuroendocrine tumors for determination of parenchyma-preserving resection: the value of gadoxetic acid-enhanced and diffusion-weighted MR imaging
S. Lim, S.H. Kim, K.M. Jang, M.J. Park, H.J. Park, D. Choi; Seoul/KR

Purpose: The purpose of this study was to evaluate the value of gadoxetic acid-enhanced and diffusion-weighted MR imaging (DWI) in predicting benign pancreatic neuroendocrine tumors (NETs) for determination of parenchyma-preserving resection.
Material and Methods: We searched radiology and pathology databases from November 2010 to July 2012 to identify patients who underwent surgery for pancreatic NETs (<4 cm). Twenty patients in the benign group and 14 patients in the non-benign group were included. Two radiologists analyzed the morphologic features, signal intensity on MR images including DWI (b=800), and dynamic enhancement pattern of the tumors with consensus. The tumor-to-parenchyma ratio and tumor apparent diffusion coefficients (ADCs) were quantitatively assessed.
Results: The benign pancreatic NETs were more often round (7/20, 35%) or ovoid (13/20, 65%) in shape and less hypovascular on the arterial phase (3/20, 15%) than were the non-benign pancreatic NETs (1/14, 7.1% and 5/14, 35.8%; 7/14, 50% respectively; $P < 0.05$). Main pancreatic duct dilatation by tumors was demonstrated only in non-benign pancreatic NETs (4/14, 28.4%; P=0.021). ADC values and ratios were significantly different between benign pancreatic NETs (mean, 1.48 x 10-3 mm^2/s, 1.11+0.25, each) and non-benign pancreatic NETs (mean, 1.04 x 10^{-3} mm^2/s, 0.74+0.13, each) ($P <0.01$). Other qualitative and quantitative analyses were not significantly different.
Conclusion: Abdominal MR imaging with DWI may be useful for differentiating benign pancreatic NETs from non-benign pancreatic NETs, which might be helpful for determination of parenchyma-preserving resection.

DOI: 10.1007/s13244-013-0254-8

SS 1.05

Reliable differentiation of malignant and benign intraductal papillary mucinous neoplasm – not an easy task

T.C. Walter, T. Denecke, L. Stelter, I.G. Steffen, C.M. Perez Fernandez, M. Bahra, B. Hamm, C. Grieser; Berlin/DE

Purpose: Retrospective evaluation of morphologic characteristics and differentiation of benign from malignant intraductal papillary mucinous neoplasm (IPMN) using CT and MRI.

Material and Methods: 42 patients (mean age, 63 years) with 61 imaging studies (CT, 14; MRI, 9; both, 19) were retrospectively evaluated. Three independent blinded observers (O1-3) were asked to evaluate each study with respect to previously published diagnostic imaging criteria (Sendai criteria – nodules, size, main duct involvement) and to grade the identified lesion or lesions as either benign or malignant. The diagnostic predictions were compared and correlated with the histological diagnoses (benign – IPMN/ Borderline, malignant – CIS/IPMC/solid tumors).

Results: Histology revealed 26 benign and 16 malignant lesions. The overall averaged accuracy of differentiation between benign IPMN and malignant IPMN was 82% for CT and 85% for MRI for all 3 observers (interobserver agreement: range 79-94% and 78-100%, respectively; $p<0.05$). Exclusion of cases with highly likely benign IPMN or solid tumors resulted in an overall averaged accuracy of 71% for CT and 68% for MRI (interobserver agreement: range 71-83% and 78-87%, respectively; $p<0.05$). Mural nodules and lesion size (>2.5 cm) were significant for malignant lesions ($p=0.017$ and $p=0.02$, respectively) whereas all other parameters were not found to be significant ($p>0.05$).

Conclusion: Differentiation of benign from malignant IPMN is possible with CT and MRI. However, if findings are equivocal, additional diagnostic measures are desirable before treatment decisions are made.

SS 1.06

The efficacy of diffusion weighted imaging for detection of acute pancreatitis and comparison of subgroups according to Balthazar classification

E. Yencilek[1], S. Telli[1], K. Meric[1], A. Ozgur[2], O. Cakir[1], M. Simsek[1]; [1]Istanbul/TR, [2]Mersin/TR

Purpose: To measure pancreatic apparent diffusion coefficient (ADC) values in acute pancreatitis and compare with CT findings based on Balthazar classification.

Material and Methods: Fifty patients with the diagnosis of clinical pancreatitis were evaluated both with multidetector CT and MRI in 24 h of presentation. We calculated pancreatic ADC values with diffusion weighted imaging (b=0 and b=1000 mm^2/sn). These values were compared with their normal counterparts (n=24). The patients with acute pancreatitis were subgrouped according to the Balthazar classification. The mean ADC values were calculated in each subgroup and they were compared with control group's ADC values.

Results: The mean pancreatic ADC values in acute pancreatitis (1.19×10^{-3} mm^2/sn ± 0.32) was significantly lower than in the normal group (1.78×10^{-3} mm^2/sn ± 0.29) ($p<0.001$). In subgroup analysis, ADC values in each group were significantly lower than normal group ($p<0,001$). In addition, according to Balthazar classification, as severity of pancreatitis increases, lower ADC values were noted.

Conclusion: DWI with MRI and ADC values are helpful in diagnosis of all subgroups of acute pancreatitis. Due to lack of CT findings in grade A patients, DWI may help the diagnosis in this group.

SS 1.07

Gadodiamide versus gadoteric acid in the evaluation of intraductal papillary mucinous neoplasms with magnetic resonance

G. Morana[1], A. Dorigo[1], V. Tavano[2], F. De Leo[1]; [1]Treviso/IT, [2]Padua/IT

Purpose: In the last decade, the detection rate of the intraductal papillary mucinous tumor (IPMN) has been increased due to an improvement in imaging modalities such as MR. MR contrast media (CM) administration allows a better definition of IPMN on T1 and T2, lowering the signal from parenchyma, thus increasing the C/N (contrast noise) between the lesion and the surrounding structures. Due to different relaxivities in CM, aim of this study was to compare the paramagnetic (T1) and superparamagnetic (T2) effect of two different CM, Gadodiamide (Omniscan@GE) and Gadoterate Meglumina (Dotarem@ Guerbet) to identify and assess IPMN.

Material and Methods: Fifty patients (mean age 67.9 years) with small branch duct IPMN were studied by using alternatively the two CM with a time gap of 6 months. MR examinations were performed on a 1.5-T scanner (Siemens Avanto): 2D HASTE, coronal 2D and 3D MCRP, axial VIBE-T1w before and during injection of CM. Statistical analysis (Matlab2010): Pearson, box plots, t test, Wilcoxon-test, Kruskal-Wallis

Results: The Wilcoxon test showed significant differences between the two groups ($p=0.0001$). The percentage of gadodiamide-enhancement resulted greater than gadoteric acid in each phase: T1_art ($p=0.0058$); T1_ven ($p=0.001$); T1_delayed ($p=0.0018$). The contrast noise-T2w (pre-post CM) was greater for gadodiamide than gadoteric acid in the IPMN ($p=0.008$) than in the Wirsung's duct ($p=0.0001$)

Conclusion: Our study showed that gadodiamide could provide a stronger T1 and T2 effects than gadoteric acid, which are needed for a better definition of IPMT and to assess morphological signs of malignant degeneration.

SS 1.08

Value of diffusion-weighted MR imaging in the diagnosis of lymph node metastases in patients with extrahepatic cholangiocarcinoma

K. Holzapfel, M. Loos, M. Eiber, E.J. Rummeny, J. Gaa; Munich/DE

Purpose: To evaluate diffusion-weighted MR imaging (DWI) in the diagnosis of lymph node metastases in patients with extrahepatic cholangiocarcinoma.

Material and Methods: In 24 patients with extrahepatic cholangiocarcinoma, MR imaging of the upper abdomen was performed prior to surgery (1.5T, Avanto, Siemens). DWI was performed using a respiratory-triggered single-shot echo-planar imaging (SSEPI) sequence (b-values 50/300/600s/mm^2). Apparent diffusion coefficient (ADC)-values and diameters of regional lymph nodes (LN) were determined. Subsequently, in all patients, surgical resection of the primary tumor and regional LN dissection were performed. Imaging results were correlated with results of histopathologic analysis. ADC-values and diameters of benign and malignant LN were compared using the Mann-Whitney U test. In addition, a receiver operating characteristic (ROC) curve analysis was performed.

Results: The mean ADC-value ($x10^{-3}mm^2$/s) of metastatic LN (1.21±0.15) was significantly lower than that of benign LN (1.62±0.33, $p<0.001$) while there was no significant difference in the mean diameter of malignant (16.8±5.4 mm) and benign LN (14.1±4.0 mm; $p=0.09$). Using an ADC-value of $1.25x10^{-3}mm^2$/s as threshold, 91.4% of LN were correctly classified as benign or malignant with a sensitivity/specificity of 83.3%/92.8% and a positive/negative predictive value of 66.7%/96.7%. The area under the ROC-curve was 0.93.

Conclusion: DWI using a respiratory-triggered SSEPI sequence is a promising imaging modality in the differentiation of benign and malignant LN in patients with extrahepatic cholangiocarcinomas.

DOI: 10.1007/s13244-013-0254-8

SS 1.09

Percutaneous cholecystostomy: single centre experience in 111 patients with an acute cholecystitis

R. Peters[1], S. Braak[1], S. Rakic[1], M. Simoens[1], S. Kolderman[2]; [1]Almelo/NL, [2]Veendam/NL

Purpose: To evaluate the safety and long-term outcome of percutaneous cholecystostomy (PC) under radiologic guidance for acute calculeous (ACC) and acalculeous cholecystitis (AAC).

Material and Methods: We performed a retrospective analysis of 111 patients who underwent PC from 2002 to 2011. Patients were divided into two groups: AAC and ACC. For all patients, comorbidity and American Society of Anesthesiologists (ASA) classification were determined. The indications, complications, recurrence rate and long-term outcome for both groups were analyzed.

Results: Twenty-four patients with AAC and 87 patients with ACC underwent PC. The procedure failed in 2 (1.8%) patients. There were 4 abscesses and 2 fistulas post-PC. Drain dislodgment was found without sequelae in 8 patients. Elective cholecystectomy was performed in 35/111 (31.5%). 51 of 87 (58.6%) patients with gallstones underwent cholecystectomy; 36/87 (41.3%) did not undergo surgery either due to a too short follow-up or they died of non-biliary disease. In the AAC group, there was no recurrent cholecystitis in 17/24 (70.8%) patients; 3/24 (12.5%) needed surgery later on and 4/24 (16.6%) patients died.

Conclusion: PC is a treatment with a low complication rate for patients with acute cholecystits who are considered to be at a high-risk for cholecystectomy. In patients with ACC, PC seems to be a valuable bridge to surgery, which will be required in the majority later on. In most of AAC-patients, no further treatment seems to be needed.

SS 1.10

ARFI of pancreatic cystic lesions

M. D'Onofrio, R. De Robertis, S. Canestrini, S. Crosara, E. Demozzi, R. Pozzi Mucelli; Verona/IT

Purpose: To prospectively evaluate the results of ARFI (Acoustic Radiation Force Impulse) ultrasound in the study of pancreatic cystic lesions using different analysis methods, compared with the final diagnosis (pathological or by MRI/EUS findings).

Material and Methods: 38 patients with pancreatic cystic focal lesions were included in the study and underwent conventional US. For every patient 5 measurements with Virtual Touch Quantification ROI were performed. In order to distinguish mucinous (potentially malignant) from serous cystic lesions (mainly benign) the result "XXXX/0" was considered meaning simple liquids (reportable to water), and the accuracy of Virtual Touch Tissue Quantification in differentiating cystic-pancreatic lesions was calculated. To consider the lesion as containing complex fluids, (potentially mucinous), two different reading methods were applied: at least two numerical values when performing five measurements; prevalence of numerical values irrespective of the number of measurements. Sensitivity, specificity, positive and negative predictive value and accuracy were calculated for the differential diagnosis between mucinous versus non-mucinous cystic lesions. .

Results: Sensitivity, specificity, PPV, NPV and accuracy in the group of cystic lesions by using the first reading method were respectively of: 68.8%, 77.3%, 68.8%, 77.3%, 73.7%. Sensitivity, specificity, PPV, NPV and accuracy in the group of cystic lesions by using the second reading method were respectively of 37.5%, 100%, 100%, 68.8%, 73.3%..

Conclusion: ARFI can be useful in non-invasive characterization of pancreatic cystic lesion during the conventional US examination.

11:00 - 12:30 **Room J**

Scientific Session 2

Imaging of the rectum

SS 2.01

Comparison between air-balloon and gel defeco MRI

F. Mazzamurro, N. Al Ansari, V. Buonocore, V. De Marco, F. Maccioni; Rome/IT

Purpose: To prospectively compare two different techniques of rectal filling for Dynamic Pelvic Floor MRI (DPF-MRI) in 22 patients affected by pelvic floor disorders. In the first technique, the rectum was inflated with air using a Foley catheter, in the second one an echographic gel was used to fill the rectum.

Material and Methods: 22 consecutive patients (22 females), mean age 57 years, with pelvic floor dysfunction underwent both rectal filling techniques during the same procedure. The two examinations were compared with regard to the evidence of rectocele, rectal invagination, cystocele, anorectal junction descent, enterocele and other pathologic findings.

Results: DPF MRI performed using gel detected 22 rectoceles, 18 invagination, 6 enteroceles, 16 cystoceles, 2 pelvic diskinesia and 0 urethral hyperpermobility. DPF MRI performed using air filling detected 19 rectoceles, 16 invagination, 10 enteroceles, 20 cystoceles, 0 pelvic diskinesia and 4 urethral hyperpermobility. Associated pelvic floor disorders of the urogenital and posterior compartment were detected in 60% patients with air and 50% of patients with gel.

Conclusion: Rectal filling with gel better evaluated pelvic diskinesia and rectocele, but it caused patient discomfort. The use of air depicted a larger number of cystoceles and urethral hypermobility, of enteroceles and of rectocele (19/22) most likely because it does not have a real evacuation phase. Although both techniques were able to detect three-compartment pelvic floor disorders, a higher sensitivity of air filling techniques was observed.

SS 2.02

Does quantitative diffusion-weighted and dynamic contrast-enhanced MRI predict pathological complete response after neoadjuvant chemoradiation therapy in rectal cancer patients?

A. Alconchel[1], I. Sosnovskikh[1], J. Garcia Bennett[2], P. Summers[1], G. Petralia[1], M. Bellomi[1]; [1]Milan/IT, [2]Reus/ES

Purpose: To evaluate the potential of quantitative diffusion-weighted MRI (DW-MRI) and dynamic contrast-enhanced MRI (DCE-MRI) to predict pathologic complete response (pCR) after neoadjuvant chemoradiation therapy (NACRT) in rectal cancer patients.

Material and Methods: 43 patients (mean age 61.7 years, range 40-81) with locally advanced rectal adenocarcinoma (T stage≥ T3, or N1-2) underwent T2-weighted, DW-MRI and DCE-MRI on a 1.5T scanner, before and after NACRT before surgery. Regions of interest (ROIs) were manually drawn on rectal cancer by a radiologist on DW and DCE images in all slices where tumour was visible. For each ROI, mean transfer constant (Ktrans), rate constant (Kep) and leakage space (Ve), or apparent diffusion coefficient (ADC) values were calculated. Based on the pathologic stage on surgical specimen, patients were grouped into those who achieved pCR (ypT0ypN0) and non-responders (nR) (including local downstaging, no local downstaging or increase in local stage).

Results: Six patients (14%) were pCR and 37 (86%) nR at final histology. Baseline and post-therapy KTrans, Kep, Ve and ADC were not significantly different between pCR and nR patients. Overall KTrans and Kep significantly decreased and Ve and ADC increased after therapy, but no difference in percentage changes of these values were observed between pCR and nR patients.

Conclusion: In our cohort, quantitative DW-MRI and DCE-MRI did not identify patients who achieved pCR after NACRT in rectal cancer patients.

DOI: 10.1007/s13244-013-0254-8

SS 2.03

High-resolution 3D T1-weighted imaging in nodal staging for locally advanced rectal carcinoma post chemoradiation – a lesion-by-lesion validation study

D. Mondal[1], D.M. Lambregts[2], L.A. Heijnen[2], M.H. Martens[2], R.G. Riedl[2], G.L. Beets[2], R. Beets-Tan[2]; [1]Oxford/UK, [2]Maastricht/NL

Purpose: The aim of this study was to assess the advantage of 3D T1-weighted gradient echo (3D-T1W GRE) imaging compared with routine multiplanar T2-weighted (T2W) imaging alone, for nodal re-staging following chemoradiation treatment in patients with locally advanced rectal cancer.

Material and Methods: Forty-one consecutive patients with locally advanced rectal cancer were retrospectively evaluated. An experienced reader scored each node as benign or malignant on T2W-MRI (1.5T) using a 5-point confidence level based on size, contour and signal heterogeneity. A week later, nodes were re-scored on 3D-T1W GRE images with 1 mm^2isotropic voxels. Each node was plotted on an anatomical map, ensuring exact lesion-by-lesion matching with histology.

Results: 609 nodes (39 N+, 570 N-) were harvested from the mesorectal fat, of which 195 (26 N+) could be identified on T2W-MRI versus 347 (31 N+) on 3D-T1W-MRI. Sensitivity, specificity, positive and negative predictive values were 58%, 95%, 65% and 94% for T2W-MRI versus 39%, 97%, 60% and 94% for 3D-T1W-MRI. Areas under the ROC-curve were 0.84 on T2W-MRI versus 0.75 for 3D-T1W-MRI (p=0.08).

Conclusion: Negative lymph nodes can be accurately predicted on MRI with a high NPV of >90%. Although it does not improve the diagnostic performance for differentiating between benign and malignant nodes, the benefit of 3D-T1W imaging compared with T2W MRI is that it increases the conspicuity and number of detected nodes.

SS 2.04

Diagnostic performance of semi-quantitative parameters of dynamic contrast-enhanced MRI for the selection of good responders after chemoradiation for rectal cancer

M.H. Martens, S. Subhani, M. Maas, L.A. Heijnen, D.M.J. Lambregts, A. Zur Hausen, G.L. Beets, E. Kluza, R.G.H. Beets-Tan; Maastricht/NL

Purpose: Response assessment after chemoradiotherapy (CRT) in rectal cancer remains difficult. Aim of this study was to investigate if semi-quantitative analysis of dynamic contrast-enhanced (DCE) MRI, using the blood-pool contrastagent gadofosveset, can identify good responders after CRT.

Material and Methods: Fifteen patients with locally advanced rectal cancer received DCE-MRI both before and 8 weeks after CRT. Kinetic parameters, i.e. initial slope, initial peak, time to peak, final slope, and area under the first 60, 90, and 120s of the enhancement curve ($IAUC_{60}$, $IAUC_{90}$, $IAUC_{120}$) were determined from relative signal enhancement-time curves. Receiver operating characteristics (ROC) curves were used to assess diagnostic performance. Good responders (n=8) were defined as patients with tumor regression grade (TRG) of 1 or 2 at histopathology. Poor responders showed a TRG of 3-5 (n=7).

Results: Significant differences between good and poor responders were found for post-CRT semi-quantitative parameters and also change in parameters. The initial slope, initial peak, $\Delta iAUC_{60}$, $\Delta iAUC_{90}$, and $\Delta iAUC_{120}$ were significant predictors for a good response after CRT. The most accurate parameter was the $\Delta iAUC_{90}$ with the area under the ROC curve ranging from 0.88 to 0.91.

Conclusion: Semi-quantitative parameters of dynamic contrast-enhanced MRI are promising tools for predicting response after chemoradiotherapy in patients with rectal cancer. Best predictor for good response was the change in area under enhancement-curve at 90 s.

SS 2.05

Apparent diffusion coefficient for discriminating metastatic from non-metastatic lymph nodes in primary rectal cancer

S.H. Kim, E.Y. Cho, J.H. Yoon, C.K. Eun; Busan/KR

Purpose: To investigate whether apparent diffusion coefficient (ADC) would be feasible to discriminate metastatic from non-metastatic lymph nodes (LNs) in patients with primary rectal cancer.

Material and Methods: 36 patients (male: 12, female: 24, mean age: 62.7, range: 37-82) who underwent 1.5-T MRI with DWI (b, 0 and 1000) and subsequent surgical resection were included. A blinded radiologist measured the ADC value in each regional LN on an ADC map after referring to T2-WI and DWI. The t-test was used to compare the mean ADC values of metastatic and non-metastatic LNs. ROC analysis was performed to calculate the diagnostic performance and to obtain the optimal cut-off value for the best accuracy for discriminating metastatic from non-metastatic LNs. Histopathologic results were used as the reference standard on a per-LN basis.

Results: 683 LNs were histopathologically identified. Of these, 116 LNs (46 metastatic and 70 non-metastatic) were radiologic-pathologically matched and analyzed. The mean ADC of metastatic LNs (0.90 ± 0.15) was significantly lower than that of non-metastatic LNs (1.06 ± 0.22) (P<0.0001). The Az was 0.746 (95% CI, 0.655 to 0.822). When an ADC of 0.99×10^{-3} mm^2/s was used as the cut-off, the accuracy of 72% was calculated for a sensitivity of 78% and a specificity of 67%.

Conclusion: ADC is feasible to discriminate metastatic from non-metastatic LNs in patients with primary rectal cancer, although the diagnostic accuracy is around 70%.

SS 2.06

Diffusion-weighted imaging in rectal cancer: comparison between 1.5 and 3T MR before, during and after neoadjuvant chemoradiotherapy

P. Lucchesi[1], C.N. De Cecco[1], M. Rengo[1], M. Ciolina[2], D. Caruso[1], A. Laghi[1]; [1]Latina/IT, [2]Rome/IT

Purpose: To compare diffusion-weighted imaging (DWI) in patients with rectal cancer studied using 1.5 and 3T MRI in terms of DWI signal intensity (SI) and apparent diffusion coefficient (ADC) values.

Material and Methods: Twenty-two patients with rectal cancer consecutively underwent 1.5 and 3T MR examination before, during and after neoadjuvant therapy, which included DWI using a 1000 mm^2/s b-values. DWI images were acquired using the following parameters: TR / TE, 667/70 ms, voxel size 2,3 x 3 x 5 mm, 30 slices, gap 1 mm, acquisition time about 5 minutes. DWI SI and ADC values were evaluated by two expert readers in separate reading sessions placing a region of interest (ROI) within rectal cancer. Paired Wilcoxon tests were used to compare DWI values.

Results: No significant difference in ADC values was found before (3 T 0.83; 1.5 T 0.84; p=0.16), during (3T 1.15; 1.5 T 1.17; p=0.16) and after (3T 1.24; 1.5 T 1.25; p=0.48) neoadjuvant therapy. 1.5T rectal cancer SI was significantly lower (p<0.05) than SI values measured on 3T before (3T 325.14; 1.5 T 68.52) during (3T 207.30; 1.5T 58.24) and after (3T 130.77; 1.5 T 41.23) neoadjuvant therapy.

Conclusion: 3T DWI shows a significant increment in rectal cancer SI without difference in ADC measurement in comparison to 1.5T.

DOI: 10.1007/s13244-013-0254-8

SS 2.07

Evaluation for rectocele patients based on the defecographic findings. How is it useful for surgery by these results?

H.J. Jeon[1], U.C. Park[2], H.S. Park[1], Y.J. Kim[1], S.I. Jung[1], S.J. Park[3]; [1]Seoul/KR, [2]Chungju/KR, [3]Goheung-Gun Chollanamdo/KR

Purpose: Defecography and a dynamic imaging modality play an important role in the diagnosis of functional and morphologic abnormalities in patients with chronic constipation. Current study was designed to assess the physiologic characteristics and clinical significance of rectocele patients with functionally obstructed defecation. Moreover, outcome of treatment was analyzed based on the physiologic characteristics.

Material and Methods: 553 patients studied defecography and cinedefecography, anal manometry (n=237), colonic transit time study (n=85), 155 female rectocele patients found to have significant rectocele. Diagnostic criteria of significant rectocele were a poor rectal emptying of barium paste from bulged outpocket of anterior rectum with a more than 3 cm, simultaneously, despite maximal trial of simulated defecation. The findings of defecography are as two types of anterior rectocele, “distension” of Type 1 (Group 1, n=102) and “displacement” or “deformity” of Type 2 (Group 2, n=53).

Results: In Group 1, clinical symptoms of obstructed defecation was not infrequently detected in comparison to Group 2 patients ($p<0.01$). In Group 2, patients showed a significantly higher frequency of the symptoms of pelvic outlet obstruction than in Group 1 patients ($p<0.001$). Current results showed improved outcome as compared with previous results of surgery before we had made these subclassification (97.0% vs. 85.7%, respectively, $p<0.01$).

Conclusion: We report defecographic features of rectocele findings. Careful selective surgical indications by using defecography are essential for the successful result.

SS 2.08

Is there a correlation between quantitative and qualitative parameters for dynamic contrast-enhanced MRI in rectal cancer?

M.H. Martens[1], N. Papanikolaou[2], E. Kluza[1], L.A. Heijnen[1], D.M. Lambregts[1], M. Maas[1], G.L. Beets[1], R.G.H. Beets-Tan[1]; [1]Maastricht/NL, [2]Heraklion/GR

Purpose: Recently several studies have been performed using dynamic contrast-enhanced MRI (DCE-MRI) in the response prediction for rectal cancer. However, both qualitative analyses (i.e. Wash in, wash out, peak enhancement) as quantitative analyses (i.e. K^{trans}, K_{ep}, V_e, V_p) are reported in current literature. The aim of this study was to compare the qualitative analysis method with the quantitative analysis method in rectal cancer patients.

Material and Methods: Twenty patients were included: 10 patients with DCE-MRI of the primary tumor, and 10 after neoadjuvant chemoradiation (post-CRT). Regions of interest were placed in the tumor and all parameters were measured. Pearson correlation test was used for comparison between the parameters. P-value <0.05 was considered statistically significant.

Results: Peak enhancement of the signal intensity curve showed strong correlation with K^{trans} ($r=0.74$-0.80, $p<0.01$), moderate to strong correlation with K_{ep} ($r=0.62$-0.75, $p=0.04$), and moderate correlation with V_e ($r=0.62$-0.70, $p=0.04$). V_p showed moderate to strong correlation with wash in ($r=0.68$-0.79, $p=0.01$).

Conclusion: There is a correlation between the quantitative and qualitative parameters derived from DCE-MRI. Of interest was the strong correlation that exists between K^{trans} and peak enhancement of the signal intensity curve, suggesting that qualitative analysis of DCE MRI may be a good alternative to a quantitative analysis.

SS 2.09

Preoperative local staging of rectal cancer using 2D T2-weighted FSE sequence and diffusion-weighted MR imaging with b-multiple SE-EPI at 3T-device

F. Donati, P. Boraschi, E. Marciano, G. Gherarducci, F. Pacciardi, R. Gigoni, E. Neri, F. Falaschi, C. Bartolozzi; Pisa/IT

Purpose: To evaluate the image quality and diagnostic performance of two-dimensional T2-weighted FSE sequence and diffusion-weighted imaging (DWI) in the local staging of rectal cancer at 3T-device.

Material and Methods: Phased-array MRI was performed in 26 consecutive patients with biopsy-proven rectal cancer. High-resolution two-dimensional T2-weighted FSE images in the sagittal, coronal, axial and axial oblique planes and DWI using an axial spin-echo echo-planar sequence with multiple b values (150, 500, 1000, 1500 s/mm^2) were obtained at 3T-device (GE DISCOVERY MR750;GE Healthcare). A set of T2-weighted images and a combined set of T2-weighted and DW images were evaluated by two experienced radiologists in consensus with regard to local disease. A quality assessment of image datasets was also performed by the observers using a five-point scale. Total mesorectal excision surgery was used as the standard of reference.

Results: Twenty patients who underwent a total mesorectal excision were enrolled in this study. Image quality was considered excellent on T2-weighted images, and good on DWI. The sensitivity and diagnostic accuracy of DWI combined with T2-weighted imaging for prediction of extramural tumor spread (92% and 88%, respectively) were significantly higher than those of T2-weighted imaging alone (67% and 65%). In particular, the measurement of the distance between the lesion and mesorectal fascia improved significantly after additional review of DWI ($p<0.05$).

Conclusion: DWI in addition to T2-weighted MR imaging can improve the local staging of rectal cancer at 3T.

SS 2.10

Does gadolinium improve accuracy of T4 diagnosis at MRI evaluation of rectal cancer?

M.J. Gollub[1], Y. Lakhman[1], K. McGinty[2], M. Weiser[1], A. Trakarnsanga[1], J. Zheng[1], M. Sohn[1], C. Moskowitz[1], J. Shia[1], P.P. Paty[1], J.G. Guillem[1], G. Nash[1], L. Temple[1], K. Goodman[1], L. Saltz[1], D. Reidy[1], N. Segal[1], J. Garcia-Aguilar[1]; [1]New York, NY/US, [2]Danville, PA/US

Purpose: To compare reader accuracy with and without gadolinium in the detection of T4 rectal cancer.

Material and Methods: From a rectal cancer surgical database (1998-2009), patients were randomly selected who had MRI scans with/without gadolinium prior to surgery and clinical T3/T4 disease or known recurrent rectal cancer. Three radiologists blinded to pathology and disease stage independently interpreted all MRI using either noncontrast images alone or combined with contrast images, with an interval between sessions of 4 weeks. Multiplanar views from a 1.5T magnet were observed. Readers evaluated involvement of surrounding structures on a 0-4 confidence scale. Pathology was the gold standard. Overall and site-specific sensitivity, specificity, NPV and PPV were calculated. ROC curves were constructed and AUC values derived.

Results: Ninety patients (mean age 59 years) included 4 T2, 49 T3 and 39 T4 stage rectal cancers. 29 organs were invaded including (2 bladders, 10 vaginas, 6 sidewall, 2 sphincters, 3 seminal vesicles and 6 prostates). Overall AUC without and with gadolinium were .74/.78, .85/.85, .80/.74 for readers 1, 2, 3, respectively. The most experienced reader had overall se/sp/PPV/NPV .74/.70,.87/84, .65/.59, .91/.89 without and with gadolinium respectively. AUC pre- and post-gadolinium for global and site-specific readings were not statistically different.

Conclusion: Gadolinium did not improve accuracy of T4 diagnosis during MRI for rectal cancer.

DOI: 10.1007/s13244-013-0254-8

11:00 - 12:30 **Room F**

Scientific Session 3

Liver imaging: Technical performance

SS 3.01

High-resolution fat suppressed 3D T1-weighted imaging using a dual-echo Dixon technique and a high-acceleration parallel acquisition for gadoxetic acid-enhanced liver MR imaging at 3T

J.H. Yoon, J.M. Lee, M.H. Yu, E.J. Kim, J.K. Han, B.I. Choi; Seoul/KR

Purpose: To determine whether multi-echo Dixon (mDixon) 3D T1-weighted (T1W) gradient-recalled-echo (GRE) technique with a high-acceleration parallel acquisition can provide better image quality than conventional 3D-fat suppressed (FS)-T1W- GRE for gadoxetic acid-enhanced liver MRI at 3T.

Material and Methods: This retrospective study was approved by our institutional review board, and informed consent was waived. 138 patients with suspected hepatic focal lesions underwent gadoxetic acid-enhanced liver MRI at 3T, including dynamic imaging using either high-resolution mDixon 3D technique (n=70). Hepatobiliary phase (HBP) imaging was obtained using standard eTHRIVE with acceleration factor (AF) of 2.6, high-resolution eTHRIVE and mDixon with AF of 5. The image quality of the arterial, portal and HBP image sets of both groups was graded independently using a five-point scale by two radiologists and they reached a final consensus.

Results: High-resolution mDixon images with AF 5 provided better overall image quality than eTHRIVE with AF 2.6 and AF 5 ($p<0.05$). In addition, among the three HBP image sets, mDixon showed significantly less pixel graininess and better fat suppression than eTHRIVE with AF 5 ($p<0.05$), despite of similar performance in terms of lesion or anatomic structure conspicuity compared with eTHRIVE with AF 5.

Conclusion: Use of high-acceleration parallel acquisition factor and mDixon sequence can provide high-resolution T1WI with better image quality and fat suppression than that of conventional 3D-FS-T1GRE sequence.

SS 3.02

Inter and intra-observer reproducibility of MRI for the measurement of NET liver metastases

J. Arfi Rouche, C. Caramella, S. Foulon, A. Laplanche, E. Baudin, C. Dromain; Villejuif/FR

Purpose: Assessment of treatment is based on metastases size measurement. Our goal was to determine the intra and inter-observer reproducibility of each MRI sequence for the measurement of NET liver metastases.

Material and Methods: 32 patients with NET liver metastases underwent 1.5-T MR imaging of the liver [T2W and T1W sequences before and after the injection of gadolinium on hepatic arterial (HAP) and portal venous phase (PVP)]. A maximum of 5 target lesions by patient was chosen by one reviewer on the MR sequence allowing the better depiction. Then measurements of target lesions diameter were performed by 3 reviewers blindly and independently in two sessions with a delay of one month.

Results: 3384 measurements were made (141 metastases, mean 4.4 per patient). The MR sequence allowing the better depiction of the target lesions was T2W in 81% of patients. Non-measurable lesions were significantly higher on HAP and PVP compared to unenhanced T1 and T2W ($p<0.001$). T2W sequence had the higher overall intra- and inter-observer inter-class correlation coefficient (0.99 and 0.98) but without significant difference compared to other sequences. No statistical difference was found between the senior and the junior radiologists.

Conclusion: MRI allows reproducible measurements with low inter and intra-observer variability. Unenhanced T2W sequence should be considered as the sequence of choice for the size measurement of NET liver metastases.

SS 3.03

Withdrawn by the authors

SS 3.04

Increased flip angle for functional liver imaging with Gd-EOB after right sided portal venous embolization

T. Denecke, D. Geisel, M. Stockmann, B. Hamm, B. Gebauer; Berlin/DE

Purpose: To prospectively evaluate the effect of an increased flip angle (FA) of a T1- weighted fat saturated 3D-sequence for the measurement of hepatocyte uptake of Gd-EOB-DTPA MRI after right portal vein embolization (PVE).

Material and Methods: 10 patients who received a PVE prior to an extended hemihepatectomy were examined 14 days after PVE using Gd-EOB-DTPA-enhanced MRI of the liver using the standard FA of 10° and the increased FA of 30°.

Results: Relative enhancement of the right liver lobe (RLL) was 0.52 ± 0.12 for 10° and 1.41 ± 0.39 for 30°, and the left liver lobe (LLL) was 0.58 ± 0.11 for 10° and 2.05 ± 0.61 for 30°. Relative enhancement of the RLL was significantly higher for 30° than for 10° ($p = 0.009$) and significantly higher in the 30° than in the 10° sequences ($p = 0.005$) for the LLL.

Conclusion: A flip angle of 30° increases the contrast between liver partitions with and without portal venous embolization. Thereby, the sensitivity for differences in uptake intensity is increased. This could be of value for a more exact determination of differences in regional liver function and, consequently, the estimation of the future remnant liver function.

SS 3.05

Diagnostic accuracy of dual energy CT in the evaluation of residual tumor within 24 h after RF ablation: ROC analysis

F. Vandenbroucke[1], S. Van Hedent[1], N. Buls[1], K. Nieboer[1], D. Belsack[1], P. Ros[2], J. De Mey[1]; [1]Brussels/BE, [2]Cleveland, OH/US

Purpose: To evaluate the diagnostic accuracy of single source dual energy CT (DECT) within 24 h after RF ablation compared to the first follow-up imaging after 8-10 weeks.

Material and Methods: Thirty-three patients with 38 malignant lesions (20 liver, 10 kidney, 8 lung) were scanned within 24 h after RF ablation with DECT technique to evaluate possible local tumor progression (LTP). The DECT data were reconstructed as monochromatic 70 keV images, grayscale iodine density and color-coded iodine density images. Two independent readers were asked to rate their confidence in the presence or absence of residual tumor. The results were compared with the follow-up imaging after 8-10 weeks. Multireader multicase receiver operating characteristic (ROC) analysis was performed with the area under the curve and 95% confidence intervals (CI) as metric for diagnostic accuracy.

Results: Ten out of 38 (26.3%) lesions showed LTP at 8-10 weeks. The mean area under the curve was 0.84 (CI: 0.75-0.93) for 70keV, 0.80 (CI: 0.67-0.93) for grayscale iodine density and 0.78 (CI: 0.65-0.90) for color-coded images. There was no significant difference observed between the three reconstruction techniques ($p=0.08$).

Conclusion: DECT can be used to make an early evaluation within 24 h after RF ablation. Results for interpretation of LTP are equal to the reconstruction techniques used in DECT.

DOI: 10.1007/s13244-013-0254-8

SS 3.06

Depiction and characterization of liver metastases in 18F-FDG PET/MRI: comparison to PET/CT

K. Beiderwellen[1], B. Gomez[1], V. Hartung-Knemeyer[1], C. Buchbender[2], F. Nensa[1], H. Kuehl[1], A. Bockisch[1], T.C. Lauenstein[1]; [1]Essen/DE, [2]Düsseldorf/DE

Purpose: To evaluate the value of PET/MRI in the diagnosis of liver lesions in patients with solid malignancies.

Material and Methods: 70 patients (31 women, 39 men) with known solid tumors underwent full-dose contrast-enhanced PET/CT with ^{18}F-FDG (Biograph mCT 128, Siemens). The patients subsequently underwent whole-body contrast-enhanced PET/MRI (Biograph mMR, Siemens). The PET/MRI protocol comprised: 1) T1 FLASH pre-contrast, 2) T2 HASTE, 3) DWI, 4) T1 FLASH post-contrast. The datasets were evaluated by two radiologists. Every depicted lesion was rated for conspicuity (4-point ordinal scale) and diagnostic confidence (5-point ordinal scale). Statistical analysis was performed using Wilcoxon's signed rank test.

Results: A total of 97 lesions were detected (malignant n=26; benign n=71). 10 patients had malignant liver lesions, whereas benign liver lesions were found in 26 patients. Using PET/MRI, all lesions could be depicted, whereas 9 benign lesions were not detected in the PET/CT datasets. Lesion conspicuity was significantly higher for PET/MRI (PET/MRI: 2.91 ± 0.30 [95% CI: 2.87 - 2.95]; PET/CT: (2.36 ± 0.92 [95% CI: 2.23 - 2.49]; $p < 0.0001$). For malignant liver lesions diagnostic confidence was significantly higher (PET/MRI: 4.81 ± 0.45 [95% CI: 4.64 - 4.98]; PET/CT: 4.52 ± 0.58 [95% CI: 4.30 to 4.74]; $p < 0.0001$).

Conclusion: PET/MRI provides significantly higher lesion conspicuity and diagnostic confidence for liver lesions, offering a high-potential alternative to PET/CT.

SS 3.07

Performance of shear wave elastography for assessment of liver fibrosis: correlation with histological staging and quantification

T. Lefort, G. Renosi, O. Guillaud, J. Dumortier, J. Scoazec, A. Guibal; Lyon/FR

Purpose: To evaluate the performance of shear wave elastography (SWE) for the quantification of liver fibrosis. Liver biopsy staging and quantification was used as the standard reference.

Material and Methods: Consecutive patients with various chronic liver diseases were prospectively included. On the same day, ultrasound SWE (Aixplorer, Supersonic Imagine, Aix-en-Provence, France), transient elastography (TE) using Fibroscan (Echosens, Paris, France), and subsequent liver biopsy were performed. Histologic analysis included staging according to the METAVIR score and digital quantification of the fibrosis area.

Results: Fifty-five patients were included for analysis. Chronic liver conditions included liver transplantation follow-up (n=21), non-alcoholic steatohepatitis (n=13), viral chronic hepatitis B or C (n=9), alcoholic liver disease (n=2), auto-immune hepatitis (n=2), chronic biliary disease (n=2), and others (n=6). Area under the ROC curve (with 95% confidence interval) for SWE and TE, respectively, were: 0.92 (0.81-0.98) and 0.91 (0.80-0.97) for F score ≥2, 0.92 (0.81-0.97) and 0.90 (0.79-0.96) for F≥3, 0.97 (0.88-0.99) and 0.97 (0.88-0.99) for F4. Liver stiffness measured with SWE and TE was significantly correlated with the fibrosis area: Spearman's coefficient was 0.76 and 0.65 ($p<0.0001$), respectively.

Conclusion: SWE can be used as a non-invasive method for quantification of liver fibrosis. Liver stiffness was significantly correlated with histologic digital quantification of fibrosis area.

SS 3.08

Acoustic radiation force impulse imaging in pediatric population: normal liver values?

L.B. Barbosa, H. Matos, M.J. Noruegas; Coimbra/PT

Purpose: Until now, the range of shear wave values (SWV) of the normal liver, obtained using the ARFI technique, in a pediatric population were not defined. We aimed to define the range of normal values in different age groups and gender evaluating differences resulting from the methodological approach.

Material and Methods: Between July and December 2011, we prospectively evaluated 90 healthy children (54 girls, 36 boys), with an age range of 2 months to 17 years. All studies were performed using the Acuson S2000 equipped with ARFI and SWV quantification. Age, gender, ROI depth, liver lobe were analyzed using different methodological approaches.

Results: Mean SWV value was 1.09±0.18 m/s (0.57 - 1.50 m/s). Significant differences were found between different age groups, respectively: 1.10±0.09 m/s to 0– 6 years; 1.09±0.09 m/s to 6– 12 years and 1.07±0.11 m/s to 12– 17 years. The mean SWV for right lobe was 1.06±0.10 m/s and for left lobe 1.18±0.15 m/s ($p<0.05$). Differences between superficial (1.17m/s) and deeper interrogation (1.10 m/s, 1.07 m/s and 1.02 m/s - with increasing depth) were significant ($p<0.05$).

Conclusion: We found a mean liver SWV value of 1.09±0.18 m/s in a normal pediatric population, ranging between 0.57 and 1.50 m/s. Depth of tissue interrogation and the ROI placement for SWV calculation (right/left lobe) may influence the results. For standardization, we propose that the SWV should be measured at right lobe, avoiding superficial and deep locations.

SS 3.09

Low-voltage CT of the abdomen: to identify cutoff patient diameters for patient selection through the analysis of the correlation between patient diameters and subjective image quality

M.C. Ambrosetti, G.A. Zamboni, F. Lombardo, R. Pozzi Mucelli; Verona/IT

Purpose: To identify cutoff patient diameters optimal for low-voltage scans through the correlation between patient diameters and subjective image quality in low-voltage and standard-voltage CT of the upper abdomen in the same patient population.

Material and Methods: 32 patients underwent MDCT of the abdomen with arterial phase at 80 kV with angular dose modulation on 64-row MDCT (test group). These examinations were compared with a previous 120kV scan on the same scanner. Patient transverse and sagittal diameters were measured at celiac axis level, and the mean was calculated. Two radiologists by consensus graded image quality on a 5-point scale (5=excellent; 1=non-diagnostic; 3 was the chosen cutoff quality). Image quality was correlated to the transverse, sagittal and mean diameter with ANOVA test.

Results: Patient diameters did not change across examinations (all p=ns). In low-voltage scans, image quality was significantly correlated to sagittal ($p=0.034$) and mean diameters ($p=0.025$), and only a trend to significance was observed for transverse diameter ($p=0.053$). In 120 kV scans, there was no significant correlation between image quality and patient diameters, and all patients received grade 4 or 5. In 80 kV scans, a subjective grade 3 corresponded to a transverse diameter of 329 mm and a sagittal diameter of 267 mm.

Conclusion: Patient size appears to influence subjective image quality more in low-voltage scans than in standard-voltage scans. For our protocol, cutoff diameters for diagnostic image quality are transverse 329 mm and sagittal 267 mm.

DOI: 10.1007/s13244-013-0254-8

SS 3.10

Controlled attenuation parameter compared with 1H-MR spectroscopy for liver fat content measurement: a pilot study

J.H. Runge, A.E. Bohte, A.J. Nederveen, U. Beuers, J. Stoker; Amsterdam/NL

Purpose: Recently, a new FibroScan device featuring the controlled attenuation parameter (CAP)-value has been introduced. The CAP-value is a quantitative measure of liver fat content, so far only compared with semi-quantitative steatosis grade at biopsy, with a Spearman's Correlation Coefficient of 0.51 ($p<0.001$). The purpose of this study was to compare CAP-values with quantitative liver fat percentages (LF-%) measured with ^{1}H-MR Spectroscopy (^{1}H-MRS).

Material and Methods: Sixteen patients were included in a study investigating CAP-value and ^{1}H-MRS in viral hepatitis. All patients had CAP and ^{1}H-MRS performed on the same day. MR spectra were measured with a PRESS sequence (TE/TR: 38/3000ms) at 3T MRI and individual T2-correction was performed. Data were described as median (range). CAP-values and LF% were compared using Spearman's correlation coefficient (r_s).

Results: CAP-values and LF% were available in 15/16 patients whose median age and BMI were 51 (22-76) and 24.7 (22.3-31.6), respectively. Median CAP and LF% were 250 (123-328) and 1.6 (0-12.7). Correlation r_s between CAP and LF% was 0.797 ($p<0.001$).

Conclusion: Our CAP results show a higher correlation with ^{1}H-MRS-derived fat percentage as compared with current literature describing correlation of CAP with liver biopsy derived steatosis grade. If this is substantiated in a larger cohort comparing CAP with ^{1}H-MRS, CAP-measurement could be established as a fast, non-invasive and quantitative biomarker of liver fat.

11:00 - 12:30 **Room H3**

Scientific Session 4

Interventional radiology

SS 4.01

Comparison of percutaneous portal vein embolization, portal vein ligation and portal vein occlusion combined with ipsilateral hepatic artery cannula implantation prior to major liver resection

P. Pajor, O. Hahn, I. Dudas, A. Zsirka-Klein, P.K. Kupcsulik; Budapest/HU

Purpose: To evaluate the results of percutaneous portal vein embolisation (PVE), portal vein ligation (PVL) and portal vein ligation combined with hepatic artery chemotherapy (PVL+can) prior to extended hepatectomy.

Material and Methods: Between 2004 and 2012, 140 patients presenting with multiple or large liver malignacies were included. Future liver remnant volume (FLR) of these patients after the planned extended hepatectomy was less than 30% (normal liver), or 40% (cirrhotic liver). To increase the FLR, portal vein occlusion techniques (51 PVE, 89 PVL alone, or PVL combined with hepatic artery cannula implantation into the ipsilateral hepatic artery - PVL+can) were performed. They were evaluated with MDCT including volume assessment, before and 8 weeks after these procedures.

Results: 112/140 patients became resectable (PVE; PVL; PVL+can; 74.3%; 80%; 88.5%). FLR increase 8 weeks after PVE, PVL or PVL+can was 17.6%, 16.5%, 19%, the complication rate of the various portal occlusion techniques were 4.5%, 3.6%, 11.5%, respectively. At least 4 segments were resected during hepatectomy. Overall postoperative morbidity and mortality rates were 13% and 2.5%, respectively. Postoperative complication and mortality rates did not differ significantly in the 3 groups.

Conclusion: Patients with previously unresectable liver tumors can benefit from resection after all kind of portal occlusion techniques. Although complication rate of portal occlusion combined with hepatic artery cannula implantion is higher, more patients become resectable due to higher increase rate of FLR in this group.

SS 4.02

Problem solving and aberrant anatomy in selective internal radiotherapy

D. Mullan, N. Kibriya, H. Laasch, P. Manoharan, J.A. Lawrance; Manchester/UK

Purpose: To discuss the incidence, consequences and outcomes of abnormal arterial anatomy in selective internal radiotherapy (SIRT) for liver metastases.

Material and Methods: 106 patients underwent SIRT work-up angiography between 21/9/5 and 14/6/12 at our institution. Angiograms and post-angiography Tc-99 uptake scans were retrospectively reviewed to record arterial anatomical variants, radio-isotope uptake, and the effect these had on planning and performing treatment. Procedural and periprocedural complications were recorded.

Results: 57/106 patients had abnormal anatomy. 7/106 were deemed unsuitable for SIRT treatment following work-up angiography due to the effects of abnormal anatomy. Chronologically, 4 of these were within the first 19/106 procedures at this institution, suggesting a learning curve when dealing with aberrant vasculature. 51/57 proceeded to treatment. 5/51 required an additional work-up and coil embolisation due to varied anatomy or initial extra-hepatic uptake. 2 patients required a two stage treatment to right and left lobes due to hepatic tumour burden and the risk of radiation hepatitis. 1 patient died prior to treatment.

Conclusion: Abnormal is the new 'normal' when considering hepatic arterial anatomy. Vascular variants will directly influence all cases and can preclude treatment. There appears to be a learning curve involved when dealing with abnormal anatomy, and understanding the effects aberrant anatomy can have will increase the probability that a patient will be deemed suitable for SIRT.

DOI: 10.1007/s13244-013-0254-8

SS 4.03

Hemorrhagic complications after percutaneous radiofrequency ablation of liver tumors: understanding of clinico-radiologic manifestation

J.Y. Lee, J.H. Kim, J.M. Lee, B.I. Choi; Seoul/KR

Purpose: To investigate hemorrhagic complications after percutaneous radiofrequency ablation (RFA) of liver tumors through understanding of its clinico-radiologic manifestation.

Material and Methods: From 2003 to 2012, 2218 patients underwent RFA in our institute. Among them, 19 patients (0.8%) had diverse hemorrhagic complications that were detected at immediate post-RFA 16-channel dynamic MDCT. Angiography was performed in 14 patients (74%) and embolization in 8 patients (42%). Ten patients (53%) were cured with conservative management. The type, location, and CT findings of bleeding, interval between RFA and symptom onset, the relationship between laboratory findings and bleeding to be treated and clinical course were analyzed.

Results: Bleeding sites were intercostal artery (n=4), internal mammary artery (n=5), segmental hepatic artery (n=3), needle entry site of the liver (n=6), and unidentified vessel (n=1). Embolization was performed in 25% of free active leak (2/8), 83% of localized active leak (5/6), none of bleeding without active leak (0/4), and one patient with hemobilia (1/1). The shape of extravasations was curvilinear along the margin of diaphragm or chest wall or irregular in course. The mean interval between RFA and blood pressure drop was 94 minutes (range, 64-165 minutes). All patients except one were successfully treated with embolization or conservative management.

Conclusion: The understanding of clinico-radiologic findings of post-RFA hemorrhagic complications may be helpful to easily detect it and accurately predict its clinical course.

SS 4.04

Safety and efficacy of percutaneous radiofrequency ablation of recurrent colo-rectal cancer liver metastases after hepatectomy

C. Valls, D. Leiva, S. Ruiz, L. Martinez Carnicero, L. Llado, A. Rafecas, E. Ramos; Barcelona/ES

Purpose: To assess the results, complications and clinical role of RFA in the treatment of recurrent colorectal liver metastases.

Material and Methods: Between 2005 and 2012, 59 patients (95 lesions) with colorectal metastases recurrence after surgery, were treated with RFA procedures if resection was not possible or the patient was not fit for surgery. Efficacy of ablation was assessed with CT at 1 month and every 6 months. The mean number of liver tumours per patient was 1.5 and mean tumour diameter was 2.3 cm (range, 0.6-5.8 cm). In 37.5% of the cases, lesions had a subcapsular location and 34% were close to a vascular structure.

Results: The morbidity rate was 18.7 %. Extrahepatic recurrence appeared in 50% of the patients. Local recurrence at the site of ablation appeared in 18% of the lesions. Local recurrence rate was 7% in lesions less than 3 cm and 52% in lesions larger than 3 cm. Actuarial survival rates at 1, 3 and 5 years were 94.5%, 65.3% and 21.7%.

Conclusion: Although our series include a selected population with poor prognosis, overall survival is comparable to surgical series. Local recurrence rate is higher than surgical resection, but it improves significantly in lesions less than 3 cm (7%). In our experience, RFA is an effective treatment in recurrent liver metastases of CRC and could be proposed as first-line treatment in lesions less than 3 cm.

SS 4.05

Trans-arterial embolization through intra-arterial injection of Ethiodol: results and follow up

F. Somma, R. D'Angelo, M. Marracino, R. Grassi, F. Fiore; Naples/IT

Purpose: Hepatocellular carcinoma is nowadays the third leading cause of cancer deaths worldwide, with over 500,000 people affected, while liver metastases are common in a wide range of malignancies, especially in patients with gastrointestinal cancers. A variety of treatment modalities have been reported including resection, transarterial chemoembolization, external irradiation, radiofrequency or ethanol ablation. Our aim is to retrospectively evaluate the efficacy and safety of transarterial embolization of hepatic malignancies using a 1:1 mixture of ethanol and lipiodol (Ethiodol), compared with other procedures.

Material and Methods: 39 patients (30.8% male; 69.2% female; range of age 36-86 years) with documented hepatic lesions of size 1.4 to 5.4 cm were elected to transarterial chemoembolization using a mixture of 50 mg Epirubicin and 5 cc Lipiodol or transarterial embolization using Ethiodol, injected directly in the tumor-feeding arteries after super-selective catheterization, followed by the injection of 70-150 µ polyvinyl-alcohol solution.

Results: Chemoembolization and embolization therapies were performed, respectively, in 19 and 20 patients. 1 month after the procedure, a Multislice Computed Tomography (MSCT) showed in all patients at least partial response to RECIST1.1 and EASL criteria, while in 24 cases, a complete resolution was observed.

Conclusion: Compared to transarterial chemoembolization, the procedure using Ethiodol showed similar radiological outcomes at 1-month MSCT but less toxicity, which makes it useful in patients with more than one lesion or in case of relapse.

SS 4.06

Use of the Fong criteria to predict local recurrence after radiofrequency ablation of colorectal liver metastases: a retrospective review

A. Wale, J. McCall, N. Wijesekera, N. Khan, K. Shahabuddin, G. Brown; Surrey/UK

Purpose: The Fong criteria have been shown to predict outcomes after hepatic resection. We evaluated these criteria in the context of radiofrequency ablation (RFA) of colorectal liver metastases.

Material and Methods: 59 patients with colorectal liver metastases had RFA to 101 colorectal liver metastases between 2005 and 2011.

Results: 52% of lesions (53/101) developed local recurrence at the site of RFA. 60% of local recurrence occurred within the first 3 months after RFA (32/53). On univariate binary logistic regression, the only significant factor which affected local recurrence was the disease-free interval from primary to liver metastases <12 months (OR 4.36, 95% CI 1.45-13.17, p=0.009). The disease free interval from primary to liver metastases <12 months was also the only significant factor which affected local recurrence on multivariate binary logistic regression (OR 3.8, 95% CI 1.21-11.88, p=0.022). The remaining factors (node-positive primary, number of hepatic tumours >1, largest hepatic tumour >5 cm, largest hepatic tumour >3 cm, carcinoembryonic antigen level >200 ng/ml) did not significantly predict for local recurrence in this series. Cox proportional hazards model found no factors were significant predictors of time to progression.

Conclusion: In this small series, disease-free interval from primary to liver metastases <12 months was the only significant predictor of local recurrence. This has implications for patient counselling before RFA as it demonstrates that, as with hepatic resection, metachronous tumours have a better outcome after RFA.

DOI: 10.1007/s13244-013-0254-8

SS 4.07

Management of arterial ammonia level with various interventional approaches

S. Bhatnagar, D. Jain, A. Mukund, S. Thapar, S. Sarin; New Delhi/IN

Purpose: To describe various techniques for reduction/occlusion of the blood flow in gastro-renal/leino renal shunts for controlling the arterial ammonia level causing hepatic encephalopathy and suggesting the best technique according to individual patient needs.

Material and Methods: In 11 patients, different technique of blood flow reduction in shunt was used according to size, shape and position and origin of the shunt. Out of 11 patients, 8 underwent for shunt obliteration, 2 underwent for splenic artery embolisation and 1 underwent for leino renal shunt reduction. For leino renal shunt reduction, a stent (preformed hour glass shape) was deployed in shunt and multiple coils of varying sizes were deployed in the space between stent and shunt wall. For obliteration of shunts, Catheter was positioned deep inside the varix and after inflating the balloon sclerosing agent in the form of foam was infused with the goal of filling the full extent of varices. For reduction of flow in shunt, polyvinyl alcohol particles were infused in lower pole branches of spleen. It causes decrease blood in splenic vein.

Results: 7/8 shunt obliteration, 1/1 shunt reduction and 2/2 partial splenic artery embolisation showed significant reduction in arterial ammonia level.

Conclusion: Ammonia level can be controlled by controlling blood flow through the shunts. Various interventional methods are available and have to select according to the size, shape, and position of shunt.

SS 4.08

Improving outcomes in percutaneous transhepatic biliary intervention – a method for tract closure

S.D. Goode, A. Dale, R. Khan, N. Hersey, R. Peck, F. Lee; Sheffield/UK

Purpose: Percutaneous transhepatic cholangiography (PTC) is an established technique for biliary drainage and stent placement. Recent publication of the UK biliary drainage and stent registry identified very high mortality and complication rates for PTC. The aim of our work was to identify the incidence of post-procedural haemorrhagic complications in patients undergoing PTC and to further assess the impact of using a dedicated liver tract closure method on patient outcomes.

Material and Methods: Retrospective analysis of all patients undergoing PTC between 11/2010 and 06/2011 to identify rates of complications and death. Further analysis was also performed between 07/2011 and 06/2012 after the incorporation of a new dedicated liver tract closure method for PTC was initiated.

Results: Initial dataset included 84 patients between 11/2010 and 06/2011. There was an 9% (n=8) haemorrhage rate and a statistically significant decrease in mean Hb was demonstrated on comparing pre- and post-procedure results (p<0.0001). Following this, we performed dedicated liver tract closure in 105 patients from 07/2011 to 08/2012. The technical success rate for closure was 98%. There was a significant decrease in the rate of haemorrhagic complications in this cohort (9% vs 3%, p=0.05).

Conclusion: Clinically significant post-procedure haemorrhage occurred in 9% of the early cohort study. Following introduction of a dedicated method for liver tract closure following PTC, we had a significant decrease in haemorrhagic complications. We advocate the use of dedicated liver tract closure following PTC to improve outcome for patients undergoing this procedure and to decrease haemorrhagic complications.

SS 4.09

Intratumoral gas in hepatocellular carcinoma following transarterial chemoembolization: factors associated and clinical implications

M. Ronot, D. Bisseret, M. Abdel Rehim, A. Sibert, M. Bouattour, L. Castera, V. Vilgrain; Clichy/FR

Purpose: To determine the frequency and factors associated with the presence of intratumoral gas-containing areas in HCC on CT obtained 4-6 weeks after TACE.

Material and Methods: From June 2010 to December 2011, all patients undergoing TACE for HCC were included. Presence of intratumoral gas was assessed on CT obtained 4-6 weeks after TACE. Clinical and biological data as well as tumoral and TACE procedure characteristics were noted. Factors associated with the presence of intratumoral gas were tested. Tumor response was assessed using the EASL criteria. Comparison between tumors containing gas and no gas was performed by uni- and multivariate analysis.

Results: 201 patients (mean age: 66, M/F 171/30, BCLC A/B 18/82%, Child A/B 81/19%) with 497 tumors underwent 286 TACE procedures. Intratumoral gas was found in 26 tumors (5%) after 26 TACE procedures (9.1%) in 26 patients (13%). Gas was related to abscess formation in only 3 of them (11.5%). On multivariate analysis, large tumor volume at baseline (P=0.003), TACE using drug eluting-Beads (P=0.033) and selective/superselective approach (P=0.024) were factors independently associated with the presence of gas. Tumors showing gas-containing areas at one month had a significantly higher response rate than those without (P<0.0001).

Conclusion: Intratumoral gas-containing areas after TACE are rarely related to abscess formation. Presence of intratumoral gas on CT obtained 4-6 weeks after TACE could be a surrogate marker for marked tumor necrosis.

SS 4.10

Interventional endovascular treatment of acute non-variceal gastrointestinal bleeding through emergency transcatheter arterial embolization

E. Bozzi, P. Scalise, F. Calcagni, A. Mantarro, F. Turini, I. Bargellini, R. Cioni, C. Bartolozzi; Pisa/IT

Purpose: To retrospectively assess the efficacy and the incidence of ischemic complications in a series of patients who underwent transcatheter arterial embolization (TAE) for the management of acute non-variceal gastrointestinal (GI) bleeding.

Material and Methods: Between January 2009 and October 2012, 32 patients underwent emergency TAE for acute GI hemorrhage. Indications for endovascular management were massive bleeding, hemodynamic compromise, patient's unsuitability to surgery, bleeding refractory to endoscopic treatment or recurrent after surgery. In all cases, abdominal contrast-enhanced Computed Tomography (CT) examination was performed to precisely localize the source of bleeding. All patients underwent diagnostic angiography with 5Fr-catheter and superselective catheterism with 3Fr-microcatheter to identify the presence of active bleeding.

Results: The commonest causes of bleeding were malignancies (n=10) and previous surgery (n=10); pancreaticoduodenal arteries were the culprit vessels in 71.8% of cases. The most commonly used embolic agents were metallic coils+gelatin sponge (n=13). Primary technical success rate was 78.1%; a second procedure was required in 7 cases (mean-time 3.1 days) with a total technical success rate of 30/32 patients (93.7%). Bowel ischemic complications occurred in 4 cases (mean-time 6.75 days).

Conclusion: In patients with both upper and lower acute non-variceal GI hemorrhage, TAE is a safe and effective procedure to obtain a rapid control of bleeding.

DOI: 10.1007/s13244-013-0254-8

SS 4.11

Outcomes following radiofrequency ablation of colorectal cancer liver metastases

A. Wale, J. McCall, N. Wijesekera, N. Khan, K. Shahabuddin, G. Brown; Surrey/UK

Purpose: The aim of this study was to determine survival outcomes according to radiofrequency ablation (RFA) treatment intent in patients with colorectal liver metastases.

Material and Methods: A total of 59 patients with colorectal liver metastases underwent their first RFA procedure between 2005 and 2010. 21 patients underwent RFA as a curative procedure, 16 patients underwent RFA as a holding procedure before hepatic resection and 22 patients underwent RFA as a palliative procedure.

Results: The median Kaplan-Meier survival for all patients was 25 months after first RFA treatment. Log Rank test showed survival was significantly different according to treatment intent; patients who underwent RFA as a holding procedure before hepatic resection had improved survival over those who underwent RFA with curative intent, who in turn had improved survival over those who underwent RFA with palliative intent (47 v 38 v 17 months, p <0.001).

Conclusion: Increasingly, RFA is performed as a holding procedure before resection and to reduce the burden of disease in patients with palliative disease. This study demonstrates that patients do best if RFA is used as an adjuvant treatment prior to hepatic resection, but demonstrates that patients undergoing RFA with curative intent do less well than those undergoing hepatic resection.

11:00 - 12:30 **Room H2**

Scientific Session 5

Challenging situations in abdominal imaging

SS 5.01

Diagnostic accuracy of MRI in diagnosing deep infiltrating endometriosis involving bowel, ureters and ligaments: comparison to laparoscopy

A. Murtaza[1], S. Tirumani[2], J. Ryan[2], S. Singh[2], M.A. Fraser-Hill[2], N. Fasih[2]; [1]Lahore/PK, [2]Ottawa, ON/CA

Purpose: To compare the diagnostic accuracy of MRI versus laparoscopy for identification of deep pelvic endometriosis, its involvement in urinary tract and bowel.

Material and Methods: This retrospective, HIPPA compliant study included 100 patients with clinical suspicion of endometriosis who underwent laparoscopy between 2005 and 2011. Their randomized MRI scans were retrospectively evaluated by two radiologists blinded to previous imaging and clinical details. Imaging and surgical findings were correlated for concordance.

Results: For bowel involvement, MRI detected 54 patients (5 false positives). Specificity, sensitivity, negative and positive predictive values were calculated at 88.3%, 87.5%, 90.7% and 82.6%, respectively with accuracy of MRI in detecting presence or absence of bowel involvement being 87%. For ureteric involvement, MRI detected 23 cases (1 false positive). Specificity, sensitivity, PPV and NPV of 98.5%, 70.9%, 95.6% and 88.1%, respectively, with accuracy of 89%. For pelvic ligaments, MRI detected 62 patients (12 false positives). Specificity, sensitivity, PPV and NPV of 73.9%, 92.5%, 80.6% and 89.4% with accuracy of 84%. Using kappa statistics, inter-observer concordance was calculated. No statistically significant variation was observed between the two readers, with p values < 0.0001 for all three variables.

Conclusion: MRI is a useful tool for the evaluation of deep pelvic endometriosis and can potentially guide treatment planning and laparoscopy. Further prospective studies on a larger scale will be beneficial for evaluating individual site-specific involvement of endometriosis.

SS 5.02

Using oral contrast: is it really necessary for the diagnosis of acute appendicitis with MDCT?

K. Hekimoglu, M. Coskun, C. Tarhan, E. Akar, U.M. Yildirim, T. Tezcaner; Ankara/TR

Purpose: To compare the diagnostic performance of IV and oral contrast-enhanced MDCT versus only IV contrast-enhanced MDCT in patients with acute appendicitis.

Material and Methods: 200 adult patients that suggested acute appendicitis were enrolled this research. Group 1 was composed of patients with combined oral and IV contrast-enhanced abdominal MDCT, and Group 2 was consisted of only IV contrast-enhanced MDCT patients. Images were evaluated by two radiologists. Acute appendicitis diagnosed with a five point Likert scale. Exact diagnosis of acute appendicitis was considered only when patients underwent surgical operation. For patients whom did not undergo an operation, medical follow-up data of patients were undertaken by another researcher. Kappa statistical analysis was planned for interobserver agreement. ROC curves were created for comparing two groups with the results of two radiologists. Sensitivity, specificity, positive predictive value, and negative predictive value were also evaluated.

Results: In ROC curves, AUCs were calculated for two readers, the values for Gp1 were 0.97 and 0.96. For Gp2, both were 0.99. There were no statistically significant differences between two readers in the AUC values in each group and no significant difference in sensitivity or specificity for the diagnosis of acute appendicitis.

Conclusion: Oral contrast do not contribute to the a better accuracy. However, in selected patients, oral contrast-added MDCT imaging may be helpful for the diagnosis of acute apendicitis.

DOI: 10.1007/s13244-013-0254-8

SS 5.03

Intraoperative contrast-enhanced ultrasound and color-coded elastography for characterization of liver lesion before surgical resection

J. Rennert, C. Stroszczynski, E. Jung; Regensburg/DE

Purpose: To evaluate if IO-CEUS and CCE allow a differentiation between malignant and benign liver lesions in comparison to histopathology.

Material and Methods: Retrospective evaluation of digitally stored intraoperative CEUS and elastography. IO-CEUS and CCE of 49 liver lesions were compared to histopathology following surgical resection. Examinations were performed using a multifrequency linear probe (6-9 MHz). CEUS was evaluated during the arterial, the portal venous and the late-venous phase. Characterization of the CCE quality using cine-loops >10 s, based upon a color-coding system. Semi-quantitative evaluation of the lesions' stiffness based upon a specified scaling of 0-6 (0 low up to 6 high) using 6 ROIs (1 central, 5 peripheral).

Results: Lesion diameter from 7 to 54 mm. All 44 malignant lesions (13 HCCs, 8 CCCs, 23 metastases) displayed a washout. 3 lesions that could not be characterized by IO-CEUS and CCE, a thrombosed hemangioma, a granuloma and a fibrosis. Two lesions were correctly diagnosed as complicated cysts using IO-CEUS. Sensitivity of IO-CEUS was 90%, PPV was 100%, NPV 40% and accuracy was 94%. Using CCE, malignant lesions were found to be inhomogenous, only partially indurated in 12 lesions, with a scaling of 5. In 8/49 lesions, only central indurations were visible (scaling 4-6). Sensitivity of the CCE was 65%. PPV was 94%, NPV 20% and accuracy was 71%.

Conclusion: Only IO-CEUS offers clear benefits for characterization of liver lesions.

SS 5.04

Diagnostic value of CT enteroclysis in small bowel pathologies

L.M.F. Tee, K.C.H. Lau, A.Y.H. Tsang, S. Lau, S. Chiu; Hong Kong/HK

Purpose: To assess the diagnostic value of CT enteroclysis (CTE) in evaluating symptomatic patients for small bowel pathologies, using surgical, endoscopic, histological or clinical follow-up findings as reference standards.

Material and Methods: At our local institution, during 2010 Nov to 2012 Oct, 104 consecutive patients underwent CT enteroclysis for evaluation of small bowel pathologies. The CTE findings were retrospectively reviewed and compared with surgical, endoscopic, histological or clinical follow-up outcomes as reference standards.

Results: CTE findings were positive in 17 patients and negative in 87 patients. 3/17 positive cases were lost to follow up and thus excluded. Positive cases were compared with histologic proof after operation or endoscopy. Negative cases were followed up clinically and radiologically. Overall sensitivity, specificity, PPV, NPV were 100%, 98.9%, 92.9% and 100%, respectively. There were 7 cases of Crohn's disease, 3 cases of gastrointestinal stromal tumour (GIST), 2 cases of Peutz-Jegher syndrome and 1 case of tuberculous ileitis. In addition, extra-enteric findings were found in 60 patients, a number of which may account for the symptoms or had an implication on management.

Conclusion: CT enteroclysis is an excellent diagnostic tool in the evaluation of small bowel pathologies, which, at the same time, can provide invaluable information on extra-enteric lesions.

SS 5.05

Dynamic MRI pelvis for investigation of persistent groin pain and inguinal herniation: a promising new technique

A. Patel, M. Denunzio, M.K. Lingam, R. Singh; Derby/UK

Purpose: Historically, groin ultrasound and herniography have been performed to investigate persistent groin pain, often with variable sensitivity and specificity. Herniography is also associated with risks of infection and bowel injury. Dynamic MRI is a new technique which shows promising results.

Material and Methods: Retrospective review of dynamic MRI performed following equivocal clinical examination and/or indeterminate ultrasound and herniography. Imaging was acquired using 1.5T Philips Achieva in relaxed phases and during Valsalva manoeuvre. MRI protocol included T2 high-resolution sagittal series, axial balanced fast field echo (BFFE) relaxed/straining, oblique BFFE relaxed/straining on affected side. Dataset included patient demographics, clinical indication, correlation with prior imaging, characterisation of herniae and other significant findings.

Results: Sample size = 65 patients. Mean age was 49.6 years (95% CI 45.1 to 54.2). Clinical indications included persistent groin pain, previous surgery and indeterminate swelling. 35 patients had prior ultrasound and/or herniography. Inguinal herniation was detected in 38/65 patients (58.4%), bilateral in 9 patients. In 95%, the hernial sac contained intra-abdominal fat only. In all positive studies, herniation was more prominent during straining. 9 patients (24%) only demonstrated herniation on straining phases. 5 patients (7.7%) revealed femoral herniation and 4 patients (6.2%) demonstrated osteitis pubis and adductor longus muscle strain.

Conclusion: Dynamic MRI is a promising non-invasive alternative to standard ultrasound and herniography. High-resolution MRI can accurately diagnose osteitis pubis and adductor muscle strain, thereby avoiding unnecessary surgical exploration.

SS 5.06

Radiologist secretarial errors: nonclinical errors using voice recognition software for radiology reports in oncological abdominal CT

M. Twomey, J. Sammon, F. Moloney, M. Breen, M. Maher; Cork/IE

Purpose: The purpose of this study is to evaluate error rates when using a voice recognition (VR) dictation system, to identify if there is a reduction in error rates over time with familiarity, and to assess if dual reading reduces errors.

Material and Methods: A total of 350 finalised reports of CT studies for abdominal oncological follow up performed between June 2008 and December 2012 were randomly selected for analysis in this study. Reports were individually scrutinized for errors which were divided into two categories: (1) significant but unlikely to alter patient management and (2) very significant with the meaning of the report affected, thus potentially negatively affecting patient management.

Results: 12% of the selected reports contained errors. In subgroup analysis, this fell from 14% in 2008 to 6% in 2012. 3% of reports contained errors that could significantly alter patient management. 60% of errors in reports occurred in dual reader studies. Two thirds of reports containing errors occurred when the report was finalised between 16:00 and 18:00 hrs.

Conclusion: Whilst there are many benefits to VR systems, there are also many pitfalls. By raising awareness of the learning curve related to error rates for radiology departments using VR lessons will be learnt. This is important in the context of ever-increasing demand on abdominal CT imaging workflow and for preventing potential detriment to our patients as a result of non-clinical errors.

DOI: 10.1007/s13244-013-0254-8

SS 5.07

Value of cardiophrenic angle lymph nodes for the diagnosis of colorectal peritoneal carcinomatosis

C. Caramella, E. Pottier, I. Borget, D. Malka, D. Goere, M. Ducreux, D. Elias, C. Dromain; Villejuif/FR

Purpose: The radiological diagnosis of peritoneal carcinomatosis (PC) is challenging. Cardiophrenic angle lymph nodes (CPALN) have been reported in patients with abdominopelvic malignancies. We aimed to assess whether CPALN detected by computed tomography (CT) scan are associated with PC in patients with colorectal cancer (CRC).

Material and Methods: Between 2007 and 2011, 550 patients with CRC, including 165 (30%) with PC, underwent abdominal surgery. We retrospectively reviewed preoperative CT-scans for the presence of CPALN, and assessed the association of CPALN with surgically confirmed PC by univariate and multivariate analyses.

Results: CPALN were present in 123 (75%) of the 165 patients with PC, but absent in 263 (68%) of the 385 patients without PC (sensitivity, 0.72; specificity, 0.68; PPV, 0.49; NPV, 0.85; odds ratio [OR], 3.3; $p<0.001$). PC was the only factor found independently associated with CPALN in multivariate analyses. The presence of CPALN was not correlated with liver or lung metastases. Among the 165 patients with PC, 99 (62%) had visible signs of PC on CT-scan; among the remaining 66 patients, CPALN were the only potential sign of CP in 41 (62%), leading to Se, Sp, PPV, and NPV in patients with no signs of CP (other than CPALN) on CT of 0.62, 0.68, 0.24, and 0.92, respectively.

Conclusion: The detection of CPALN on CT may be of valuable help for the diagnosis of PC in patients with CRC.

SS 5.08

First in-human MR-visualisation of surgical mesh implants for inguinal hernia treatment

N.L. Hansen, A. Barabasch, M. Distelmaier, A. Ciritsis, N. Kuehnert, J. Otto, J. Conze, U. Klinge, C.K. Kuhl, N.A. Kraemer; Aachen/DE

Purpose: This study evaluates the MR-conspicuity of iron-loaded mesh implants in patients treated for inguinal hernia.

Material and Methods: A prospective study with thirteen patients receiving an iron-loaded mesh implant via laparoscopic (TAPP, n=8) or open (Lichtenstein, n=5) surgery was performed between March and September 2012. The study was approved by the local ethics committee. MRI was conducted on the first postoperative day at a 1.5T scanner using three conventional gradient echo (GRE1-3) and one T2-weighted turbospin echo (TSE) sequences. Three radiologists independently assessed the following criteria using a 4-point-scale: visual contrast-to-noise ratio, conspicuity to air artifacts, and diagnostic quality rating with respect to the mesh and to the surrounding anatomy. In addition, mesh's crease formation and localisation in relation to the hernia were rated. Wilcoxon signed-rank test was used for statistical analysis.

Results: All GRE sequences facilitated a good delineation of the mesh implant. GRE1 was rated best (3.6, $p<0.05$) for diagnostic quality with respect to the mesh whereas both GRE2 and GRE3 were suited best for evaluation of mesh localisation in respect to the hernia (3.3, $p<0.05$). TSE was preferred for evaluation of the anatomy (3.8, $p<0.05$) but insufficient in mesh delineation.

Conclusion: Using a combination of different MRI sequences, iron-loaded mesh implants can be clearly visualised for localization and configuration after hernia repair. Their use could help to identify mesh-related problems and reduce the need for surgical revision.

SS 5.09

Withdrawn by the authors

SS 5.10

Mesenteric panniculitis is not a paraneoplastic phenomenon

Ö. Gögebakan, M.A. Osterhoff, A. Reimann, T. Albrecht; Berlin/DE

Purpose: Mesenteric panniculitis (MP) is an underdiagnosed inflammatory condition of mesenteric adipose tissue. Previous studies suggested that MP is associated with malignancy. In order to reassess this hypothesis, we performed the first-matched case-control study comparing the prevalence of malignancy and other disease in patients with PM versus controls.

Material and Methods: By keyword search from our RIS database, we identified patients with MP undergoing abdominal CT between 2010 and 2012. For each patient with a MP, two control patients matched for age, gender, abdominal diameter and CT protocol were chosen from the same database. The diagnosis MP was independently confirmed by two readers according to established criteria. Concomitant disease was recorded for MP patients and controls.

Results: A total of 13485 patients underwent abdominal CT in the study period; MP was diagnosed in 77 patients (prevalence 0.58%). There was a male predominance (3.3:1). 50.6% of the patients with MP had a malignancy, while the rate of malignancy was 60.2% in the control group ($p \leq 0.157$; Fisher's exact test). There was also no difference in the rate of other frequently encountered concomitant diseases, such as arterial hypertension, diabetes, previous surgery, cholecystolithiasis or raised CRP between the two groups.

Conclusion: Contrary to previous reports, our matched case control study suggests that MP is not a paraneoplastic phenomenon and is also not associated with other disease.

DOI: 10.1007/s13244-013-0254-8

11:00 - 12:30 **Auditorium**

Scientific Session 6

Imaging of pancreatic neoplams

SS 6.01

Radiopathological correlation in T4 pancreatic cancer: prognostic implications

C. Cappelli, R. Cervelli, S. Mazzeo, D. Campani, U. Boggi, C. Bartolozzi; Pisa/IT

Purpose: To discuss the correlation between CT and pathology in T4 pancreatic cancer.

Material and Methods: 31 arteries (6 celiac axis, 10 hepatic arteries, 8 splenic arteries-SA, 7 superior mesenteric artery), resected in 17 patients were analyzed. The relationship between tumor and artery was graded as: 0, no contact; I, focal contiguity; II, tumor surrounding partially (a) or completely (b) the artery; III tumor surrounding (a) or (b) the vessel with lumen reduction. For each artery, the contact length with the tumor was reported. The neural plexus (NP) and celiac ganglia (CG) involvement was graded with a score between 1 and 3.

Results: At CT, 1 resected artery was graded as 0, 2 as I, 17 as IIa, 3 as IIb, 5 as IIIa and 3 as IIIb (all SA). At pathology, none of 0, I and IIa arteries was infiltrated, irrespective to the NP and CG score. Adventitial infiltration was identified in 2 IIb, 2IIIa and all IIIb arteries. Arterial infiltration was significantly related to CG involvement (p=0.014), while no correlation with NP grading was found (p=0.37). No correlation with survival existed considering arterial infiltration (p=0.66), while significance (p=0.0097) was reached considering CG involvement.

Conclusion: Radiological T4 poorly correlates with pathology. Current CT-grading system should be revised because of the structural differences between arteries and veins, and the key role of CG involvement in predicting arterial infiltration and prognosis.

SS 6.02

Does arterial encasement on CT always mean vascular invasion at surgery in pancreatic cancer and what is the cause of false-positivity in assessment of unresectability?

V.I. Egorov, R.V. Petrov, E. Solodinina, G. Karmazanovsky, N. Starostina, N.M. Kurushkina; Moscow/RU

Purpose: Indication of pancreatic cancer (PC) unresectability is the superior mesenteric (SMA) and celiac artery (CA) encasement, signaling arterial invasion. Computed tomography (CT) is the gold standard for PC detection and its resectability evaluation.

Material and Methods: Preoperative radiology data were compared with findings at 51 standard, 58 extended, 17 total pancreaticoduodenectomies (PDs), 9 distal resections with CA excision (DPCA) and 28 palliative bypasses for PC. Survival of 11 patients with controversial data of CT and EUS in regard to arterial invasion, after R0/R1 procedures, was compared to survival of 8 patients after R2 resection (Group B) and of 12 patients with locally advanced cancer after bypass surgery (Group C).

Results: CT showed peripancreatic arteries' encasement in 11 cases. In all cases an operative exploration was performed, basing on equivocal yield of endoUS, and no invasion of the arterial wall was revealed. The 1-year survival in Group A was 88.9%, 2-year – 26.7% with 22-month median follow-up. One-year survival was not attained in Groups B and C. Survival difference between groups was significant (Pa-b = 0.0029,Pb-c = 0.003)

Conclusion: Peripancreatic arterial encasement on CT does not necessarily signify arterial wall invasion, which means that PC can still be radically removed. Whenever PC is considered unresectable endoUS should be used; without recourse to an extended pancreatectomy with skeletalisation of the SMA and CA, PC resectability cannot be reliably appraised based on CT data.

SS 6.03

Different lobar distribution of liver metastases based on the site of primary pancreatic carcinoma

M.C. Ambrosetti, G.A. Zamboni, F. Lombardo, R. Pozzi Mucelli; Verona/IT

Purpose: To investigate whether the different site of pancreatic adenocarcinoma affects the lobar distribution of metastases in the liver.

Material and Methods: From all the patients who underwent MDCT for first staging of pancreatic adenocarcinoma, we selected 51 consecutive patients (26 Males, 25 Females; mean age 60 years) with pathological proven liver metastases. 23 patients had a tumor in the head (Group A) and 28 in the body-tail (Group B). We analyzed site, diameter and vascular invasion of the pancreatic adenocarcinoma and number of metastases in each lobe of the liver using Cantlie's line. Total number of metastases was compared between the two groups with unpaired t-test while Fisher's test was used to compare the number of metastases in the two lobes.

Results: As expected, the number of liver metastases was significantly higher in group B than in group A ($p<0.05$). The ratio of metastases in the right and left lobes was 6.5:1 for group A compared to 3.3:1 for group B (p=0.0018).

Conclusion: Although liver metastases are more numerous in the right than in the left lobe in both groups, there is a significant difference in the ratio of metastases between the right and the left hemiliver. This can support the existence of a "fast track" to the left liver lobe when the carcinoma invades the splenic vein, and may help in detection of liver metastases.

SS 6.04

Diagnostic performance of MRI for important prognostic factors in pancreatic cancer

J.H. Kim, H.W. Eun, J.M. Lee, J.K. Han, B.I. Choi; Seoul/KR

Purpose: Tumor size, T-stage, N-stage, vascular invasion, and cell differentiation are most important prognostic factors in pancreatic cancer. To investigate diagnostic accuracy of MR for determining these factors.

Material and Methods: 41 patients with resectable pancreatic cancer who underwent preoperative MR were included in this study. We measured tumor size on different MR sequences. Two radiologists retrospectively accessed T-stage, N-stage, vascular invasion. They also accessed MR findings including SI on T2WI, enhancement patterns, duct dilation, presence of diffusion restriction, and ADC values. Each MR finding was used to compare these prognostic factors. Statistical analyses were performed using ROC analysis, McNemar test, and paired t test.

Results: All pancreatic cancers were detected on FS GRE T1WI. Tumor size on FS GRE T1WI and DWI was closest to pathological size without difference ($p>0.05$). Diagnostic accuracy for T-stage was 92.6 and 95.1% with moderate agreement ($\kappa=0.41$). Accuracy for N-stage was 70.7 and 65.8% with moderate agreement ($\kappa=0.576$). Accuracy for peripancreatic invasion, bile duct invasion, and duodenal invasion were 88 and 93%, 90 and 93%, 83 and 83% with almost perfect agreement. Accuracy for determining vascular invasion was 92%. MR findings were not different according to T-stage, N-stage, cell differentiation, and gross pattern.

Conclusion: MR is useful for preoperative evaluation of tumor size, T-stage, and vascular invasion, but it has limitation for N-metastasis. However, each MR finding is not different according to T-stage, N-stage, cell differentiation, and gross pattern.

DOI: 10.1007/s13244-013-0254-8

SS 6.05

Value of MDCT angiography in predicting R0 resectability of pancreatic adenocarcinoma

G.A. Zamboni, M.C. Ambrosetti, F. Lombardo, G. Malleo, R. Pozzi Mucelli; Verona/IT

Purpose: To assess the value of MDCT in the preoperative staging of pancreatic adenocarcinoma, with special regard to predicting R0 resectability.
Material and Methods: We reviewed in this retrospective study the images from the CT scans performed on 154 consecutive patients who underwent MDCT angiography at our institution for diagnosis and/or preoperative staging of pancreatic carcinoma. The diagnosis of pancreatic adenocarcinoma was confirmed at pathology in all patients. Imaging findings were compared with surgical reports, pathology reports and patient follow up. Sensitivity, specificity, positive predictive value (PPV) and negative predictive value (NPV) for overall resectability and for R0 resectability were calculated with Fisher's test.
Results: Patient population included 88 males and 66 females (mean age 63.8 years, range 37-81). 52 patients underwent resection while 102 underwent palliative procedures because of unresectability. According to MDCT criteria, 66 patients were potentially resectable and 88 nonresectable. When analyzing all the performed resections, CT for the prediction of resectability had 92.3% sensitivity, 82.4% specificity, 72.7% PPV and 95.5% NPV. When only R0 resections were considered as true positives, CT had 93.1% sensitivity, 68.8% specificity, 40.9% PPV and 97.7% NPV.
Conclusion: The value of MDCT in predicting overall resectability is well known, and our results are in line with those presented in the literature. For patient outcome, however, R0 resectability might be a more important parameter: MDCT appears to be of value also in this assessment.

SS 6.06

MRI of pancreatic adenocarcinoma including diffusion-weighted imaging: assessment of tumour conspicuity and pathologic correlation

L. Legrand, V. Duchatelle, V. Molinié, I. Boulay-Coletta, E. Sibileau, M. Zins; Paris/FR

Purpose: To identify the best MR sequences for pancreatic adenocarcinoma conspicuity and to determine whether MR signal and apparent diffusion coefficient (ADC) correlate with pathological findings.
Material and Methods: Twenty-two consecutive patients with pancreatic adenocarcinoma who underwent MRI (1.5 or 3T) before surgical resection were included. Fat-suppressed (FS) T1 and T2-weighted sequences, 3D FS dynamic T1-weighted gadolinium-enhanced gradient-echo (GRE) during arterial, portal and delayed phases, and diffusion-weighted imaging (DWI) with b values of 600-800 s/mm^2 were obtained. Lesion conspicuity was assessed on each sequence qualitatively (three-point rating scale) and quantitatively (tumour-to-proximal and distal pancreas contrast), and compared using paired Wilcoxon tests. Histological characteristics were correlated with MRI features.
Results: 95% of pancreatic adenocarcinomas were hypointense on 3D FS T1 GRE arterial phase, which was the best sequence for tumour conspicuity ($p \leq 0.02$). DWI was not useful for delineating 25% of tumours. Maximum diameter at pathological examination was 33±10 mm. It was best correlated with MR tumour size on DWI. Progressive enhancement curve was associated with extensive and dense fibrous stroma ($p \leq 0.03$). No correlation was found between ADC (mean value: 1.76×10^{-3} mm^2/s) and differentiation, fibrosis or necrosis.
Conclusion: 3D FS T1 GRE arterial phase sequence is superior to DWI for pancreatic adenocarcinoma conspicuity but it underestimates the size of the tumour. DWI could be the best sequence for size evaluation when the tumour is correctly delineated.

SS 6.07

MDCT features of pancreatic adenocarcinoma before and after chemotherapy: do they change? Do they affect interobserver agreement?

G.A. Zamboni, M.C. Ambrosetti, F. Lombardo, R. Pozzi Mucelli; Verona/IT

Purpose: To compare the MDCT features of pancreatic adenocarcinoma before and after chemotherapy, and to assess the effect on interobserver agreement.
Material and Methods: Two readers reviewed independently the MDCT scans performed before and after gemcitabine chemotherapy on 31 patients with advanced pancreatic cancer, assessing tumor margins, density, necrosis, infiltration of peripancreatic fat and vessels, liver metastases, ascites and carcinosis. Post-treatment tumor changes were analyzed with Student and Mann-Whitney tests, interobserver agreement was calculated with kappa statistics.
Results: 16/31 patients had stable disease, 15/31 disease progression. Tumor size, margins, homogeneity, necrosis, conspicuity, adipose tissue infiltration, presence of liver metastases, ascites or carcinosis were not significantly changed post-treatment (all p=n.s). A significant increase was observed post-treatment in main duct caliber (7mm vs 6mm) and lymphnode size (16.8 mm vs 12.6 mm). Post-treatment, venous invasion increased in 8/31, decreased in 1/31 and remained stable in 22/31 patients. Arterial invasion increased in 9/31, decreased in 2/31 and was stable in 20/31 patients. Interobserver agreement did not change post-treatment for tumor homogeneity, presence of necrosis, adipose tissue infiltration or carcinosis (all good agreement), and ascites (very good agreement). Interobserver agreement decreased for tumor margins (from good to moderate) and liver metastases (from perfect to good).
Conclusion: Post-chemotherapy, the CT features of pancreatic adenocarcinoma do not appear to change significantly; interobserver agreement decreases for tumor margin evaluation and for liver metastases, possibly as an effect of treatment.

SS 6.08

Solid and pseudopapillary tumours of the pancreas: are the epidemiology and imaging features changing?

M.-P. Vullierme, G. Goujon, J. Cros, V. Vilgrain; Clichy/FR

Purpose: Solid and pseudopapillary tumours (SPT) are rare pancreatic tumours known to be large in size and affecting young women. Due to the trends in imaging methods, their presentation of may have changed over the past years, individualising new aspects. We retrospectively revisit the epidemiologic and radiological features in a series of patients with resected SPT.
Material and Methods: 36 patients (28 women, 8 men), median age 30 years (14-57) underwent surgery between 2002 and 2011. The diagnosis of pancreatic tumour was suspected following non-specific abdominal pain (n=24) or fortuitously (n=12). It was located in the head (n=19), the neck (n=10) or the body/tail (n=7). All patients underwent CT scan, MRI and EUS. In doubtful cases, EUS-biopsy or somatostatin-receptors scintigraphy (SRS) were performed in 12 and 6 patients, respectively.
Results: In 9 cases (25%), there was a differential diagnosis with a neuroendocrine tumour (NET) (n=6) or a mucinous cystadenoma (n=3), underlying two atypical patterns, a solid well-circumscribed lesion pattern, and a purely cystic pattern some with large shell-like calcifications. A peripheral fibrous capsule was present in 22 cases (61%) and this pattern was not described with other cystic and solid lesion.
Conclusion: This series suggests that the presentation of SPT has changed with half of patients aged >30 years and/or with small solid lesions (<3 cm), 1/3 male. Atypical imaging features (entirely cystic or NET-like lesions) can be encountered as well.

DOI: 10.1007/s13244-013-0254-8

SS 6.09

Complications after major pancreatic surgery: MDCT features

F. Lombardo, G.A. Zamboni, M.C. Ambrosetti, R. Pozzi Mucelli; Verona/IT

Purpose: To review the MDCT features of complications after major pancreatic surgery for pancreatic tumors.

Material and Methods: We reviewed 50 consecutive emergency MDCT scans performed after major pancreatic surgery. Patient population included 22 Females and 28 Males, mean age 61.8 years. Surgeries included 37 pancreatico-duodenectomies, 1 total pancreatectomy, 4 intermediate resections, 2 enucleations and 6 distal pancreatectomies. The resected tumors at pathology included 25 adenocarcinomas, 11 endocrine tumors, 2 mucinous tumors, 2 serous cystoadenomas, 6 intraductal papillary mucinous neoplasms, 2 duodenal GISTs, 1 solid-pseudopapillary tumor and 1 mesenchimal tumor.

Results: Mean interval between surgery and CT was 6.8 days. The pancreatic remnant was normal in 39/50 cases and atrophic in 11/50 cases. The complications included 12 anastomotic leakages, 25 fluid collections, 5 bleedings/hematomas, 8 free peritoneal fluid. 11/12 anastomotic leakages involved the pancreatic anastomosis. In 8/12 cases of leakage, the pancreatic remnant was normal while in 4 cases, it was atrophic. Fluid collections were hypoattenuating in 40 cases, hyperattenuating in 5 cases and mixed in 5 cases. Free air was seen in all cases of anastomotic leakage and in 10/25 cases with fluid collections.

Conclusion: Complications after major pancreatic surgery are not uncommon, even in high-volume referral centers, and range from small amounts of free fluid to anastomotic leakage or hemorrhage. Complications appear to be more common in patients with a normal pancreas than in those with atrophic parenchyma.

SS 6.10

Diagnostic performance of MR for pancreatic neuroendocrine tumor according to the WHO classification compared with the TNM stage

J.H. Kim, H.W. Eun, J.M. Lee, J.Y. Lee, J.K. Han, B.I. Choi; Seoul/KR

Purpose: According to WHO 2010 classification, pancreatic neuroendocrine tumor (PNET) was classified as NETG1, NETG2, and NEC. Our study investigates diagnostic performance of MR for PNET according to WHO 2010 classification compared with TNM stage.

Material and Methods: Our study consisted of 39 patients with surgically proven PNET (NETG1; n=24, NETG2; n=12, NEC; n=3) who underwent preoperative MRI. Two radiologists retrospectively reviewed MR findings including margin, SI on T2WI, enhancement patterns, degenerative change, presence of diffusion restriction, duct dilation, and ADC value. They also assessed T-stage, N-stage, and tumor size. Statistical analyses were performed using Chi-square tests, ROC analysis, and Fisher's exact test.

Results: Statistically specific findings for NEC were ill-defined borders (p=0.001) and hypo-SI on venous- and delayed-phase (p=0.016). ADC value showed significant difference between G1 and G2 (p=0.007). Az of ADC value for differentiating G1 from G2 was 0.743. Tumor size on MR was not different from pathologic size (p=0.452). Accuracy for T-staging was 77 and 85%, and for N-staging was 92 and 87% with substantial agreement (κ=0.78, κ=0.79). T-stage showed significant difference according to tumor grade (p<0.001), although there was no significant difference in tumor size (p=0.252) or N-stage (p=0.565).

Conclusion: Ill-defined borders and hypo-SI on venous- and delayed-phase are common findings of NEC, and ADC value is helpful for differentiating G1 from G2. MR is useful for the evaluation of T-stage, N-stage, and tumor size, and T-stage showed significant difference according to tumor grade.

11:00 - 12:30 **Room J**

Scientific Session 7

Detection and management of focal liver lesions in the non-cirrhotic liver

SS 7.01

Preoperative evaluation of colorectal liver metastases after chemotherapy: a combined approach of diffusion-weighted imaging with b-multiple SE-EPI and Gd-EOB-DTPA MR sequences at 3T

F. Donati, P. Boraschi, L. Urbani, G. Gherarducci, F. Pacciardi, M.C. Della Pina, R. Gigoni, G. Masi, F. Falaschi, C. Bartolozzi; Pisa/IT

Purpose: To compare diffusion-weighted imaging (DWI) with b-multiple SE-EPI and Gd-EOB-DTPA MR sequences alone and in combination at 3T-device for detecting colorectal liver metastases in patients previously undergone preoperative chemotherapy.

Material and Methods: Twenty patients with colorectal cancer and focal liver lesions underwent MR imaging at 3T-device (GE DISCOVERY MR750;GE Healthcare) after preoperative chemotherapy. Three images sets were reviewed by two observers in conference: (1) DWI using a spin-echo echo-planar sequence with multiple b values (150, 500, 1000, 1500 s/mm^2); (2) Gd-EOB-DTPA Lava-flex sequence including both dynamic and hepato-biliary phase; (3) combined DWI and Gd-EOB-DTPA images. The MRI findings were correlated with surgery and histopathology, which was our gold standard. Only clear benign lesions at intraoperative ultrasound remained unresected. Statistical analysis was performed on a per-lesion basis.

Results: A total of 146 lesions were detected; of these, 106 were metastases (72.6%), whereas the remaining 40 (27.4%) were characterized as benign lesions (cysts and hemangiomas). Image set 1 correctly identified 92 out of 106 metastases (sensitivity 86.7%, specificity 50%, diagnostic accuracy 76.7%), image set 2 correctly detected 98 out of 106 metastases (sensitivity 92.4%, specificity 70%, diagnostic accuracy 86.3%), and image set 3 correctly diagnosed 104 out of 106 metastases (sensitivity 98.1%, specificity 95%, diagnostic accuracy 97.2%). Differences were statistically significant (p<0.001).

Conclusion: DWI in combination with Gd-EOB-DTPA sequences at 3T-device significantly increases the diagnostic performance of MRI in detecting preoperative colorectal liver metastases.

SS 7.02

Growth of colorectal liver metastases in the embolized and non-embolized liver after portal vein embolization

M. Ronot, R. Pommier, F. Cauchy, S. Gaujoux, M. Abdel Rehim, A. Sibert, V. Paradis, S. Faivre, J. Belghiti, V. Vilgrain; Clichy/FR

Purpose: To compare tumor progression in both embolized and non-embolized lobes after portal vein embolization (PVE) in patients with bilobar colorectal liver metastases (CLM).

Material and Methods: From 2002 to 2012, 42 consecutive patients displaying initially unresectable bilobar CLM and undergoing right PVE to achieve resectability after chemotherapy downstaging (median 12 cycles) were included. Before PVE, all patients had at least one lesion in the future non-embolized lobe. Right and left livers tumoral and non-tumoral volumes as well as volume variations were measured on CT before and after PVE. Influence of neoadjuvant and post-PVE chemotherapy (n=26) on tumor growth was assessed.

Results: After a median of 34 days (28-37) following PVE, the median right liver volume decreased 17% (P<0.0001), while left liver volume increased 32% (P<0.0001). A tumoral volume increase was observed in both embolized and non-embolized lobes in 25 (60%) patients. Right and left tumoral volumes had a significant median increase of 48% (P<0.0001) and 31% (P<0.0001), respectively. After PVE, increases in right and left tumoral volume were correlated (r=0.54, p=0.0004). In both livers, tumor growth was not significantly reduced in patients who received chemotherapy after PVE (right liver, p=0.21; left liver, p=0.86).

Conclusion: Tumor growth after PVE can be observed in both embolized and non-embolized liver lobes and is not influenced by post-PVE chemotherapy.

DOI: 10.1007/s13244-013-0254-8

SS 7.03

Performance of gadoxetic acid-enhanced MRI for the differentiation of FNH and HCA: a single centre experience

C.M. Perez Fernandez, T. Denecke, I.G. Steffen, D. Seehofer, I. Kramme, B. Hamm, C. Grieser; Berlin/DE

Purpose: Evaluation of enhancement characteristics of focal nodular hyperplasia (FNHs) and hepatocellular adenomas (HCAs) with gadoxetic acid-enhanced magnetic resonance imaging (MRI).

Material and Methods: Eighty-six patients who underwent MRI at 1.5 T were retrospectively included. Examination protocol contained: T1-in- and opposed phase; T2-weighted UTSE and fat-saturated T1-weighted (WATS; LAVA) with and without contrast media (Gd-EOB-DTPA; arterial, portal venous, venous and hepatobiliary phase. Standard of reference was surgical resection (n=53) or biopsy (n=15) available for 114 lesions. All cases were read by two independent radiologists in consensus. Lesion intensity was visually compared with the intensity of the surrounding liver parenchyma. Furthermore, relative signal intensity (SI) values (%) in contrast to native SI-values were recorded for the different contrast phases.

Results: 114 lesions (FNHs, n=44; HCAs, n=70) were evaluated. On unenhanced MRI, presence of fat (P<0.001; accuracy=54%), haemorrhage (P=0.071; accuracy=57%) and "wash-out'' were indicative for HCA (P<0.001; accuracy=63%), whereas presence of a central scar was indicative for FNH (P<0.001; accuracy=85%). Regarding signal intensities on hepatobiliary phase images, an iso-/hyperintense appearance of FNHs and hypointensity of HCAs were the best discriminators between both entities (P<0.001; acc=92%).

Conclusion: An iso-/hyperintensity of FNHs and hypointensity of HCAs on hepatobiliary phase images are highly accurate discriminators between both entities. In case of conclusive findings of FNH on gadoxetic-enhanced MRI, biopsy may be dispensable.

SS 7.04

Differentiating hepatic abscess from malignant mimickers: the value of diffusion-weighted imaging with an emphasis on the periphery of the lesion

H.J. Park, S.H. Kim, K.M. Jang, M.J. Park, S.J. Lee, D. Choi; Seoul/KR

Purpose: To evaluate the efficacy of diffusion-weighted imaging (DWI) in differentiating hepatic abscess from malignant mimickers with an emphasis on periphery of the lesions.

Material and Methods: 39 patients with hepatic abscess and 74 patients with malignant hepatic tumors were included. Patients underwent gadoxetic acid-enhanced 3T conventional MRI and DWI. For qualitative and quantitative analysis, signal intensity and ADC values of periphery of the lesions on MRI and DWI with ADC maps were assessed. Two observers independently reviewed the DWI and ADC maps and rated them using 5-point scale. Diagnostic performance was evaluated using ROC curve analysis. Accuracy, sensitivity, specificity, PPV and NPV were calculated.

Results: Periphery of hepatic abscesses showed T1-hypointense, arterial hyperintense and hypointense on hepatobiliary phase less frequently than that of malignant tumors (P<0.05). No hepatic abscesses showed peripheral washout on 3-min late phase compared to malignant tumors (59.5%) (P<0.001). Both groups showed a hyperintense rim on DWI, but 37 (94.9%) abscesses revealed a hyperintense rim on the ADC map compared to one (1.4%) malignant tumor (P<0.001). Mean ADC value of abscesses was significantly higher than that of malignancies. Diagnostic performance (area under the ROC curve [Az]) of DWI in identifying hepatic abscess was 0.986 and 0.982 in each observer. Interobserver agreement was excellent.

Conclusion: In addition to conventional MRI, DWI is helpful in differentiating hepatic abscess from malignant mimickers.

SS 7.05

Detection of liver metastases in patients with adenocarcinomas of the gastrointestinal tract: comparison of [18F]FDG-PET-CT and MRI

C. Maegerlein, A.A. Fingerle, M. Souvatzoglou, E.J. Rummeny, K. Holzapfel; Munich/DE

Purpose: To compare the diagnostic performance of [18F]FDG-PET-CT and MRI in the detection of liver metastases in patients with adenocarcinomas of the gastrointestinal tract.

Material and Methods: Thirty-four patients with adenocarcinomas of the gastrointestinal tract who had undergone [18F]FDG-PET-CT and MRI of the liver within a maximum interval of 4 weeks were included in this study. The MRI protocol included diffusion-weighted imaging (DWI) and dynamic contrast-enhanced imaging after intravenous application of Gd-DTPA using a VIBE (volume interpolated breathhold examination) sequence. Images were acquired in the arterial, portal venous and equilibrium phase. Two datasets (PET-CT and MRI) were analyzed by a blinded reader with a time interval of 4 weeks between both datasets. Imaging results were correlated with histopathologic findings or results of follow-up imaging studies. Sensitivities of both modalities in the detection of liver metastases were compared using the Mann Whitney U-Test.

Results: A total of 94 metastases were confirmed in 34 patients. Sensitivity of MRI in detecting metastases was 91.2% and was significantly higher than that of PET-CT (77.0%; p<0.001). Regarding metastases with a diameter of ≤10 mm, the difference was even more pronounced with sensitivities of 71.4% (MRI) and 16.7% (PET-CT; p<0.0001).

Conclusion: MRI including diffusion-weighted imaging and dynamic contrast-enhanced imaging is significantly superior to PET-CT in detecting liver metastases in patients with adenocarcinomas of the gastrointestinal tract, especially in detecting metastases ≤10mm.

SS 7.06

Whole liver ADC histogram analysis in patients with liver metastases from rectal cancer

N. Papanikolaou[1], D. Lambregts[2], A. Nikiforaki[1], M.H. Martens[2], D. Mondal[3], L.A. Heijnen[2], G.L. Beets[2], R. Beets-Tan[2]; [1]Vasilika Vouton/GR, [2]Maastricht/NL, [3]Oxford/UK

Purpose: ADC measurements have been proposed to characterize focal liver lesions in the basis of restricted diffusion pattern due to hypercellularity. The aim of this study was to explore whether whole liver ADC histogram metrics may be used to differentiate between patients with colorectal liver metastasis and controls with no liver disease.

Material and Methods: Ten patients with colorectal liver metastasis and 10 controls with no focal or diffuse liver disease were included. Whole liver segmentation was performed on ADC maps and a corresponding histogram was generated. In addition, quantitative histogram metrics were calculated and compared between the patients and normal controls. P-value <0.05 was considered statistically significant.

Results: Mean ADC value of patient group was significantly lower than that of normal controls ($0.958x10^{-3}$ and $1.22x10^{-3}$, respectively, p<0.05), while both skewness and kurtosis were not significantly different (p=0.176 and p=0.056, respectively). In the patient group mode, 5% percentile and 95% percentile were significantly lower to the normal controls ($0.936x10^{-3}$ and $1.140x10^{-3}$, p<0.001, $0.475x10^{-3}$ and $0.7x10^{-3}$, p<0.05, $1.466x10^{-3}$ and $1.833x10^{-3}$, p<0.05).

Conclusion: Whole liver histogram ADC analysis revealed a significant shift towards lower ADC values in patients with colorectal liver metastasis compared to controls without liver disease. These results show that ADC histogram analysis could be a promising tool for detecting occult colorectal liver metastasis.

DOI: 10.1007/s13244-013-0254-8

SS 7.07

Evaluation of radiological prognostic factors of hepatic metastases in patients with non-functional pancreatic neuroendocrine tumors

A.D.J. Baur, C.M. Perez Fernandez, C. Ihm, I.G. Steffen, E. Tischer, R. Arsenic, M. Pavel, T. Denecke; Berlin/DE

Purpose: In non-functional well to moderately differentiated (G1 and G2) pancreatic neuroendocrine tumors (pNET) with irresectable hepatic metastases, watchful waiting until tumor progression is a well-established approach. Treatment with somatostatin analogues (SSA) is optional. Goal of this study was to identify radiological prognostic factors predicting rapid tumor progression.

Material and Methods: In 44 patients, we retrospectively evaluated features of hepatic metastases on contrast-enhanced multiphase CT and MR imaging including contrast enhancement, presence of necrosis and macrovascular infiltration as well as number of metastases and tumor burden. These features were correlated with time to tumor progression (TTP) according to RECIST 1.0.

Results: In the initial patient cohort, none of the evaluated parameters was found to be a statistically significant predictor of TTP. This patient cohort included 14 patients who had received treatment with SSA. Since treatment with SSA was associated with an increased TTP (p=0.01), we also analyzed a subgroup of 30 patients without any antitumoral therapy. In this subgroup of patients, hypoenhancement of hepatic metastases during early contrast phases was found to be an independent prognostic factor predicting rapid tumor progression (p=0.018).

Conclusion: Hypovascularization of hepatic metastases from G1 and G2 pNET reflected by hypoenhancement during the early contrast phases seems to be associated with rapid tumor progression. In patients with hypoenhancing metastases, early initiation of antitumoral therapy as well as repeated biopsy for grading of these metastases should be considered.

SS 7.08

The preoperative assessment of hepatic tumours: evaluation of UK regional multidisciplinary team performance

M.G. Wiggans, E.M. Armstrong, D.A. Stell, S. Jackson; Plymouth/UK

Purpose: In the UK, all patients where liver resection is contemplated are discussed at hepatobiliary multi-disciplinary team (MDT) meetings. The Peninsula HPB unit is a tertiary referral facility in the South-West of England. Our aim was to assess MDT performance by identification of patients where radiological and final pathological diagnoses differed.

Material and Methods: A prospective database of cases has been maintained since the inception of the unit. The presumed diagnosis as a result of radiological investigation and MDT discussion is recorded at the time of surgery. Imaging was reviewed by specialist gastrointestinal radiologists and results agreed by consensus. A review of patients undergoing surgery from Mar 2006 to Jan 2012 was performed.

Results: We identified 417 patients who underwent hepatic resection. There was a significant increase in the use of preoperative imaging modalities ($p \leq 0.01$) but no change in the rate of discrepant diagnosis over time. 42 individuals were identified whose final histological diagnosis differed to the outcome of the MDT discussion (9.6%). These included 30% of patients diagnosed pre-operatively with hepatocellular carcinomas and 25% diagnosed with cholangiocarcinoma of a major hepatic duct.

Conclusion: The highest rate of discrepancies occurred in patients with focal liver lesions without a history of chronic liver disease or primary cancer, where hepatoma was over-diagnosed during MDT discussion and peripheral cholangiocarcinoma under-diagnosed. Additional care should be taken in these groups and high-quality preoperative multi-modality imaging considered.

SS 7.09

Importance of arterial phase CT imaging for detection and management of liver metastasis

F. Willemssen, S. Van Koeverden, G. Krestin, R.S. Dwarkasing; Rotterdam/NL

Purpose: To evaluate the arterial phase imaging for detection of liver metastasis and the effect on therapeutic management.

Material and Methods: From January until December 2008, patients with histological proven colorectal or breast carcinoma, who underwent a CT examination in both arterial and portal-venous phase were included. Contrast material used was 120-150 ml iodixanol 320 mgI/ml (Visipaque, GE Healthcare Inc, Cork, Ireland), injection rate 3-3.5cc/s. Arterial phase was acquired at 30 s, the portal-venous phase at 70 s. All CT examinations were evaluated in the portal-venous phase and compared to portal-venous and arterial phase. Difference in number of metastases was assessed. Follow-up CT examinations (3-30 months) were used to evaluate the aetiology of detected lesions. Change over time of a lesion was defined as metastasis.

Results: In this retrospective cohort follow-up study, 317 patients were included. 74 (23.5%) patients were excluded, because no follow-up was available. In 171 (54.3%) patients, there was neither difference in the number of metastases detected in both phases, nor new lesions developed. 72 (22.9%) patients developed new metastasis during follow-up. In 17 (23.6%) patients of this group, additional metastases were detected due to arterial phase imaging. Management would have changed in only 1 (1.4%) patient.

Conclusion: Combined arterial and portal-venous phase CT-imaging allows detection of additional metastases in patients with colorectal and breast carcinoma. However, therapeutic consequences related to higher number of detected liver metastases is extremely low.

SS 7.10

Differential findings between hepatic adenoma and focal nodular hyperplasia at DWI and hepatobiliary imaging

N. Al Ansari, V. De Marco, V. Buonocore, F. Mazzamurro, F. Maccioni; Rome/IT

Purpose: To characterize imaging features of hepatic adenoma (HA), confirmed at follow-up imaging, as well as radiologically proven focal nodular hyperplasia (FNH) using delayed hepatobiliary MR imaging with gadoxetic acid and DWI.

Material and Methods: 20 patients with radiologically proven HAs were retrospectively analyzed on liver MRI studies performed with gadoxetic acid and imaging acquired during the delayed hepatobiliary phase. 25 patients with radiologically diagnosed FNH lesions were identified. Only patients with non-cirrhotic liver were evaluated. Two readers, blinded to the clinical information and the radiological diagnosis, reviewed all images in terms of signal intensity (SI) features on dynamic, and hepatobiliary phase images. Signal intensity ratios relative to adjacent liver were measured on selected imaging sequences. Agreement between the 2 observers was evaluated with kappa statistic.

Results: All 20 HA (100%) demonstrated hypointensity relative to adjacent liver on delayed imaging whereas FNH were either hyperintense (70%) or isointense (30%) relative to the adjacent liver on delayed imaging. None of the FNHs was hypointense relative to liver. Interobserver agreement was excellent (k=1). On the other hand, DWI signal was not significantly different between HA and FNH.

Conclusion: HA and FNH showed distinct imaging characteristics on delayed gadoxetic acid-enhanced MRI, whilst DWI was not effective in differentiating these lesions. The use of gadoxetic acid-enhanced MR imaging with hepatobiliary phase images plays a primary role in the differentiation of FNH from HA.

DOI: 10.1007/s13244-013-0254-8

11:00 - 12:30 **Room F**

Scientific Session 8

Imaging of inflammatory small bowel diseases

SS 8.01

A technique for global small bowel motility assessment using dynamic MRI

A. Menys[1], A. Plumb[1], S.A. Taylor[1], A. Ahmed[1], A. Alam[1], F. Odille[2], A. Emmanuel[1], S. Halligan[1], D. Atkinson[1]; [1]London/UK, [2]Nancy/FR

Purpose: To develop an MRI-based index of small-bowel motility, test its repeatability in human volunteers and to test its ability to detect changes induced by pharmacological challenge.

Material and Methods: 20 healthy volunteers (mean age 28, 13 male) underwent baseline cine MRI utilising 3D Balanced Turbo Field Echo to capture small bowel motility in 15 cm volume blocks over a 20-s breath hold. A randomised blinded, placebo-controlled cross-over study of either 0.5 mg Neostigmine or saline (n=10) or 20 mg IV Butylscopolamine or saline (n=10) was performed with motility MRI at baseline and repeated at mean 4 weeks (range 2-7). Two readers drew regions of interest around small bowel independently, and motility was quantified using a registration algorithm that provided a global motility metric in arbitrary units (AU). Repeatability of mean baseline AU was assessed using Bland Altman (BA) and within-subject coefficient of variation (wCV). Changes in mean AU following drug administration was compared to placebo using paired t-testing.

Results: Repeatability between baseline measurements of motility was high; BA mean difference -0.0025, range 0.28 to 0.4, 95% Limits of Agreement at ±0.044AU and wCV of 4.9%. Measured motility following neostigmine (mean 0.39AU) was significantly higher than placebo (mean 0.34AU), $p<0.001$, whilst that following Butylscopolamine (mean 0.13AU) was significantly less than placebo (mean 0.30AU) $p<0.001$.

Conclusion: MRI-generated software-quantified small bowel motility in healthy volunteers is repeatable and sensitive to changes induced by pharmacological manipulation.

SS 8.02

Validation of dynamic contrast-enhanced and diffusion-weighted imaging for quantitative Crohn's disease assessment based on histologic characterization

J.A.W. Tielbeek[1], M. Ziech[1], Z. Li[2], C. Lavini[1], S. Bipat[1], W. Bemelman[1], J. Roelofs[1], C.Y. Ponsioen[1], F. Vos[2], J. Stoker[1]; [1]Amsterdam/NL, [2]Delft/NL

Purpose: To prospectively compare conventional MRI, dynamic contrast-enhanced (DCE)-MRI and diffusion-weighted imaging (DWI) sequences to histopathology of surgical specimens in Crohn's disease (CD).

Material and Methods: 3T MR enterography was performed in 25 consecutive CD patients scheduled for surgery within 4 weeks. Features such as mural thickness, T1 signal ratio and T2 signal ratio were determined; ROI's were drawn on DCE-MRI for maximum enhancement (ME), initial slope of increase (ISI), time to peak (TTP) and on DWI for apparent diffusion coefficient (ADC). All were compared with location matched-histopathologic grading of acute inflammation score (AIS) and fibrostenosis score (FS) by Spearman correlation, Kruskal Wallis and Mann-Whitney test.

Results: Twenty patients (mean age 38 years, range 21-73, 12 females) were included and 50 bowel locations were matched to AIS and FS. Mural thickness, T1 signal ratio, T2 signal ratio, ME and ISI correlated significantly to AIS ($r = 0.634, 0.392, 0.485, 0.520, 0.510$, respectively, all $p<0.05$). Mural thickness, T1 signal ratio, T2 signal ratio, ME and ISI differed significantly between the grades of FS ($p<0.001$, $p=0.001$, $p=0.021$, $p=0.005$ and $p=0.020$, respectively). ADC values differed significantly between the non-fibrotic sections and the fibrotic sections ($p=0.023$).

Conclusion: Quantitative parameters from conventional, DCE-MRI and DWI sequences correlate significantly to histopathologic scores of surgical specimens. DCE-MRI and DWI give comparable results but do not outperform conventional MRI parameters.

SS 8.03

Diffusion-weighted MRI enterography: assessment of Crohn's disease activity

A. Centola, E. Cleopazzo, C. Bristogiannis, P. Milillo, L.P. Stoppino, R. Vinci, L. Macarini; Foggia/IT

Purpose: To investigate the diagnostic accuracy of diffusion-weighted MRI (DW-MRI) in Crohn's disease (CD) activity by differentiating acute, chronic and remission stage, evaluating the changes in apparent diffusion coefficient (ADC) values.

Material and Methods: 50 patients (mean age: 22-69) with histological diagnosis of CD underwent a magnetic resonance enterography (MR-E) including dynamic contrast-enhanced MRI on a 1.5T MR unit. Before i.v. contrast agent administration, we acquired DWI sequence with b values 0 and 800 mm-2. We used 1.5 x 10^{-3} mm^2/s as cut-off value to distinguish active from chronic disease and 2.0 x 10^{-3} mm^2/s to distinguish chronic to inactive disease.

Results: We analysed a total of 298 segments. DWI identified active disease in 54 bowel segments, chronic disease in 12, and inactive disease in the remaining 116. The sensitivity, specificity, accuracy, PPV, NPV were 84.3%, 94,8%, 93%, 81,8%, 95,7%, respectively. In the quantitative assessment, ADC values in the disease-active area were lower than those in chronic-disease and inactive areas (1.47 ± 0.34 x 10^{-3} mm^2/s, 1.67 ± 0.42 x 10^{-3} mm^2/s and 2.46 ± 0.47 x 10^{-3} mm^2/s, respectively).

Conclusion: DWI allows the detection of CD active affected segments. Qualitative and quantitative analysis is a useful tool for follow-up and post-treatment assessment. Further studies are necessary to assess the role of ADC values in long-term post-therapy follow-up.

SS 8.04

Automated evaluation of bowel motility in patients with Crohn's disease by development of a colour coding algorithm for cine MRI

M.L. Hahnemann, F. Nensa, S. Kinner, G. Gerken, T.C. Lauenstein; Essen/DE

Purpose: There are only few studies using cine MRI to consider bowel motion disorders in Crohn's disease. Furthermore, this method lacks an objective view and reproducible quantification of bowel motility. The aim of this study was to establish an automated algorithm for visualizing and quantifying bowel motion disorders in Crohn's disease by cine MRI.

Material and Methods: Twenty patients with suspected or diagnosed Crohn's disease underwent MR examination on a 1.5T scanner (Avanto, Siemens). In addition to the standard MRI bowel protocol, coronal T2-weighted cine MR images were acquired with a temporal resolution of 7.5s continuously over a time span of 150s. After affine 2D respiratory motion correction, bowel motility was estimated from cine MRI using an optical flow algorithm. The resulting motion vector magnitudes were color coded into bowel motility maps.

Results: Increased or decreased bowel movement visualized by intuitive heat mapping within the cine MRI allows for detecting segments of abnormal bowel motility. The different colors were defined by abnormally increased or decreased peristaltic motion compared with adjacent bowel. Particularly, inflamed bowel segments exhibited a decreased motility.

Conclusion: Bowel motilities highlighted by different colors within the T2w cine MRI is a feasible and promising new approach for detecting bowel motility disorders in Crohn's disease. In future, this method may be useful to identify pathological conditions or abnormalities of bowel segments with only subtle signs of inflammation on static images.

DOI: 10.1007/s13244-013-0254-8

SS 8.05

MR enterography for planning fluoroscopically assisted endoscopic balloon dilatation in small bowel Crohn's strictures

E.M. Thomson, J. Hamlin, H. Lambie, N. Mohammed, F. Majeed, R. Hyland, D.J.M. Tolan; Leeds/UK

Purpose: Intestinal strictures are a complication of Crohn's disease (CD). While surgical treatment was standard management, endoscopic dilatation offers an attractive alternative. We set out to (1) determine the correlation of MR enterography (MRE) with endoscopic findings in intestinal strictures complicating CD and whether MRE can select patients for dilatation treatment and (2) evaluate our experience and success of fluoroscopically assisted endoscopic dilatation.
Material and Methods: Retrospective review of patients undergoing balloon dilatation for CD-related strictures. All had undergone MRE prior to dilatation procedures. Outcomes evaluated were correlation of MRE and endoscopy findings; endoscopic success (able to traverse the stricture endoscopically after dilatation); clinical success (symptomatic improvement); and complications both immediate and longer term including the need for escalation of medical therapy, further dilatation or surgical intervention.
Results: 65 dilatations were performed in 37 patients with a median age of 47 years. Median follow-up period was 21 months. MRE findings correlated with endoscopic findings in 30/37 (81%) of cases. Endoscopic success was seen in 34/37 (91%) and clinical success in 32/37(86%) of cases. 1 patient (3%) developed perforation following dilatation.
Conclusion: MRE findings correlate well with endoscopic findings and can be used effectively to help plan dilatation. Fluoroscopic screening helps to avoid surgery by facilitating safe and effective dilatation of CD-related strictures with good endoscopic and clinical success rates.

SS 8.06

Specific features of pediatric Crohn's disease detected at MRE

N. Al Ansari, F. Mazzamurro, R. Giovannone, V. De Marco, F. Maccioni; Rome/IT

Purpose: To retrospectively describe Crohn's disease (CD) in paediatric patients (PP) in terms of the location and activity of intestinal lesions.
Material and Methods: 70 children (mean age 15 years) with proven CD underwent magnetic resonance enterography (MRE), after the administration of negative or biphasic contrast agent, according to age and compliance of the patients, to localize lesions and to detect their activity in 9 segments of the small and large bowel. The results were analyzed on a per patient and per segment basis. Ileo-colonoscopy was performed in all patients.
Results: Involvement of terminal ileum was observed in 60% of PP. The colon was diseased in 87% of PP. In particular, left colonic segments were significantly involved in PP (descending colon 58%; rectum 68%, sigmoid colon 58%). The maximal disease activity was found in the left colonic segments.
Conclusion: MRE detected significant features of CD in PP, showing a more extensive and severe involvement of the left colon than distal ileum, differently from adult patients. The causes of the severe left colonic disease in children are unknown and may have relevant clinical-diagnostic implications.

SS 8.07

The accuracy of CT enterography in the diagnosis of terminal ileal disease: a retrospective analysis

T. Mistry, G. Bhatnagar, E. Lemoniati, H.S. Sidhu, R. Ilangovan, S. Thomas-Gibson, M. Marshall; Harrow/UK

Purpose: CT enterography (CTE) is reported to have high sensitivity and specificity for diagnosing Crohn's disease. Due at least in part to the lack of a gold standard examination for small bowel disease, there is little high-quality published data relating to the earliest signs of mucosal disease. We examine the accuracy of CTE for terminal ileitis in comparison to terminal ileoscopy (TI).
Material and Methods: CTE and TI findings were reviewed in patients attending St Mark's hospital between June 2011 and May 2012. Discrepant cases were re-evaluated by 3 independent GI radiologists blinded to the prior CTE and TI report.
Results: 36 patients underwent CTE and TI (mean interval 7 days). Prevalence, sensitivity, specificity, PPV and NPV for terminal ileitis on CTE were 36% (95%CI 21%-54%), 69% (95%CI 39-90%), 83% (95%CI 60-94%), 69% (95%CI 39-90%), 83% (95%CI 60-94%), respectively. Re-evaluation of discrepant cases demonstrated fair to moderate inter-observer correlation (kappa values 0.3-0.5 (Landis & Koch 1977)) between the three readers with mildly improved accuracy.
Conclusion: CTE is an important diagnostic tool in Crohn's disease. However, identification of early inflammation is challenging. We demonstrate that not all radiographic signs reported to depict inflammation are reliable in accurately diagnosing terminal ileitis. Furthermore, we demonstrate significant variation in interpretation between expert readers. We recommend further studies to demonstrate correlation between radiological signs on CTE and pathology.

SS 8.08

Low-dose abdominopelvic CT in active Crohn's disease: image quality and diagnostic accuracy with model-based iterative reconstruction

S.B. O'Neill, L. Crush, K.N. O'Regan, O.J. O'Connor, M. Maher; Cork/IE

Purpose: We designed a prospective, intra-individual study to determine the feasibility and diagnostic accuracy of low-dose CT (LD-CT) reconstructed with model-based iterative reconstruction (MBIR) in the setting of active Crohn's disease (CD). We compare the diagnostic performance of LD-CT with MBIR with synchronously acquired conventional dose CT (CD-CT).
Material and Methods: CD-CT and LD-CT datasets were acquired in 34 consecutive patients with active CD. LD-CT images were reconstructed with MBIR, 40% and 70% adaptive statistical iterative reconstruction (ASIR). Image quality parameters were subjectively scored and image noise was objectively measured. LD-CT images were clinically interpreted by 2 radiologists in random order with interpretation of the CD-CT images after a 6-week delay.
Results: Mean ED was 1.27±0.87 mSv for LD-CT compared with 4.8±2.99 mSv for CD-CT. Reconstructing LD-CT images with MBIR resulted in a significant decrease in mean objective noise when compared with ASIR-40 and ASIR-70 images ($p<0.001$). No acute complication of CD was missed on the LD-CT MBIR images with excellent statistical agreement between the findings identified on LD-CT MBIR and CD-CT images ($k= 0.871$). There was also substantial inter-rater agreement with LD-CT MBIR interpretations ($k=0.715$).
Conclusion: Abdominopelvic CT at doses close to 1 mSv reconstructed with MBIR detected all acute complications in patients with active CD. This protocol has potential to effect substantial cumulative effective dose reductions in this cohort.

DOI: 10.1007/s13244-013-0254-8

SS 8.09

Pilot study to assess the diagnostic performance of MRI in the identification of adhesions between the abdominal wall and small bowel loops, using a time efficient protocol

G. Bhatnagar, R. Tandon, A. Hansmann, P. Lung, H.S. Sidhu, R. Ilangovan, M. Marshall, A. Gupta; Harrow/UK

Purpose: Abdominal adhesions following surgery are the commonest cause of small bowel obstruction. Accurate identification of adhesions has been reported using MR fluoroscopy sequences. We report our results utilising a time efficient protocol.

Material and Methods: 10 patients scheduled for open colorectal surgery and who had undergone previous abdominal surgery were recruited over 4 months (mean age 44; range 29-59). The abdomen was divided into 9 segments prior to MR and surgery enabling accurate correlation. Using a 1.5T scanner (Siemens Avanto), T2 sagittal, axial, sagittal true-FISP 30s cine sequences were obtained in inspiration, expiration and abdominal strain within 8 min. Adhesions were identified by consensus following independent analysis from 4 readers and compared to laparotomy (the gold standard).

Results: Of 90 abdominal segments, adhesions were identified in 44% at laparotomy and 34% on consensus MR opinion. 31 segments demonstrated adhesions on MR; 74% (95% CI 64%-83%) correlated at surgery, whilst the remainder was found in adjacent segments (26%). Sensitivity, specificity, PPV and NPV were 60% (95% CI 43%-75%), 86% (95% CI 73%-94%), 77% (95% CI 59%-90%) and 73% (95% CI 60%-84%), respectively.

Conclusion: Our results suggest utilisation of a time-efficient MR protocol in identifying adhesions between the bowel and anterior abdominal wall is feasible, and may represent a non-invasive application in the research of adhesion-preventative techniques. Reader performance rose during our study and further improvements may be realised in a larger trial.

SS 8.10

Comparison of magnetic resonance enterography and small bowel follow through in intestinal tuberculosis

N. Kalra, J.S. Krishna, P. Singh, R. Kochhar, R. Gupta, R. Singh, N. Khandelwal; Chandigarh/IN

Purpose: To compare magnetic resonance enterography (MRE) and small bowel follow through (SBFT) in intestinal tuberculosis.

Material and Methods: 30 consecutive patients who presented with clinical and radiologic suspicion of intestinal tuberculosis were enrolled in this prospective study. MRE and SBFT were done within 2 weeks of each other. The imaging findings were evaluated by two radiologists who were blinded to each other. 19 of the 30 patients were finally diagnosed as tuberculosis. The remaining 11 patients were either normal (n=6) or had alternate diagnoses (n=5).

Results: Out of the 19 patients with tuberculosis, 9 patients had ileocaecal junction involvement which was detected by both MRE and SBFT. Strictures in jejunum and ileum were seen in 7 of the 19 patients by both these imaging techniques. However, MRE detected more strictures (n=34) compared to SBFT (n=23). MRE also showed segmental mild mural thickening in 6 patients out of which only one could be demonstrated on SBFT. MRE detected extraenteric findings like lymphadenopathy (n=17), ascites (n=5), peritoneal involvement (n=6), splenic granuloma (n=1) and spondylodiscitis (n=1). Overall MRE had higher sensitivity and specificity for diagnosis of tuberculosis (100%, 95% confidence interval, CI: 1.000-1.000 and 72.73%, 95% CI: 0.464-0.990, respectively) compared to SBFT (88.23%, 95% CI: 0.729-1.036 and 70%, 95% CI: 0.416-0.984, respectively).

Conclusion: MRE is an alternative to SBFT and has the potential to become a one-stop imaging technique for intestinal tuberculosis.

11:00 - 12:30 **Room H3**

Scientific Session 9

Diffuse liver diseases

SS 9.01

Shear wave elastography for liver stiffness measurement in clinical ultrasound examination: evaluation of intraobserver reproducibility, technical failure and unreliable stiffness measurement

J.H. Yoon, J.M. Lee, J.K. Han, B.I. Choi; Seoul/KR

Purpose: To evaluate technical failure, unreliable stiffness measurement and intraobserver reproducibility of shear wave elastography (SWE) in assessing liver stiffness (LS) during clinical ultrasound (US) examinations.

Material and Methods: This retrospective study was approved by our institutional review board, and informed consent was waived. 423 patients who underwent abdominal US including SWE were enrolled in this study. SWE was performed by using a convex probe. In each patient, two sessions of SWE were carried in the liver right lobe, five times a session. Technical failure was defined when no or little signal was obtained in the SWE box for all acquisitions, and unreliable results of SWE was determined as coefficient of variant (CV) exceeds 25%. Intraobserver agreement was assessed by intraclass correlation coefficient (ICC) and 95% Bland-Altman limits of agreement.

Results: Technical failure occurred in 35 patients (8.3%). Unreliable measurements occurred in 58 patients (13.7%). Among the reliably measured 330 cases, there was no significant difference of median LS values between the two sessions (6.8 kPa vs. 6.7 kPa; p >0.05). CVs of the 1st and 2nd sessions were 15.6±6% and 16±5.92%, respectively. The overall intraobserver reproducibility was excellent (ICC=0.97). The 95% limit of agreement between the repeated SWE measurements was 2.88 kPa and -2.56 kPa.

Conclusion: SWE using median LS value seems to be a reproducible noninvasive method, although relatively large CV of SWE necessitates multiple LS measurements.

SS 9.02

First intention-to-diagnose comparison of ARFI and Fibroscan in chronic liver diseases

V. Cartier, D. Bardou, J. Boursier, J. Lebigot, S. Michalak, I. Fouchard, C. Aube; Angers/FR

Purpose: To compare ARFI and Fibroscan in an intention-to-diagnose (ITD) basis for the non-invasive diagnosis of liver fibrosis.

Material and Methods: 219 consecutive patients with chronic liver disease and biopsy were included. Liver stiffness measurements were performed by ARFI (right lobe: ARFI-D, left lobe: ARFI-G) and Fibroscan (right lobe). ARFI-DG corresponded to the median value of all valid measurements obtained in both lobes. Reference for fibrosis was Metavir F staging. Diagnostic accuracy was evaluated using AUROC and Obuchowski index (adjusted AUROC). For ITD analysis, failures of elastographic measurement were replaced by the median value measured in the opposite group of the biopsy diagnosis.

Results: Fibrosis stage prevalence: F≥2: 50%, F≥3: 26%, F4: 9%. Rate of measurement failure: ARFI-D or ARFI-G: 0.5% versus Fibroscan: 5.9% (p=0.002). In per-protocol analysis, AUROCs of Fibroscan were significantly higher than those of ARFI-D for each diagnostic target (p<0.022), and those of ARFI-G or ARFI-DG for F4 (p<0.028). In ITD analysis, Fibroscan AUROCs decreased showing no significant difference with ARFI-D, ARFI-G, and ARFI-DG for each diagnostic target. Comparison of Obuchowski indexes showed the same results.

Conclusion: ARFI and Fibroscan have close and high accuracy for liver fibrosis diagnosis. Due to a higher failure rate, accuracy of Fibroscan decreases in the ITD analysis but remains not significantly different from ARFI accuracy.

DOI: 10.1007/s13244-013-0254-8

SS 9.03

CT texture as a novel biomarker of liver fibrosis

M.Y.S. Wan, B. Ganeshan, K. Miles, J. Karani; London/UK

Purpose: To determine if CT texture of liver and spleen is related to liver fibrosis severity.

Material and Methods: Histology and radiology databases (2009-2011) in a tertiary liver centre were reviewed. Patients with chronic viral hepatitis who had a contrast-enhanced CT and liver biopsy within 3 months of each other were selected. Severity of liver fibrosis was staged using modified histology activity index (HAI – Ischak). Patients whom had CT for other indications, without risk factor for liver disease were used as control. Regions of interests were drawn around the liver and spleen and analysed using a proprietary software (TexRad) which quantified Entropy, Uniformity, Kurtosis, Skewness, Standard-deviation on prefiltered CT images, using different filters (fine, medium, coarse).

Results: 29 patients (mean age 43.8) and 10 controls (mean age 42.8) were identified. Median for HAI was 3, standard deviation 1.8. Spearman's rank correlation shows significant strong correlation between HAI and venous phase liver texture parameters: $Kurtosis_{(medium)}$ ($r=-0.667$, $p\leq0.001$), $Skewness_{(medium)}$ ($r=-0.725$, $p=<.0001$) and Mean $density_{(unfiltered)}$ ($r=-0.583$, $p<0.001$). There is a significant strong correlation between HAI and the arterial phase spleen Mean $density_{(unfiltered)}$ ($r=-0.589$, $p<0.001$).

Conclusion: We have established the feasibility of CT texture as a novel biomarker for liver fibrosis. Kurtosis and skewness of the venous phase liver CT are strongest predictors of severity of liver fibrosis.

SS 9.04

Interobserver agreement for 3T magnetic resonance elastography and histological liver fibrosis stage

J.H. Runge[1], A.E. Bohte[1], J. Verheij[1], V. Terpstra[2], A.J. Nederveen[1], C.M. Van Nieuwkerk[1], R.J. De Knegt[3], L.C. Baak[1], P.L. Jansen[1], R. Sinkus[4], J. Stoker[1]; [1]Amsterdam/NL, [2]The Hague/NL, [3]Rotterdam/NL, [4]Paris/FR

Purpose: To compare interobserver agreement for MR-Elastography (MRE) of the liver and histological fibrosis staging.

Material and Methods: 103 patients with viral hepatitis B or C who underwent liver biopsy were scanned with MRE at 3T. Mechanical waves were applied with a vibrating piston at 50Hz. Using a SE-EPI sequence, elasticity and displacement-amplitude maps were generated, voxel size: 4x4x4mm. Two readers independently selected a region of interest (ROI) in the liver, avoiding liver edges, large vessels and areas with displacement-amplitudes <4.5µm. Mean elasticity was derived from each ROI. Two pathologists independently scored biopsies for fibrosis using the Metavir scoring system (0-4). All were blinded to clinical data. Interobserver agreement for MRE and biopsy was assessed with intraclass correlation coefficients (ICC).

Results: MRE and biopsy data were available for 81/103 patients. Spearman's correlation between MRE and fibrosis stage was 0.687. For histological grading, ICC of fibrosis stage was 0.905 (95%-CI:0.857-0.938). For MRE, ICC of elasticity was 0.992 (95%-CI:0.977-0.996) which was significantly higher (p=0.0001). Median difference in ROI-size between MRE readers was 135 voxels [IQR:60-213].

Conclusion: Although interobserver agreement of fibrosis staging using histopathology was very good, interobserver agreement of MRE was even higher. This difference was statistically significant. Variation in ROI-size between MRE readers had a minor effect on the ICC of MRE. The high accuracy and ICC of MRE support its use as a screening tool for fibrosis.

SS 9.05

MRI biomarkers on type-II diabetes mellitus patients: which role for multi-echo GRE and IVIM-DWI imaging?

S.I. Goncalves, F. Caseiro Alves, M. Castelo Branco; Coimbra/PT

Purpose: Evaluate the role of ME-GRE [2] and IVIM-DWI [3] as surrogate biomarkers of NAFLD [1] in patients with type-II diabetes mellitus (DM).

Material and Methods: Thirty-two asymptomatic patients (mean age 60±8) and 37 controls (mean age 49±7) were prospectively enrolled. IVIM-DWI and ME-GRE on a 3T scanner (Magnetom Trio, Siemens): FOV=400×400 mm, 1 slice 10 mm thick; IVIM-DWI - TR/TE=3800/67 ms, 16 b-values, 3.12×3.12 mm in-plane resolution; ME-GRE - TR/TE=30/2.46, 3.69, …, 15.99 ms (12 echoes), 2.08×2.08 mm in-plane resolution. Quantification for (a) liver fat fraction (FF) (b) T2* values as in [2]; (c) molecular diffusion (D ($\times10^{-3}$ mm^2/s)), (d) pseudo-diffusion (D*($\times10^{-3}$ mm^2/s)), and e) perfusion fraction (f) as in [3].

Results: 5% (31%) of controls (patients) showed FF values higher than 10%. D, D* and f of patients (1.17±0.27, 65±24, 0.26±0.09) and controls (1.22±0.27, 66±28, 0.27±0.08) were not significantly different (p=0.05). However, D (1.04±0.13) and D* (54±10) for fatty liver (FL) patients (n=10) were significantly lower (p=0.05) compared to controls [4]. FF, D and D* differentiate FL patients from controls; T2* values not significantly different.

Conclusion: ME-GRE and IVIM-DWI are sensitive to NAFLD in the context of type II DM patients. References: [1] Neuschwander-Tetri et al., Hepatology, 37(5), 1202-1219, 2003, [2] O'Reegan et al., Radiology, 247(2), 550-557, 2008; [3] Luciani et al., Radiology, 249 (3), 891-899, 2008; [4] Guiu et al., Radiology, 265, 96-103, 2012.

SS 9.06

Diagnostic algorithm for high liver iron overload

J.M. Alústiza; San Sebastian/ES

Purpose: To develop and validate a diagnostic algorithm for high iron overload (HIO) based on laboratory and genetic variables.

Material and Methods: We collected a retrospective cohort with consecutive patients studied by MRI to determine liver iron concentration (LIC). We analyzed all variables using univariate statistics with the MRI acting as the gold standard. We validated the algorithm in a prospective cohort. HIO is considered if the hepatic iron index >1.9 (estimated by MRI).

Results: Retrospective cohort: 242 patients. 36 had HIO. 117 had both transferrin saturation index (TSI) and ferritin elevated and 28 (11.5%) were C282Y homozygous. Final algorithm: We consider a patient as having HIO with TSI and ferritin elevated and C282Y homozygosis. HIO is discarded if TSI or ferritin is normal. The rest should be studied by MRI. Prospective cohort: 177 patients. 5 were TSI and ferritin elevated with C282Y homozygosis. Four of them proved to have HIO by MRI, PPV=80% (37.6-96.4) Specificity= 99.4% (96.8-99.9). 131 had TSI or ferritin within normal values. Two of them had HIO NPV=99.2% (95.8-99.9), Sensitivity=83.3% (43.6-97). 23% needed to have a diagnostic MRI for HIO.

Conclusion: MRI is not necessary in 77% of the patients for HIO diagnosis. MRI is indicated in patients who are C282Y non-homozygous with raised TSI and ferritin.

DOI: 10.1007/s13244-013-0254-8

SS 9.07

Quantitative analysis of arterial enhancement fraction in Hepatitis C viral-related chronic liver diseases using dual energy multiphasic CT as objective index for assessment of hepatic hemodynamic alteration: initial experience

S. Kobayashi[1], O. Matsui[1], T. Gabata[1], W. Koda[1], T. Minami[1], K. Kozaka[1], A. Kitao[1], K. Otani[2], B. Krauss[3]; [1]Kanazawa/JP, [2]Tokyo/JP, [3]Forchheim/DE

Purpose: The purpose of this study was to clarify whether quantitative color map of arterial enhancement fraction (AEF) generated with arterial and portal phase images of contrast-enhanced dual energy CT (DECT) can reflect hemodynamic differences of hepatitis C viral (HCV)-related chronic liver diseases.

Material and Methods: 22 patients who underwent abdominal multiphasic DECT for closer examination of HCV positive hepatic disease (chronic hepatitis, CH-C n=12; cirrhosis without major portosystemic collateral, LC-C PS (-) n=7; cirrhosis with major portosystemic collateral, LC-C PS (+) n=5), and normal control liver (NL n=8) were included in this study. AEF color map was generated with prototype software. The mean AEF of each groups were compared with t-test. In addition, AEF of hepatic central zone (AEF-cz) and hepatic peripheral zone (AEF-pz) were also compared within each group.

Results: Average AEF in each groups were as follows; CH-C -57.0±11.4%, LC-C PS(-) -61.0±10.9%, LC-C PS(+) -44.9±18.8%, NL -44.7±10.3%. There were significance differences between CH-C and NL (P=0.02), LC-C PS (-) and NL (P=0.01). However, there were no significant differences between AEF-cz and AEF-pz within each group.

Conclusion: Quantitative AEF map generated with DECT might be useful as objective index to assess the hemodynamic differences of HCV-related chronic liver diseases.

SS 9.08

Gd-EOB-DTPA-enhanced MRI: estimation of liver function using T1 mapping

M. Haimerl, N. Verloh, C. Fellner, C. Niessen, A.G. Schreyer, C. Stroszczynski, P. Wiggermann; Regensburg/DE

Purpose: To determine the ability of T1 mapping of liver on Gd-EOB-DTPA-enhanced MR imaging (MRI) for estimating liver function and to compare the estimated liver function to the Model for End-Stage Liver Disease (MELD) score.

Material and Methods: 75 patients underwent Gd-EOB-DTPA-enhanced MRI on a 3T system. Patients were classified into two groups: MELD-Score < 9 (n=49) and MELD-Score ≥ 9 (n=26). Two TurboFLASH sequences (TI = 400 ms, 1000 ms) were acquired before and 20 min after Gd-EOB-DTPA administration to obtain T1 maps. T1 relaxation times were determined indicating Gd-EOB-DTPA liver-uptake and correlated to the MELD-Score.

Results: Significant changes between T1 relaxation times of non-enhanced MRI (778 ± 133 ms) and Gd-EOB-DTPA-enhanced MRI (339 ± 120 ms) were observed (p<0.001). T1 relaxation time for non-enhanced MRI showed no significant differences (p=0.526) between the group with MELD-Score < 9 (777 ± 150 ms) and the group with MELD-Score ≥ 9 (780 ± 97 ms). After administration of Gd-EOB-DTPA T1 relaxation time of patients with MELD-Score < 9 (299 ± 103 ms) and patients with MELD-Score ≥ 9 (416 ± 112 ms) shows a significant difference (p<0.001).

Conclusion: Patients with advanced liver disease showed significantly lower changes in T1 mapping. Therefore, evaluation of changes in T1 mapping of the liver parenchyma may serve as a useful method to determine whole liver function, to improve the estimation of segmental liver function and finally to define the grade of liver disease.

SS 9.09

Fulminant hepatic failure: correlation among different aetiologies, MDCT findings and histopathology in adult transplanted patients

A. Pecchi, D. Corniani, M. De Santis, L. Maccio, L. Losi, N. De Ruvo, F. Di Benedetto, P. Torricelli; Modena/IT

Purpose: To describe the main features at MDCT of fulminant hepatic failure of different aetiologies, and correlating them with histopathological findings on explanted livers.

Material and Methods: The MDCT-exams of 11 patients transplanted between 2003 and 2011 were retrospectively evaluated and correlated with the histopathological examinations.

Results: MDCT revealed hepatomegaly in 6/11 patients, 5 confirmed by macroscopic evaluation. All patients showed smooth liver surface at MDCT imaging and at macroscopic examination. A diffuse hepatic parenchymal hypoattenuation was observed in 10/11 patients, correlating with the diffuse hepatocytes necrosis at histopathology. In all exams, we found periportal hypoattenuation and in 7 of them diffused peribiliary THADs corresponding to periportal inflammatory infiltration and ductular proliferation. All patients had thickened gall-bladder wall corresponding to inflammatory infiltration. Ascite was present in 9/11 patients, splenomegaly in 6/11 and thickened colon wall in 3 patients.

Conclusion: A diffuse hepatocytes necrosis and an inflammatory cell infiltration were the main histopathological findings on explanted liver for fulminant hepatic failure. They were the pathological basis of the main features founded on MDCT imaging: diffuse parenchymal and periportal hypoattenuation and thickened gall bladder wall. The regenerative liver processes might be at the basis of parenchymal heterogeneous density, such as THAD.

SS 9.10

Opportunistic screening for hereditary hemochromatosis using unenhanced CT: determination of an optimal liver attenuation threshold

P.J. Pickhardt, B.D. Pooler, E. Lawrence; Madison, WI/US

Purpose: To evaluate for a liver attenuation threshold at unenhanced CT that might allow for sensitive and specific detection of unsuspected hereditary hemochromatosis.

Material and Methods: To establish normal distribution of liver attenuation and test-positive rates of various thresholds, hepatic attenuation was measured at unenhanced CT in 3,357 consecutive asymptomatic adults (mean age, 57.0 years) undergoing colorectal cancer screening. To assess sensitivity, hepatic attenuation was measured at unenhanced-CT in 12 patients (mean age, 48.3 years) with genetically confirmed hemochromatosis (homozygous for C282Y mutation of HFE gene), including three cases detected by screening CTC.

Results: Mean liver attenuation in asymptomatic adults was 59.4±12.7 HU, compared with 78.7±13.1 HU (range, 59-105 HU) in the hemochromatosis cohort (p<0.001). Test-positive rates for triggering iron/ferritin studies in the screening cohort was 30.6% (n=1,028) at 65 HU, 8.2% (n=275) at 70 HU, 1.2% (n=39) at 75 HU, and 0.2% (n=7) at 80 HU. Corresponding sensitivity for hemochromatosis at these thresholds was 83.3% at 65 HU, 83.3% at 70 HU, 83.3% at 75 HU, and 50.0% at 80 HU.

Conclusion: An unenhanced-CT liver attenuation threshold of 75 HU would be both sensitive (83%) and specific (~99%) for the detection of clinically relevant hereditary hemochromatosis. Unexplained liver attenuation ≥75 HU (1% prevalence among asymptomatic adults) should trigger a blood draw, since early intervention with phlebotomy can prevent significant organ damage.

DOI: 10.1007/s13244-013-0254-8

11:00 - 12:30 **Room H2**

Scientific Session 10

GI Tract: From oesophagus to rectum

SS 10.01

CT colonography with rectal iodine tagging: evaluation of diagnostic accuracy and image quality

A. Mantarro, L. Faggioni, P. Bemi, R. Scandiffio, P. Vagli, E. Neri, C. Bartolozzi; Pisa/IT

Purpose: To evaluate diagnostic accuracy and image quality of CT-colonography (CTC) examinations performed with rectal iodine tagging.
Material and Methods: Thirty-five patients (male:female=19:16, age 49-78 years, mean 62 years) with a total of 44 lesions (37 sized between 6 and 9 mm, and 7 between 10 and 30 mm) were selected from a screening population for colorectal cancer (500 patients). Patients underwent CTC on a 64-row CT scanner following a 3-day low-residue diet plus a low dose of Macrogol 4000 and bisacodyl after lunch, and immediately before CTC they were rectally administered 50 mL of diatrizoate dimeglumine (Gastrografin®, Bayer Schering) diluted in 300 mL warm tap water, followed by automatic insufflation of 3 L carbon dioxide. Patients were asked to turn themselves on the CT table to ensure homogeneous luminal enhancement. CTC findings were compared with optical colonoscopy, and per-segment image quality was assessed visually using a semiquantitative score (1=poor, 2=adequate, 3=excellent).
Results: Sensitivity and specificity of CTC in lesion detection were 94.6% ($CI_{95\%}$ 80.5±99.1%) and 98.8% ($CI_{95\%}$ 95.3±99.8%) for lesions between 6 and 9 mm, and 100% ($CI_{95\%}$ 56.1±100%) and 99.4% ($CI_{95\%}$ 96.2±100%) for lesions between 10 and 30 mm, respectively. Mean image quality was adequate to excellent in all colonic segments (from 2.3 in the cecum to 3 in the sigmoid colon).
Conclusion: CTC performed with rectal tagging showed high sensitivity and specificity for all lesion sizes with overall good image quality.

SS 10.02

Technical feasibility of elastosonography in the assessment of bowel wall in inflammatory bowel disease and inter-observer variability

A. Colleoni[1], L. Romanini[1], M. Ravanelli[1], V. Cantisani[2], L. Grazioli[1], P. Ricci[2], R. Maroldi[1]; [1]Brescia/IT, [2]Rome/IT

Purpose: To investigate the feasibility of US-elastosonography to evaluate the abnormal bowel wall and the inter-observer variability as well.
Material and Methods: In this prospective study, we examined 35 consecutive patients who underwent US examination of the bowel and showed at least one segment with thickened wall underwent an additional elastosonography assessment. Overall, 39 abnormal thickened bowel segments were evaluated. GE E9 equipment was used, with a linear 6-15 MHz probe. In 39 segments, the elastosonography was acquired with 7.5 MHz in 30/39, with 5 MHz in 33/39, and in 24/39 with both frequencies. All studies were performed by the same operator. The images acquired were subsequently evaluated by two other radiologists, separately. Inter-observer variability was calculated by Cohen's test (between two operators) and Randolph's test (comparing three operators).
Results: All but 4 segments (35/39; 89.7%) were assessable by elastosonography. The elastosonography was considered adequate when the wall layers distinguished on standard ultrasound were equally detected in the color map (grading wall stiffness). The average thickness of the bowel segments was 6 mm. The Randolph test demonstrated a moderate agreement among the three operators (63%), while Cohen test provided a lesser agreement (k=0.39).
Conclusion: The preliminary results indicate the feasibility of US-elastosonography assessment of abnormal bowel segments in inflammatory bowel disease. This could offer the possibility to differentiate fibrotic from inflammatory thickening. However, only moderate correlation was observed.

SS 10.03

Diffusion-weighted imaging in the follow-up of patients after primary surgical and non-surgical treatment for rectal cancer

D.M.J. Lambregts, M.J. Lahaye, L.A. Heijnen, M.H. Martens, B.E. Heidemann, M. Maas, G.L. Beets, R.G.H. Beets-Tan; Maastricht/NL

Purpose: To evaluate the value of diffusion-weighted MRI (DWI) in the follow-up of patients after primary surgical or non-surgical rectal cancer treatment.
Material and Methods: The study group (n=117) consisted of 36 patients who had previously undergone standard surgery (+/- neoadjuvant treatment), 40 a local excision (15 after chemoradiotherapy) and 41 a 'wait-and-see'-policy. During clinical follow-up (FU), patients underwent ≥1 FU-MRIs (1.5T) including DWI, as a part of routine FU or because of a suspected local recurrence. Two readers in consensus evaluated each MRI and scored the (b1000) DWI-images as 'no high signal/no recurrence', 'high signal suspected of recurrence' or 'not adequately assessable due to focal image artefacts'.
Results: Patients underwent a mean number of 3 FU-scans (range 1-11) with a mean FU-time of 44 months (4-144). 27/117 patients developed a local recurrence, of which 23 (85%) were accurately detected on DWI. The other 90 patients together underwent a total of 261 FU scans, of which 194 (74%) remained negative (no high signal) on DWI. 57 DWI-scans (19%) could not adequately be assessed due to artefacts. 14 DWI-scans were false positive (mainly at the first FU after surgery/local excision) of which 50% again normalised during further FU.
Conclusion: DWI is a useful imaging tool in the follow-up of patients after primary rectal cancer treatment. False positives may occur immediately after surgery, but the DWI signal normalises again during follow-up.

SS 10.04

Structured reporting in rectal cancer staging: a proposal

R. Scandiffio, A. Mantarro, L. Faggioni, P. Vagli, R. Balestri, P. Buccianti, E. Neri, C. Bartolozzi; Pisa/IT

Purpose: To highlight the relevant information that should be included in a structured MRI report for rectal cancer (RC) staging.
Material and Methods: From March 2012 to January 2013, 100 patients with rectal cancer were prospectively evaluated at 3T MRI. A structured report was used by 3 experienced radiologists to describe relevant findings in 50 patients. Report included the following information: tumor location, longitudinal extent and maximum thickness parietal involvement; lumen stenosis; distance from the distal margin of the lesion and puborectal muscles; extent of extramural invasion; lesion morphology (infiltrative or nodular); distance from the mesorectal fascia; relationship with elevator muscles and extramural vessels; lymph node involvement. Diagnostic accuracy and mean reporting time was assessed.
Results: Diagnostic accuracy resulted superimposable in structured and non-structured reporting (75% and 77%); mean reporting time resulted in 15 and 20 min, respectively.
Conclusion: The main advantages of a well-structured report include reduction of reporting time, the possibility of creating an easily accessible database and clearer description of imaging findings to clinicians, allowing for detailed comparison with previous MRI examinations.

DOI: 10.1007/s13244-013-0254-8

SS 10.05

MDCT evaluation of bowel obstruction: can the radiologist's experience make a difference?

R. Basilico, V. Calamita, A.R. Ferri, E. Rodolfino, N. Civitareale, A. Lella, A.R. Cotroneo; Chieti/IT

Purpose: To evaluate the diagnostic performance of MDCT in the detection of site and cause of bowel obstruction and in the diagnosis of bowel wall ischemia or infarction, by assessing the added value of the radiologist's experience.

Material and Methods: The MDCT reports of 110 patients with surgical and istological diagnosis of bowel obstruction were retrospectively analyzed. We calculated the diagnostic accuracy of MDCT reports in the evaluation of the cause and the site of obstruction and the sensitivity, specificity, diagnostic accuracy values in the detection of bowel wall ischemia or infarction. The same MDCT examinations were then reviewed by an experienced abdominal radiologist, to compare her results with those of the original MDCT reports.

Results: The diagnostic accuracy in determining the cause of bowel obstruction and in defining the site of obstruction were respectively 89% and 91% for MDCT reports and 92% and 94% for the experienced reader. The sensitivity, specificity and diagnostic accuracy of MDCT reports in identifying bowel wall ischemia or infarction were respectively 73%, 96% and 91%. The sensitivity value for bowel wall ischemia or infarction significantly increased to 83% for the abdominal radiologist.

Conclusion: MDCT is very accurate in diagnosing the cause and the site of bowel obstruction. The radiologist's experience in abdominal disease represents an added value in the diagnosis of bowel wall ischemia or infarction occurring in bowel obstruction.

SS 10.06

Morphological and functional evaluation of sleeve gastrectomy: MDTC and cMR imaging

M. Rengo, D. Caruso, D. Bellini, A. Iossa, M.M. Maceroni, C.N. De Cecco, G. Silecchia, A. Laghi; Latina/IT

Purpose: To evaluate morphological and functional changes after laparoscopic sleeve gastrectomy (LSG) using volumetric multidetector computer tomography (MDCT), for the evaluation of gastric volumes and thoracic migration, and cine magnetic resonance (cMR) of the esophagus, for the evaluation of motility anomalies and gastroesophageal reflux.

Material and Methods: Thirteen patients, presenting gastroesophageal reflux after LSG, underwent both volumetric MDCT of the stomach and cMR of the esophagus. All patients presented gastroesophageal reflux. Gastric volume, stomach length, sleeve length, antrum length thoracic migration and staple line length were evaluated on MDCT. Motility anomalies of the esophagus and the presence of gastroesophageal reflux were evaluated on cMR.

Results: Gastroesophageal reflux was detected by cMR in all patients. Thoracic migration was founded in 50% of patients. Mean gastric volume increase after surgery (initial volume 200 ml) was 105.3 ml. Antrum or proximal sleeve dilatation was found in all patients.

Conclusion: Volumetric MDCT and cMR can identify both morphological and functional cause of gastroesophageal reflux and can be helpful in the planning of reintervention.

SS 10.07

Prognostic significance of novel 18F-FDG PET/CT defined tumour parameters in patients with oesophageal cancer

K.G. Foley, P. Fielding, W.G. Lewis, A. Karran, D. Chan, P. Blake, S.A. Roberts; Cardiff/UK

Purpose: Radiological staging of oesophageal cancer (OC) includes CT, endoscopic ultrasound (EUS), and 2-[18F]-fluoro-2-deoxy-D-glucose (FDG) positron-emission tomography/computed tomography (PET/CT). The aim of this study was to determine the prognostic significance of radiologically defined OC tumour volume, including total lymph node metastasis volume, as measured by both EUS and PET/CT.

Material and Methods: 103 consecutive OC patients were staged using CT, EUS and PET/CT. PET/CT was used to measure tumour volume, including that of the primary tumour, nodal involvement and any metastases. Primary outcome measure was survival from diagnosis.

Results: 94% of patients had FDG-avid tumours on PET/CT. On multivariable analysis, 4 factors were found to be independently and significantly associated with survival; EUS T stage (HR 10.302 p=0.041); mean standardized uptake value (SUVmean, HR 0.797 p=0.025); PET/CT OC tumour and lymph node metastasis volume (HR 1.041 p=0.002); and PET/CT defined lymph node metastasis count (HR 3.271 p=0.007). EUS volume and PET/CT stage were not significant factors in the multivariate analysis.

Conclusion: PET/CT is an important predictor of survival and further research is needed to identify critical prognostic values. Current PET/CT reporting strategies should arguably include SUVmean, tumour and lymph node metastasis volume and count to enrich prognostic modelling.

SS 10.08

Role of preoperative imaging with MDCT in the management of patients with gastroesophageal reflux disease symptoms, candidate to sleeve surgical revision

M. Rengo, D. Caruso, F. Vecchietti, L. Bertana, A. Iossa, C.N. De Cecco, G. Silecchia, A. Laghi; Latina/IT

Purpose: To evaluate if multidetector computed tomography (MDCT) can be helpful and useful in the decision-making process in sleeve patients with gastroesophageal reflux disease (GERD) symptoms and to demonstrate the reproducibility and accuracy of the technique.

Material and Methods: Twenty-three patients submitted to LSG, complaining upper GI symptoms and/or weight regain and scheduled for a sleeve surgical revision were investigated. All patients underwent MDCT scan, upper GI barium swallow study and endoscopy. MDCT was compared to barium and endoscopy features as concern: esophageal dilatation, neo-fundus development and volume, hiatal hernia, sleeve size in toto and atrum dilatation. All patients underwent laparoscopic sleeve revision. Surgical findings were considered "as gold standard".

Results: A total of 21 patients with hiatal hernia, neo-fundus or sleeve dilatation underwent surgical correction. All findings identified at MDCT were confirmed by intraoperative findings. The presence of hiatal hernia was significantly underestimated by both barium and endoscopy with a sensitivity of 57.1% and 50%, respectively (P=0.04, P=0.02).

Conclusion: MDCT is an accurate method for the detection of hiatal hernias and quantification of gastric volumes and can be considered as non-invasive method to guide surgery.

DOI: 10.1007/s13244-013-0254-8

SS 10.09

N-staging of oesophageal carcinoma: is there still a role for EUS in patients staged N0 on PET/CT?

K.G. Foley, P. Fielding, W.G. Lewis, A. Karran, D. Chan, P. Blake, S.A. Roberts; Cardiff/UK

Purpose: Accurate exclusion of lymph node metastases in oesophageal cancer (OC) may prevent unnecessary preoperative chemotherapy. Endoscopic ultrasound (EUS) has been shown to be the most accurate method of assessing nodal status. However, with the increasing utilisation of 2-[18F]-fluoro-2-deoxy-D-glucose (FDG) positron-emission tomography/computed tomography (PET/CT), our study aims to assess whether separate EUS N-staging is still of prognostic value in those staged N0 on PET/CT.
Material and Methods: Ninety-nine consecutive patients (median age 66, 72 male, 80 ACA, 18 SCC, 1 other) staged as N0 on PET/CT were separated into two groups: EUS N0 (n=59) and EUS ≥N1 (n=40). Kaplan-Meier survival analysis was performed. Primary outcome was survival from diagnosis.
Results: There was a significant difference in survival between EUS N0 (mean survival 35.8 months, 95% CI 32.343 - 39.428) and EUS ≥N1 (mean survival 26.4 months, 95% CI 20.727 – 32.106, p=0.002) in patients staged N0 on PET/CT.
Conclusion: EUS N-staging still has prognostic value in patients staged N0 on PET/CT. PET/CT and EUS continue to have complimentary roles in OC staging.

SS 10.10

Preoperative MDCT assessment for lymphatic gastric cancer spread in the era of neoadjuvant treatment

P. Mercuri, M.A. Mazzei, A.V. Parrinello, C. Pozzessere, S. Guerrini, N. Cioffi Squitieri, F.G. Mazzei, L. Volterrani; Siena/IT

Purpose: To validate the feasibility and accuracy of MDCT for the preoperative lymphatic gastric cancer spread.
Material and Methods: 104 patients with primary gastric cancer (mean age 68.67 years) who consecutively underwent MDCT scan followed by radical surgical treatment were prospectively evaluated. Regional lymph nodes were considered involved when the short-axis diameter was >5mm for the lymph nodes of group 1 and >8mm for the lymph nodes of other group according to the Japanese Classification of Gastric Carcinoma. All patients underwent a radical lymph node dissection (D2-D3) according to Japanese Research Society for Gastric Cancer (JRSGC) guidelines. The removal of nodal stations was always preceded by Indian-ink injection in the lesser and greater curvature of the stomach; after operation, single lymph nodes were retrieved on the fresh specimen by the surgeon, and classified in JRSGC nodal stations for pathological examination.
Results: Lymph node invasion was found in 85 cases (81.73%) with a MDCT sensitivity and specificity of 89% and 85%, respectively. The rate of understaging was higher (15%) than that of overstaging (8%). Lymph node status of early forms was correctly staged in all cases. Furthermore, all N3 cases were correctly staged.
Conclusion: MDCT is a useful technique in the preoperative assessment of lymphatic cancer spread and could have a positive impact in clinical decision making in the era of neoadjuvant treatment.

DOI: 10.1007/s13244-013-0254-8

11:00 - 12:30 **Auditorium**

Scientific Session 11

Focal lesions in the cirrhotic liver

SS 11.01

Diagnostic performance of multi-detector CT and magnetic resonance imaging for the detection of hepatocellular carcinoma: a systematic review and meta-analysis

Y.J. Lee[1], J.M. Lee[2], J.K. Han[2], B.I. Choi[2], J.S. Lee[2]; [1]Seongnam-Si, Gyeonggi-do/KR, [2]Seoul/KR

Purpose: To perform a systematic review and meta-analysis of the diagnostic accuracy of CT and MRI for the detection of HCC and update previously summarized estimates.

Material and Methods: We searched MEDLINE, EMBASE, and Cochrane Library to identify studies providing per-patient or per-lesion diagnostic accuracy data of CT and MRI for the detection of HCC in patients with chronic liver disease. Studies published from January 2000 to December 2012, having a reference standard based on histopathology and/or follow-up, were included. Summary estimates of diagnostic accuracy were obtained using random-effects model with further exploration using meta-regression and subgroup analyses.

Results: Forty-one studies (18 CT, 35 MRI) were included, evaluating 1135 patients for CT and 2348 patients for MRI. Overall per-patient sensitivity of MRI was 87% with a specificity of 92%. Overall per-lesion sensitivity of MRI was higher than CT when pooling sensitivity data of all studies (MRI vs. CT: 78% vs. 72%) and when pooling studies with cross-tabulation data only (79% vs. 70%). Per-lesion specificity was not significantly different (91%). The use of Gd-EOB-DTPA for MRI showed a significantly higher per-lesion sensitivity than other contrast agents (P=0.01). There was a tendency of lower diagnostic accuracy for lesions smaller than 2 cm and for studies using explanted liver as the only reference standard.

Conclusion: MRI is more sensitive than CT for the detection of HCC with comparable specificity, in patients with chronic liver disease.

SS 11.02

Comparison of hepatobiliary phase Gd-EOB-DTPA-enhanced magnetic resonance imaging and diffusion-weighted imaging for detecting malignant focal liver lesions

D. Akata, I.C. Kose, M. Ozmen, M. Karcaaltincaba; Ankara/TR

Purpose: To compare the role of high-b-value diffusion-weighted imaging (DWI) and hepatobiliary phase of gadoxetic acid disodium (Gd-EOB-DTPA)-enhanced dynamic magnetic resonance imaging (MRI) to detect malignant focal liver lesions.

Material and Methods: 24 patients with 114 liver metastases and 17 patients with 50 hepatocellular carcinomas (HCC) underwent DWI and Gd-EOB-DTPA-enhanced MRI for suspected or known malignant liver lesions according to previous imaging findings. Gd-EOB-DTPA-enhanced MRI included T(2) weighted TSE sequence, early dynamic T(1) weighted sequences and 20-min delayed hepatobiliary phase sequence. Each sequence was evaluated separately from other sequences. Lesions detected either at hepatobiliary phase or at DWI or detected in at least two other sequences were defined as true lesions. Sensitivity for detecting malignant focal liver lesions were compared among high-b-value diffusion weighted images and hepatobiliary phase images.

Results: Hepatobiliary phase of Gd-EOB-DTPA-enhanced MRI yielded significantly higher sensitivity (87.8%) for detecting HCC than high-b-value diffusion weighted images (63,3%) (Mc Nemar test $p<0.05$). Hepatobiliary phase yielded equal sensitivity to DWI for detecting metastases (80% at both of them). For overall malign lesions, hepatobiliary phase had higher sensitivity (82.3%) than DWI (75%) but it was not significant at Mc Nemar test ($p>0.05$).

Conclusion: Hepatobiliary phase of Gd-EOB-DTPA-enhanced MRI has highest sensitivity for detecting HCC among all sequences. However, sensitivity for detecting metastases at hepatobiliary phase and DWI are equal.

SS 11.03

HCC detection on CT: can multi-energy spectral CT improve lesion conspicuity?

F. Legou[1], M. Chiaradia[1], P. Richard[2], M. Djabbari[1], F. Pigneur[1], C. Costentin[1], J. Calderaro[1], A. Laurent[1], A. Rahmouni[1], A. Luciani[1]; [1]Creteil Cedex/FR, [2]Buc/FR

Purpose: To determine the effect of spectral images obtained on multi-phasic spectral energy CT on HCC conspicuity.

Material and Methods: 14 patients with 35 advanced HCC (BCLC C, follow up under oral adjuvant therapy) underwent an abdominal contrast material-enhanced spectral CT (Discovery CT 750HD; GE Healthcare, Wisconsin, USA), in liver-arterial phase, and portal venous phase, with final HCC diagnosis based on liver biopsy (n= 9) or AASLD imaging criteria with a median follow-up of 18 months (n=5). 140 kVp polychromatic images were compared to the monochromatic images datasets (40 to 140 keV, 1 keV step) derived from the spectral acquisition. Tumor-to-liver CNR and HCC signal intensity obtained on arterial phase whether using polychromatic (UH) or monochromatic images were compared (ANOVA, Post hoc Dunn). Effective radiation doses were estimated based on $CTDI_{vol}$.

Results: 33 HCC were identified with polychromatic images vs 34 on spectral imaging (P=0.75). On monochromatic images obtained at the single energy optimal level of 49 keV, the mean HCC CNR was significantly higher than that obtained on polychromatic images (1.96 vs. 0.67; $P<0.001$). The HCC signal intensity was significantly higher on monochromatic images than on polychromatic images (4.45 vs 3.88; P=0.0099). Mean $CTDI_{vol}$ was 12.3 mGy.

Conclusion: Monochromatic energy levels at 49 keV can increase conspicuity of HCC in keeping with the usual standardized HCC enhancement profile, and with an acceptable radiation exposure.

SS 11.04

Small (≤1cm) hepatocellular carcinoma: diagnostic performance and imaging features of gadoxetic acid-enhanced Liver MRI

M.H. Yu, J.H. Kim, Y.D. Cho, J. Yoon; Seoul/KR

Purpose: To investigate the diagnostic performance and imaging features of gadoxetic acid-enhanced MRI for detection of small (≤1cm) hepatocellular carcinoma (HCC) in patients with chronic liver disease.

Material and Methods: Sixty patients (M:F=56:4, 60.1 years) having HCCs (n=146; 70>1cm, 76≤1cm) underwent gadoxetic acid-enhanced MRI including DWI. HCCs were confirmed by surgical resection (n=72) or by showing interval growth with typical enhancement pattern on follow-up dynamic CT/MRI (n=74). Two radiologists graded the possibility of HCC on MRI using a 5-point confidence scale and assessed their MR imaging features. The jackknife free-response receiver operating characteristic (JAFROC) method was used.

Results: The average JAFROC figure of merit (FOM) for small (≤1cm) HCC was 0.717, meanwhile FOM for large HCC (>1cm) was 0.973 with substantial agreement (κ=0.676). The sensitivity and specificity were as follows: 46% and 42% in small HCC vs. 95% and 70% in large HCC. Eleven small HCCs (14.5%) were not demonstrated on MRI. MR imaging features of small HCC included arterial enhancement (n=60, 78.9%), hypointensity on hepatobiliary phase (n=52, 68.4%), washout on portal phase (n=38, 50%), T2 hyperintensity (n=33, 43.4%), T1 hypointensity (n=24, 31.6%), and restriction on DWI (n=20, 26.3%).

Conclusion: The diagnostic performance of gadoxetic acid-enhanced MRI for small HCC detection is lower than that of large HCC. The arterial enhancement and hypointensity on hepatobiliary phase are the most common MR imaging features of small HCCs.

DOI: 10.1007/s13244-013-0254-8

SS 11.05

Contrast-enhanced MDCT follow-up of HCC treated by TACE with iodized oil: correlation between oil deposition and residual enhancement, and effect on interobserver agreement

G.A. Zamboni, M.C. Ambrosetti, F. Lombardo, R. Pozzi Mucelli; Verona/IT

Purpose: To evaluate CT for follow-up HCC patients treated with TACE with oil, assessing the relationship between tumor sizes, complete filling with oil and residual enhancement. In addition, to assess how the presence of oil affects interobserver agreement in evaluating tumor filling with oil and presence of residual enhancement.

Material and Methods: The 64-row MDCTs performed 4 weeks after TACE on 62 patients with HCC (52M, 10F; mean age 69 years) were reviewed: unenhanced, arterial, portal-venous and equilibrium phase images were available. Two readers reviewed independently the exams evaluating ≤3 tumors/patient and assessed completeness of tumor filling with oil and presence of residual enhancement. Their relation with tumor size (t-test, Fisher's test) and interobserver agreement (kappa-statistics) were calculated.

Results: 98 nodules were analyzed (mean diameter 31.7 mm). Tumors completely filled with oil were significantly smaller than those who were not (16.5±1.3 mm vs 42.2±4 mm; $p<0.0001$). Tumors with residual enhancement were significantly larger than those without (44.5±5.8 mm vs 21.7±1.8 mm; $p<0.0001$). Complete filling with oil was significantly associated with lack of residual enhancement ($p<0.0001$). Interobserver agreement was perfect for complete filling with oil ($k=1$) and very good for presence of residual enhancement ($k=0.888$).

Conclusion: Multiphasic CT is commonly used to follow-up HCC after TACE. Tumor size correlates directly with rate of complete filling with oil and inversely with presence of residual enhancement. Since interobserver agreement is very good/perfect, the technique can be safely used for treatment assessment.

SS 11.06

Withdrawn by the authors

SS 11.07

Italy meets Japan: comparison among Western and Eastern pathologists about histological classification of a series of nodules within cirrhosis showing atypical findings after Gd-EOB-DTPA contrast-enhanced MR

V. Battaglia[1], U. Motosugi[2], T. Ichikawa[2], L.E. Pollina[1], D. Campani[1], M. Sakamoto[3], M. Nakano[3], C. Bartolozzi[1]; [1]Pisa/IT, [2]Yamanashi/JP, [3]Tokyo/JP

Purpose: Actually available guidelines for diagnosis and management of nodules in cirrhosis still focus on lesions with typical vascular pattern at dynamic imaging. MR with hepatospecific contrast agents can give additional clues for a more precise classification of atypical nodules, frequently detected in cirrhotic livers. Purpose of the study was to understand the pathological meaning of nodules' atypia at MR and to define a correspondence between Western and Eastern pathological interpretations.

Material and Methods: Thirty-one nodules on 15 explanted cirrhotic livers were retrospectively analysed. At MR examinations prior to OLT, performed after Gd-EOB-DTPA injection, all nodules did show atypical findings (hypo-isointense on arterial phase; hypo-isointense on late phase). On HB phase, nodules were hypointense. All nodules were histologically analyzed both by Italian and Japanese expert pathologists. Results from blinded pathological assessments by two groups of experts were then compared.

Results: Complete agreement among pathologists was achieved in 12 nodules (7 early HCCs, 4 overt HCCs, 1 characterized as regenerative nodule). Remnant 29 nodules were judged at first evaluation both as early HCC or as high-grade dysplastic nodules; agreement among pathologists about definite nodules' diagnosis was achieved in a second time.

Conclusion: Despite different histological interpretations between Western and Eastern experts, MR atypical nodules should be considered as preneoplastic/early neoplastic lesions, thus giving a more accurate stratification of risk patients. Final report of agreement among Western and Eastern pathologists is upcoming.

SS 11.08

Detection of hepatocellular carcinoma in gadoxetic acid-enhanced hepatobiliary phase MR imaging at 3T: comparison of high and low flip angle

H.J. Cho[1], Y.K. Cho[1], M.Y. Kim[1], J.M. Lee[2]; [1]Seoul/KR, [2]Bucheon, Gyounggi/KR

Purpose: To compare the detectability of hepatocellular carcinoma (HCC) on fat-suppressed 3D T1-weighted gradient echo sequences acquired with both low and high flip angle (FA) during hepatobiliary phase liver MRI using gadoxetic acid, quantitatively and qualitatively.

Material and Methods: Our institutional review board approved this retrospective study. 267 consecutive patients underwent 3T liver MR imaging with low and high FA (10° and 25°) sequences at hepatobiliary phase. Among 125 patients diagnosed as HCC, 47 patients with 62 HCCs were enrolled in this retrospective study. To quantitative analysis, a radiologist measured signal intensities of the lesion, the liver and the spleen, and calculated liver-spleen contrast, lesion-to-liver contrast-to-noise ratios and SAR. To qualitative analysis, three reviewers independently reviewed the image sequences using a five-point rating scale, focused on hypointense lesion detection and the image qualities.

Results: The high FA sequence had significantly higher liver-spleen contrast and lesion-to-liver CNR compared to those of low FA ($p<0.05$, respectively). The per-lesion and per-person sensitivities of high FA were higher than those of low FA in all three reviewers ($p<0.05$, respectively). There was statistical differences for the detection of HCCs smaller than 1.5 cm in two of three reviewers ($p<0.05$, respectively). Interobserver agreements were more than moderate degree.

Conclusion: Increasing the FA in T1-weighted hepatobiliary phase liver MRI with gadoxetatic acid improves lesion detection and conspicuity for smaller lesions and helps the diagnosis of HCC.

SS 11.09

Imaging features of combined hepatocellular carcinoma and intrahepatic cholangiocarcinoma in patients undergoing liver surgery

N. Leo, L. Ricca, C. Balasa, S. Bivol, C. Guettier, E. Vibert, M. Lewin; Villejuif/FR

Purpose: To clarify imaging features of combined hepatocellular and intrahepatic cholangiocarcinoma (cHCC-CC).

Material and Methods: This retrospective study includes 10 patients (10 males, mean age 65 years) who had either an hepatectomy (n=5) for HCC and CC, either a liver transplantation (LT) (n=5) for HCC. All the patients were evaluated with presurgical imaging study by US (n=10), MRI (n=6) and CT (n=10). All patients had a clinical history of chronic liver disease and 4/10 were treated with presurgical Transarterial Chemoembolization (TACE). After histologic and immunohistochemical stain confirmation, two radiologists analyzed the imaging features of cHCC-CC: size, shape, margins, signal intensity, components of tumor, enhancement pattern, satellite tumors, metastasis, lymphadenopathy, vascular invasion, biliary dilatation and findings of liver disease.

Results: The cHCC-CC was a single mass (8/10) with a mean size of 4 cm (range 1-10 cm), heterogeneous signal (6/10), hyperintensity on T2-weighted and hypointensity on T1-weighted images (6/10). On post-contrast imaging, cHCC-CC were divided in 3 enhanced patterns: HCC-like (early enhancement with wash-out on later phases, 4/10), CC-like (early ring-enhancement with progressive enhancement in central portions, 4/10) and hypovascular pattern (2/10). Other findings included chronic hepatopathy (10/10), late capsule enhancement (2/10), lymphadenopathies (2/10), portal venous invasion (1/10) and biliary dilatation (1/10).

Conclusion: In our study, cHCC-CC presents in male patient most commonly as a single mass, heterogeneous, hyperintensity on T2-weighted images with 2 predominant enhanced patterns.

DOI: 10.1007/s13244-013-0254-8

SS 11.10

Diagnostic imaging after Yttrium 90 therapy in patients with hepatocellular carcinoma: comparison of magnetic resonance imaging with Gd-EOB-DTPA and gadobutrol

S. Kinner, C. Kloeters, J. Theysohn, J. Ertle, M. Forsting, T. Lauenstein; Essen/DE

Purpose: A precise evaluation of tumour response after Yttrium-90 therapy is essential for adequate clinical management. However, evaluation of imaging may be hampered as Y90 itself can lead to reactive liver changes with similar appearance to progress. We aimed to compare a liver specific agent (Gd-EOB-DTPA) to gadobutrol MRI concerning therapy response evaluation.

Material and Methods: 20 patients with HCC underwent contrast-enhanced CT and gadobutrol-MRI on the day before and Gd-EOB-DTPA MRI directly before Y90 therapy. Follow-up images were performed 30, 90 and 180 days after therapy. Two radiologists reviewed gadobutrol and Gd-EOB-DTPA MRI in consensus using a 4-point-scale: 1=definitely response, 2=probably response, 3=probably no response, 4=definitely no response. CT in combination with laboratory parameters served as reference standard.

Results: CT and laboratory parameters revealed progress in 5 patients after 30, 3 patients after 90 and 7 patients after 180 days. With Gd-EOB-DTPA MRI radiologists were more determinate compared to gadobutrol-MRI (mean values day 30 for responders with Gd-EOB-DTPA=1.4; gadobutrol=1.9). In each patient, on day 90 and 180, radiologists rated gadobutrol-MRI as probable response while Gd-EOB-DTPA MRI revealed definite progress which was confirmed by AFP values.

Conclusion: Gd-EOB-DTPA MRI allows a more precise assessment of tumour response after Y90 therapy. The liver specific contrast-enabled earlier diagnosis of tumour progress compared to gadobutrol MR and also to CT and can differentiate between therapy induced changes and real tumour progress.

11:00 - 12:30 **Room J**

Scientific Session 12

CT Colonography: Implementation and technical performance

SS 12.01

Population screening with CT colonography: preliminary findings of a randomized multicenter trial

G. Iussich[1], L. Correale[2], C. Senore[2], D. Campanella[1], N. Segnan[2], G. Galatola[1], C. Laudi[1], S. Montemezzi[3], A. Bert[2], D. Regge[1]; [1]Candiolo/IT, [2]Turin/IT, [3]Verona/IT

Purpose: To report preliminary findings of a population-based screening CTC trial.

Material and Methods: Subjects aged 58-60 years without a personal history of cancer/adenomas were mailed a personal invitation. Respondents were randomized to either CTC or sigmoidoscopy. CTC bowel preparation consisted of a 3-day mild laxative (movicol) with same-day fecal tagging (gastrographin). Exams were read by experienced radiologists using a paradigm with first reader CAD. Patients with lesions ≥6 mm were referred for colonoscopy. Outcome measures included colonoscopy referral, reporting time, extracolonic findings (ECFs). Detection of advanced neoplasia (AN) was estimated on a subset of patients for which colonoscopy and histological data were available.

Results: Between December 2010 and September 2012, 1019 (521 men) subjects were randomly assigned to CTC screening. Exam quality was inadequate in 30 (2.9%) patients. A total of 121 lesions ≥6 mm, including 8 masses, in 103 (10%) patients were found at CTC; 39 (3.8%) had lesions ≥10 mm. On a subset of 917 patients, including 72 positive CTC results, detection rate for AN was 4.4% (95% CI: 3.1-5.9%) and the PPV was 55.6% (95% CI: 43.4-67.3%). Forty-three (4.2%) patients had ECFs of any significance; only 8 (0.9%) required further work-up. The mean reporting time was 239 s (range, 60-1020).

Conclusion: As a primary colorectal screening tool, CTC has acceptable low referral rate, adequate reporting times and a high concordance of positive findings at colonoscopy.

SS 12.02

Use of CT colonography in the English national Bowel Cancer Screening Programme

A. Plumb[1], S. Halligan[1], C. Nickerson[2], P. Bassett[1], A. Goddard[3], S.A. Taylor[1], J. Patnick[2], D. Burling[4]; [1]London/UK, [2]Sheffield/UK, [3]Derby/UK, [4]Harrow/UK

Purpose: To examine use of CT colonography (CTC) in the English Bowel Cancer Screening Programme (BCSP) and investigate neoplasia detection rates and positive predictive value.

Material and Methods: Between June 2006 and July 2012, asymptomatic screenees undergoing CTC as their first-line colonic test following a positive faecal occult blood result were identified via the BCSP national database. Referral rates for further testing (usually endoscopy), neoplasia detection and positive predictive value for CTC were calculated. Variation between screening centres was assessed with risk-adjusted funnel plots. Multilevel logistic regression examined factors associated with variable neoplasia detection.

Results: 2753 CTC were performed over 6 years, spanning 3 rounds of biennial FOBt screening. Overall neoplasia detection rate was 24.4% (95%CI 21.7, 27.0%). Referral rate for further testing after CTC was 40.6% (95%CI 35.7, 45.6%). Positive predictive value (PPV) for neoplasia was 67.9% (95%CI 64.6%, 74.4%) and was highly variable between screening centres. After adjusting for confounders, one centre had a significantly lower detection rate. Centres with highly experienced radiologists (1000+ lifetime total CTC cases interpreted) had higher neoplasia detection rates and PPV. 3D interpretation was associated with greater neoplasia detection.

Conclusion: Neoplasia detection following positive FOBt is highly variable across screening centres and is lower than colonoscopy. Radiologist experience and use of 3D visualisation are associated with greater detection rates. High yield centres also have high PPV.

DOI: 10.1007/s13244-013-0254-8

SS 12.03

What did the barium enema teach us? Comparison of paired decubitus CT colonography to supine prone CT colonography

S.A. O'Connor, J.M. Hanson, A.D. Quinn; Drogheda/IE

Purpose: The purpose of the study was to assess the equivalence of paired decubitus imaging compared to supine prone imaging and to assess patient preference for positioning in CT colonography (CTC).

Material and Methods: Fifty consecutive symptomatic patients referred for CTC for failed colonoscopy were enrolled prospectively. Each patient was put into all four positions: prone, supine and both decubitus for the time taken to scan and were asked to grade the comfort on a linear scale. 50 supine/prone and 50 paired decubitus CTC were retrospectively scored by 2 experienced reporters for visual distension for each of 6 segments of the colon. 1=inadequate distension of the segment. 2=inadequate distension of a part of the segment. 3=diagnostic distension of the entire segment. 4=optimal distension of the entire segment.

Results: The patient position survey showed the least comfortable position being prone 66% (p=0.001 Student t test). The most comfortable pair of positions was decubitus 78% (p=0.001 Student t test). On statistical input, comparison of equivalence of distension was made using two one-sided tests with equivalence shown at p=0.001 t_{cv}=3.175.

Conclusion: Paired-decubitus imaging in CTC gives equivalent distension to supine prone. Paired-decubitus imaging is the preferred positioning and should be considered as an alternative strategy to conventional supine prone imaging.

SS 12.04

Natural history trial of small colorectal polyps: in vivo volumetric growth rates for assessing clinical behavior

P.J. Pickhardt[1], D. Kim[1], B.D. Pooler[1], J.L. Hinshaw[1], B. Cash[2]; [1]Madison, WI/US, [2]Bethesda, MD/US

Purpose: We report the results of a prospective natural history trial assessing behavior of small (6-9 mm) colorectal polyps at longitudinal CTC.

Material and Methods: In vivo CTC surveillance was performed on 306 small (6-9 mm) polyps initially detected at screening CTC in 243 consenting asymptomatic adults (mean interval, 2.3 years; range, 1-7 years). Volumetric and linear polyp measurements at initial and surveillance CTC were correlated with histologic subgroups.

Results: Applying a polyp volume threshold of ±20%/year to categorize growth, 22% progressed (n=68), 50% were stable (n=153), and 28% regressed (n=85), including complete resolution in 10% (n=32). 91% of advanced adenomas progressed, compared with 37% of non-advanced adenomas, and 8% of all other lesions (p<0.0001). Mean polyp volume change was +77%/year for advanced adenomas (n=23), +16%/year for non-advanced adenomas (n=84), and -13%/year for all non-neoplastic or unresected polyps (p<0.0001). An absolute polyp volume >180 mm^3 at surveillance CTC identified advanced neoplasia with 92% sensitivity, 94% specificity, 58% PPV, and 99% NPV. In general, volume assessment amplified small linear changes, as only sixteen 6-9 mm polyps (6%) exceeded 10 mm at follow-up.

Conclusion: Volumetric growth assessment of small colorectal polyps represents a powerful biomarker for determining clinical relevance. Advanced adenomas demonstrate more rapid growth than non-advanced adenomas, whereas most other small polyps remain stable or regress over time.

SS 12.05

Colonic morphology at CTC in men versus women: quantitative assessment using novel software

C.N. Weber[1], A.S. Lev-Toaff[1], H.M. Zafar[1], M.S. Levine[1], A. Wilmot[1], S. Sudarsky[2], L. Guendel[3], B. Geiger[2]; [1]Philadelphia, PA/US, [2]Princeton, NJ/US, [3]Forchheim/DE

Purpose: We developed novel CTC software for quantitative analysis of colonic morphology to determine if there are significant differences between genders which may explain higher rates of incomplete optical colonoscopy among women.

Material and Methods: 8CTC datasets from 20 men and 20 women with incomplete optical colonoscopies were compared using software to determine total/segmental colonic length, volume, tortuosity (number of 90° angles with 8 cm limbs), compactness (volume containing colon/segments divided by length), and height of the sigmoid apex relative to the lumbosacral junction.

Results: Women had greater tortuosity (turns) of the total colon (10.60 vs 7.40, p<.001), rectum (0.85 vs 0.32, p<.001), sigmoid (4.40 vs 3.28, p=.005), and transverse colon (3.65 vs 2.20, p=.002). Women had greater compactness (mm^2) of the total colon (6457 vs 8246, p<.001), sigmoid (2961 vs 3554, p=.032), descending (1534 vs 2165, p=.021) and transverse colon (3320 vs 4132, p=.005). Men had greater volumes (liters) of the total colon (2.10 vs 1.65, p=.006), sigmoid (0.54 vs 0.31, p<.001) and ascending colon (0.28 vs 0.35, p=.029). Women had lower height (mm) of the sigmoid apex (46.47 vs 90.39, p=.004). There were no significant differences in total/segmental colonic length between genders.

Conclusion: Our novel CTC software enables quantitative analysis of colonic morphology. Significant differences between the genders in tortuosity, compactness, volumes, and sigmoid apex height may explain differences in optical colonoscopy performance. This software may have other beneficial applications.

SS 12.06

Withdrawn by the authors

SS 12.07

Low-dose CT colonography using model-based iterative reconstruction: findings in 65 patients

V. Vardhanabhuti, J. James, R.R. Nensey, E.M. Armstrong, C.A. Roobottom, B. Fox, S. Jackson; Plymouth/UK

Purpose: To compare image quality of CT images acquired at standard dose (SD) and low dose (LD) using adaptive statistical iterative reconstruction (ASIR) and model-based iterative reconstruction (MBIR) techniques.

Material and Methods: 65 patients were prospectively recruited with informed consent. They underwent SD and LD CT colonography. Both sets of scans were reconstructed with ASIR and MBIR. Objective and subjective image qualities were assessed as well as diagnostic accuracies for significant colonic and extra colonic lesions (e.g. polyps, colonic cancer, liver lesions, etc.). Effective doses for each scans were recorded.

Results: Objective image analysis supports significant noise reduction and superior contrast-to-noise ratio with low-dose scans using MBIR technique (p<0.05) compared to SD ASIR. Subjective image parameters were equivalent for LD MBIR and SD ASIR for both colonic and extra-colonic findings (p>0.05, overlapping 95% CI). Diagnostic accuracies for polyp detection were comparable although the numbers were too few to reach significance (p>0.05). Substantial dose reduction was achieved with LD scan (average 4.2 mSv) compared to SD scan (average 8.9 mSv) in our population group.

Conclusion: MBIR shows superior reduction in objective noise whilst maintaining subjective image quality and most importantly substantial dose reduction can be achieved. This small study confirms feasibility of using MBIR in performing low-dose CT colonography. A larger study is underway to assess diagnostic accuracies specifically for polyp detection.

DOI: 10.1007/s13244-013-0254-8

SS 12.08

CT colonography with adaptive statistical iterative reconstruction: estimation of dose radiation and diagnostic accuracy in a screening population

R. Scandiffio, A. Mantarro, L. Faggioni, E. Neri, C. Bartolozzi; Pisa/IT

Purpose: Dose reduction is a hot topic in imaging, especially for screening examination such as CTC. Aim of the paper is to evaluate and validate a method to reduce dose in CTC and control image noise using an adaptive statistical iterative reconstruction (ASiR).

Material and Methods: From March to December 2012, 253 patients underwent CTC for colorectal cancer screening on a 128-row CT scanner. Examination protocol included both supine and prone acquisition; a very low-dose protocol was used, and static tube current was set at 30 mAs. ASiR was used to subtract noise. Three experienced radiologists reviewed examinations; in case of positive findings, endoscopy was performed and was considered the gold standard. DLP, CTDI were evaluated; per-segment image quality was assessed visually using a semiquantitative score (1=poor, 2=adequate, 3=excellent). Sensitivity and specificity were assessed.

Results: Mean DLP and CTDI resulted significantly lower than in usual CTC protocol (mean value 45.35 mGy/cm and 0.90 mGy, respectively). Image quality was considered adequate (mean value: 2). Sensitivity and specificity in lesion detecting were 94.6% and 98.8% for lesions between 6 and 9 mm, and 100% and 99.4% for lesions between 10 and 30 mm.

Conclusion: ASiR allows a significantly dose decreasing preserving image quality, anatomical details and technique efficacy.

SS 12.09

Review of CT colonography: real-life experience of one thousand cases in a tertiary referral centre

A.E. Smyth, C.F. Healy, P. Macmathuna, H.M. Fenlon; Dublin/IE

Purpose: The purpose of this study was to review the indications for and findings of 1000 most recent CT colonography examinations performed in a tertiary referral hospital campus.

Material and Methods: Data on patient demographics, indications and findings were analysed from a dedicated database.

Results: Over a 5-year period (January 2008 - December 2012), 1000 CT colonography studies were performed. The median age of patient was 70 years (interquartile range 60-78). Patients were symptomatic in 86% of cases, while screening accounted for 8% and surveillance in patients with a history of polyps or colorectal cancer accounted for 6%. In 42% of patients, the study was performed following an incomplete optical colonoscopy. CT colonography was normal or had benign findings in 75% of patients. Neoplasia was observed in 19%: colorectal carcinoma 5.5%, polyps >1cm in 7.7% and smaller polyps <1cm in 5.7%. In this patient group, there was an extracolonic finding that required further evaluation in 18.5% with 5.5% found to have a potentially clinically significant finding. There was no significant procedure related complications.

Conclusion: This review describes the real life experience of CT colonography in a largely elderly, symptomatic patient group. In this patient group, CT colonography safely confirmed the need for no further bowel tests in 75%, identified colorectal cancer in 5.5% and clinically significant extracolonic findings in 5.5% of cases.

SS 12.10

Evaluation of two minimal-preparation iodine only regimes for CT colonography: implications for patient compliance and mucosal cleansing and correlation with bowel habit

H.S. Sidhu, G. Bhatnagar, R. Ilangovan, P. Shorvon, J. Muckian, R. Baldwin, K. Smith, M. Marshall, D. Burling, A. Gupta; Harrow/UK

Purpose: Minimal iodine-only preparations are increasingly established at CTC in optimising patient acceptability whilst producing diagnostic-quality studies. Debate exists concerning optimal regime and little is known regarding variation with bowel habit (BH). This study compares use of 2-day preparation with 1-day regime in compliance, mucosal cleansing and correlation with BH.

Material and Methods: Prospective study with 400 consecutive patients receiving Regime-1 (R1, N=200) two doses of 50 ml iodinated-contrast over 2 days (with low residue diet; LRD) or Regime-2 (R2, N=200) two doses of 50 ml contrast over 1 day (LRD). Interview at CTC recorded compliance with contrast and LRD. BH recorded on four-point frequency scale. CTC mucosal cleansing adequacy scored by experienced GI-radiologists.

Results: R1 compliance with iodinated-contrast 97% and LRD 95.5% (non-compliant excluded subsequently). Overall adequacy mucosal cleansing 92.0%, by BH: 94.4% (134/142) BO>1/day, 88.9% (24/27) BO>1/two-days, 80% (12/15) BO>1/five-days, 66% (2/3) BO<1/five-days. R2 compliance with iodinated-contrast 99.5% and LRD 96.2%. Overall adequacy mucosal cleansing 94.4%, by BH: 97.5% (157/161) BO>1/day, 92% (23/25) BO>1/two-days, 77.8% (7/9) BO>1/five days, 50% (1/2) BO<1/five-days. Significantly greater compliance with iodinated-contrast in R2 ($p<0.05$) with improved LRD compliance. No statistical difference ($p=0.34$) in mucosal cleansing adequacy. Trend towards poorer mucosal cleansing with decreasing BO frequency in both regimes.

Conclusion: One-day minimal-regime results in significantly greater compliance with no statistical difference in mucosal cleansing. There is a trend towards suboptimal cleansing with decreasing frequency of bowel opening.

DOI: 10.1007/s13244-013-0254-8

11:00 - 12:30 **Room F**

Scientific Session 13

Liver functional imaging and response assessment

SS 13.01

Assessment of liver cirrhosis using T1 mapping on Gd-EOB-DTPA enhanced 3T MRI

M. Haimerl, N. Verloh, C. Niessen, C. Fellner, A.G. Schreyer, C. Stroszczynski, P. Wiggermann; Regensburg/DE

Purpose: To assess differences in T1 maps of liver parenchyma between normal and cirrhotic livers on contrast- enhanced MRI obtained with GD-EOB-DTPA.

Material and Methods: A total of 71 patients with normal (n=36) and cirrhotic liver (n=35; Child-Pugh class A, n=16; B, n=14; C, n=5) underwent Gd-EOB-DTPA-enhanced 3T MRI. To obtain T1 maps, two TurboFLASH sequences (TI=400ms, 1000ms) were acquired before and 20 min after Gd-EOB-DTPA administration. Region-of-interest measurements were used to define signal intensity of T1 maps in normal and cirrhotic liver parenchyma indicating Gd-EOB-DTPA liver uptake and T1 relaxation time.

Results: T1 relaxation time of non-enhanced MRI (778±136ms) and Gd-EOB-DTPA-enhanced MRI (339±121ms) were significantly different ($p<0.001$): mean decrease of T1 relaxation time was 56 ± 14%. T1 relaxation time for non-enhanced MRI showed no significant differences between normal and cirrhotic livers (p= 0.59- 0.98). After administration of Gd-EOB-DTPA T1, relaxation time increased significantly between normal-liver and Child-Pugh class B and C patients, respectively ($p<0.001$). There was a constant, significant increase of T1 relaxation time from Child-Pugh class A up to class C patients (Child-Pugh class A, 311±84ms; B, 438±87ms; C, 545±71ms) coming along with a constant decrease of Gd-EOB-DTPA liver uptake (Child-Pugh class A, 60±9%; B, 43±11%, C, 30±6%).

Conclusion: Evaluation of changes in T1 mapping of the liver parenchyma may serve as a useful method to determine severity of liver cirrhosis.

SS 13.02

Comparison between CT perfusion and indocyanine green retention test results in the assessment of hepatic function

R. De Robertis, M. D'Onofrio, S. Crosara, S. Canestrini, G. Puntel, R. Pozzi Mucelli; Verona/IT

Purpose: To assess the reliability of perfusion CT for the estimation of liver function in patients scheduled for hepatic resection, comparing these results with those obtained with the indocyanine green retention.

Material and Methods: 31 patients with hepato-biliary malignancies (13/31 hepatocarcinomas; 5/31 peripheral cholangiocarcinomas; 12/31 hilar cholangiocarcinomas; 1/31 colonic adenocarcinoma metastases), scheduled for liver resection, were prospectively included in this study. In all cases, a pre-operative perfusional CT and the indocyanine green retention test were performed. The results were compared using Pearson's correlation test.

Results: The comparison between single arterial input time to peak values and indocyanine green retention values at 15 min (ICGR15) and plasma disappearance rate (PDR) showed high correlation (R=0.84 and -0.80); the comparison between single portal input time to peak values, ICGR15 and PDR showed high correlation (R=0.88 and -0.83).

Conclusion: Perfusion CT may be a method to estimate liver function. Time to peak values obtained with single input analysis had shown good correlation with IGR15 and PDR values.

SS 13.03

Effects of liver cirrhosis on Gd-EOB-DTPA enhanced 3 T MRI

M. Haimerl, N. Verloh, J. Rennert, R. Müller-Wille, C. Fellner, P. Wiggermann, E.M. Jung, C. Stroszczynski; Regensburg/DE

Purpose: The purpose of this study was to assess differences in enhancement effects of liver parenchyma between normal and cirrhotic livers on dynamic, Gd-EOB-DTPA-enhanced 3 T MRI.

Material and Methods: 93 patients with cirrhotic liver (normal, n=54; Child-Pugh class A, n=18; B, n=16; C, n=5) underwent contrast-enhanced 3 T MRI. T1-weighted volume interpolated GRE sequences with fat suppression were acquired before contrast injection in the arterial phase (AP), in the late arterial (LAP) phase, in the portal venous phase (PVP), and in the hepatobiliary phase (HBP) after 20 min. The relative enhancement (RE) of the signal intensity of the liver parenchyma was calculated for all phases.

Results: Mean RE for patients with normal liver and patients with a Child-Pugh score A increased significantly over time in all phases ($p\leq0.002$-0.001). Child-Pugh class B patients showed no increase between the PVP (0.50±0.22) and the HBP (0.46±0.17) ($p=0.501$). Patients with a Child-Pugh Score C showed a significant increase ($p=0.043$) between AP (0.15±0.11), LAP (0.45±0.12) and PVP (0.50±0.13) and a significant ($p=0.043$) decrease for HBP (0.29±0.04). RE in the hepatobiliary phase was significantly different among all evaluated groups and with increasing severity of liver cirrhosis, a constant reduction of RE could be shown ($p\leq0.021$-0.001).

Conclusion: RE of liver parenchyma is negatively affected by increased severity of liver cirrhosis. Evaluation of RE might help to define the grade of liver disease.

SS 13.04

Assessment of liver perfusion by multi-parametric MR-DWI: correlation with phase-contrast portal venous flow measurements

F. Regini[1], S. Colagrande[1], L.N. Mazzoni[1], S. Busoni[1], B. Matteuzzi[1], P. Santini[2], R. Wyttenbach[2]; [1]Florence/IT, [2]Bellinzona/CH

Purpose: To verify in vivo the bi-exponential model of signal decay in diffusion-weighted imaging (DWI) in liver parenchyma by evaluation of related parameters: apparent diffusion coefficient (ADC), slow diffusion coefficient (D), fast diffusion coefficient (D*) and perfusion fraction (PF).

Material and Methods: Forty healthy volunteers (19 f, mean age 32 years; range 20-52 years), underwent MR imaging at 3.0 T including 2D-Phase-Contrast (PC) acquisitions (Venc=40 cm/s) to measure portal venous flow, and DWI acquisitions (free breath, 14 b-values, b-range=0-800 s/mm^2), repeated before and 30 min after a standard meal (600 Kcal). DWI parameters were calculated using signal intensities at every b value, measured with four different circular ROIs drawn on right liver lobe. Paired sample t-test and Pearson correlation coefficient test were performed to evaluate differences in various parameters when calculated before and after the meal and to detect possible correlation with portal flow.

Results: After the meal portal flow increased in all the subjects (mean increment±SD=887±281 ml/min; 96±33%). ADC, D, and PF did not show a statistically significant increment after meal at t-test, while D* did (mean increment±SD=34±46%, $p<0.001$). Pearson correlation coefficient did not show a significant correlation of portal flow and D* increment when calculated before and after the meal.

Conclusion: D* increases significantly with portal flow, confirming its dependence on perfusive phenomena, as hypothesized originally by Le Bihan. This observation underlines the possible role of D* evaluation in conditions involving perfusional changes.

DOI: 10.1007/s13244-013-0254-8

SS 13.05

Quantitative evaluation of hepatocellular uptake function with use of gadolinium disodium-enhanced MR imaging: comparison of dynamic pharmacokinetic analysis and static signal intensity analysis

A. Yamada[1], S. Yanagisawa[1], M. Kurozumi[1], Y. Fujinaga[1], K. Ueda[1], M. Kadoya[1], S. Miyagawa[1], K. Maruyama[2]; [1]Matsumoto/JP, [2]Tokyo/JP

Purpose: The purpose of this study is to compare dynamic and static methods in the quantitative evaluation of hepatocellular uptake function with use of gadolinium disodium-enhanced MR imaging.

Material and Methods: We retrospectively evaluated 23 consecutive patients who underwent dynamic gadoxetate disodium-enhanced MR imaging and indocianine green (ICG) clearance test. T1-weighted images with fat suppression were obtained at pre-contrast and 25, 28, 31, 34, 37, 40, 43, 46, 60, 120, 180, 1200 s after intra-venous administration of contrast agent using k-space weighted image contrast reconstruction (Radial-VIBE). Intracellular uptake rate (Ki) at the region of interest located in the part of the liver was determined applying obtained images into dual-inlet two-compartment uptake model. Hepatocellular uptake index (HUI) and volume (V) of the whole liver were determined from static contrast enhanced-images at hepatobiliary phase. The correlation coefficients for power regression between plasma disappearance rate of ICG (ICG-PDR) and parameters (V, Ki, Ki*V and HUI) were evaluated.

Results: The 95% confidence interval of correlation coefficient was significantly higher in HUI (0.76 to 0.78) than in the other parameters (0.10 to 0.12 for V; 0.61 to 0.63 for Ki; 0.64 to 0.66 for Ki*V).

Conclusion: Hepatocellular uptake function can be evaluated quantitatively and efficiently with use of HUI determined from static gadoxetate disodium-enhanced MR images at hepatobiliary phase.

SS 13.06

Prediction and monitoring of treatment effect using T1-weighted dynamic contrast-enhanced MRI in colorectal liver metastases: potential of whole tumour ROI and selective ROI analysis

K. Coenegrachts, A. Bols, M. Haspeslagh, H. Rigauts; Bruges/BE

Purpose: To evaluate dynamic contrast-enhanced magnetic resonance imaging (DCE-MRI) for prediction and early monitoring of treatment in colorectal liver metastases.

Material and Methods: Ten patients were included. Baseline and follow-up DCE-MRI examinations were evaluated by whole tumour and selected ROI placements calculating Kep-values. Selective ROIs, concentric-like and hot spot, were drawn on early arterial phase images. Monitoring of treatment was performed comparing RECIST1.1 criteria with whole tumour and selected ROI placement. To evaluate treatment effect between responders and non-responders, independent samples t-test was used on Kep-values.

Results: In each patient, largest lesion was evaluated totalling 10 target lesions. At baseline, for whole tumour ROI placements mean Kep-values in responders were significantly higher than mean Kep-values in non-responders ($t = 7.481$, $p<0.001$). Selective ROI placement comparison of mean Kep-values at baseline and after 6 weeks of treatment (first follow-up measurement) showed significant decrease in responding patients ($t=4.706$, $p=0.003$) whereas increase in Kep-values in non-responding patients was not statistically significant.

Conclusion: This preliminary study shows that baseline Kep for whole tumour ROI is a predictor for treatment outcome. Decrease of Kep using selective ROIs allows early identification of response after 6 weeks of treatment.

SS 13.07

Assessment of treatment response after selective internal radiation therapy using diffusion-weighted imaging

A. Barabasch, A. Ciritsis, N.A. Kraemer, C.K. Kuhl; Aachen/DE

Purpose: Fluorodeoxyglucose-uptake quantified by standardized uptake value (SUV) in positron-emission-tomography (PET)/CT-scans is an established parameter for tumour response following SIRT. Aim of the study was to compare the accuracy of liver-MRI to PET/CT for early treatment response assessment 8 weeks after SIRT.

Material and Methods: Between June 2010 and June 2012, 103 SIRTs in 57 patients were performed for treatment of liver metastasis. 18 patients (12 female; 10 colorectal, 7 breast and 1 cholangiocellular carcinoma) received contrast-enhanced liver-MRI and contrast-enhanced PET/CT-scans within 6 weeks prior and 8 weeks after SIRT of the right liver lobe. Three target lesions per patient were defined. In both modalities, changes of tumour size, contrast-enhancement, apparent diffusion coefficient (ADC)-values and SUV were compared before and after SIRT and validated by long-term follow up.

Results: After SIRT, average maximal SUV decreased from 7.86 to 5.34 (-32%; $p<0.02$) and average minimal ADC-value increased from 540×10^{-6} mm²/s to 729×10^{-6} mm²/s (+35%; $p<0.05$). No significant changes in tumour size and contrast enhancement were observed on MRI or PET/CT scans. Follow-up imaging confirmed response to SIRT in patients with significant ADC changes.

Conclusion: These preliminary results indicate that changes of ADC-values in liver-MRI are useful to predict response to SIRT well before any change of tumor size or perfusion. Accordingly, liver-MRI with DWI can be used to evaluate treatment response just as PET/CT.

SS 13.08

Transient sinusoidal dilatation appearing as mosaic pattern on CT/MR imaging can be related to extrahepatic infectious or inflammatory states

M. Ronot, A. Kerbaol, M. Zappa, M.-P. Vullierme, P. Bedossa, V. Vilgrain; Clichy/FR

Purpose: To describe CT/MR findings of patients who had sinusoidal dilatation associated with extrahepatic infectious or inflammatory disease.

Material and Methods: From 2005 to 2012, patients who had extrahepatic infectious or inflammatory disease, and CT and/or MR of the liver showing mosaic enhancement pattern (MP) were selected. MP was defined as areas of high signal intensity of the liver on T2-weighted sequences and reticular enhancement on arterial and/or portal phases, which appear homogeneous on delayed phase. Clinical, biological, and imaging features were noted at the time of diagnosis and at follow-up.

Results: All (n=12) patients were women (median age: 30 years; 18-68) and among them 5 patients (42%) had OC intake. No patients had hepatic venous outflow impairment. Extrahepatic diseases were as follows: pyelonephritis (n=7), pancreatitis (n=2), pneumonia (n=1), septicaemia (n=1), and colitis (n=1). MP was seen on both arterial and portal phases in 7/12, 58% and on portal phase only in 2/12, 17%. MP was diffuse in all livers but more prominent in the sub-capsular areas. Four patients (33%) had liver biopsy, which showed sinusoidal dilatation. Nine patients (75%) had follow-up imaging with a median delay of 60 days, and abnormal liver enhancement disappeared in 7/9 cases (78%).

Conclusion: Extrahepatic infectious or inflammatory disease can be responsible for transient sinusoidal dilatation, which appears as mosaic pattern on CT/MR imaging.

DOI: 10.1007/s13244-013-0254-8

SS 13.09

Perfusion CT of hepatocellular carcinoma with the axial shuttle technique and iterative image reconstruction: preliminary experience

L. Faggioni, F. Pancrazi, I. Bargellini, P. Vagli, R. Sacco, G. Bresci, C. Bartolozzi; Pisa/IT

Purpose: To assess the feasibility of CT perfusion imaging (pCT) of hepatocellular carcinoma (HCC) on a 64-row scanner with extended lesion coverage and iterative image reconstruction.
Material and Methods: Thirteen patients (total 18 HCC) underwent pCT on a 64-row CT scanner (Discovery CT750 HD, General Electric) with z-axis coverage of 8 cm obtained through continuous table toggling (axial shuttle) and an iterative image reconstruction algorithm (ASIR™). Blood flow (BF), blood volume (BV), mean transit time (MTT), hepatic arterial fraction (HAF), and permeability-surface product (PS) parameters were computed in the HCC and the surrounding liver parenchyma (P). The rate of non-assessable HCC due to incomplete lesion coverage and dose-length product (DLP) values were compared with those achieved on 14 patients (total 23 HCC) previously evaluated on a 64-row scanner with 4 cm coverage and standard filtered backprojection (LightSpeed VCT).
Results: BF, BV, HAF, and PS were higher, and MTT lower in HCC than in P ($p<0.01$). The rate of non-assessable lesions was lower in the 8-cm coverage, ASIR™ group than in the 4-cm group (17% vs 26%, $p=0.024$). DLP was also lower in the 8-cm ASIR™ group (221.6±75.9 vs 598.2±135.4 mGy cm, $p<0.01$).
Conclusion: Compared with a standard pCT protocol, pCT of HCC lesions with extended lesion coverage and iterative image reconstruction is associated with a significantly higher rate of assessable lesions and lower radiation dose.

SS 13.10

Evaluation of T1rho as a potential MR biomarker for liver cirrhosis: comparison of healthy control subjects and patients with liver cirrhosis

I. Rauscher[1], C. Ganter[1], P. Martirosian[2], E.J. Rummeny[1], K. Holzapfel[1]; [1]Munich/DE, [2]Tübingen/DE

Purpose: To compare mean liver $T_{1\rho}$ values in patients with liver cirrhosis and healthy control subjects in order to evaluate $T_{1\rho}$ as a potential MR biomarker for liver cirrhosis.
Material and Methods: Ten healthy control subjects and 17 patients with clinically diagnosed and/or biopsy-proven liver cirrhosis were examined at 1.5T. $T_{1\rho}$-weighted images were acquired using a 2D Turbo FLASH sequence (TR/TE 3000/1.31 ms, FA 8°, FoV 309×380mm, resolution 2×2×6 mm, acquisition time 15 s) with Spin-Lock preparation. $T_{1\rho}$ maps were calculated from five breath-hold measurements, performed with different Spin-Lock-times (4, 8, 16, 32, 48 ms). Mean liver $T_{1\rho}$ values were calculated and compared using two-tailed student-t-test. In addition, a receiver operating characteristic (ROC) curve analysis was performed to evaluate the utility of mean liver $T_{1\rho}$ for the prediction of liver cirrhosis.
Results: Mean liver $T_{1\rho}$ values in patients with liver cirrhosis (57.7 ± 8 ms) were significantly higher than those of healthy control subjects (48.6 ± 3.5 ms; $p=0.006$). According to the ROC analysis at a threshold value of 51.4 ms, the sensitivity and specificity of mean liver $T_{1\rho}$ in predicting liver cirrhosis were 86.7 and 88.9%, respectively. The area under the ROC curve was 0.87.
Conclusion: Mean liver $T_{1\rho}$ values in patients with liver cirrhosis were significantly higher than those in healthy subjects suggesting a potential role of liver $T_{1\rho}$ as a MR biomarker for liver cirrhosis.

11:00 - 12:30 **Room H3**

Scientific Session 14

Imaging of the colon and rectum

SS 14.01

Does imaging of the pattern of relapse justify the hypothesis for benefit in more radical right colon surgery?

R. Balasubramaniam, A. Tan, D. Jayne, D.J.M. Tolan; Leeds/UK

Purpose: To evaluate the pattern of recurrence following elective right hemicolectomy for colon cancer and extrapolate potential benefit of D2 from more radical D3 resection in patients with right colon adenocarcinoma.
Material and Methods: Retrospective analysis was performed on patients undergoing D2 right hemicolectomy for adenocarcinoma in a tertiary referral centre over 6 years from 2005 to 2010. All post-operative imaging was independently reviewed by two radiologists blinded to histology to assess the pattern and form of relapse.
Results: Of 267 patients undergoing elective right hemicolectomy, 41 developed disease recurrence. Of these 10.5% (28/41) presented first with haematogenous metastasis; in these, liver was the commonest site (36.6%) and earliest organ affected followed by pulmonary metastasis (24.4%). Isolated nodal recurrence was rare (1/41, 2.4% of metastases). Metastatic disease did not arise in any patients with node negative T2 or less primary tumours of the right colon.
Conclusion: Right colon cancers tend to first undergo haematogenous metastasis (28/41). The higher incidence of pulmonary metastasis reinforces the importance of pre- and post-operative CT thorax. The low incidence of nodal recurrence provides no evidence to justify a routine practice of a more radical D3 resection in elective curative right colon cancer surgery. The absence of recurrence in node negative T2 primary disease indicates a more customised post-operative follow-up protocol based on the histology could prove more efficient as early surveillance for low-grade tumours appears unnecessary.

SS 14.02

Regorafenib therapy effects on human colon carcinoma xenografts monitored by dynamic contrast-enhanced computed tomography with immunohistochemical validation

C.C. Cyran, P.M. Kazmierczak, H. Hirner, M. Moser, M. Ingrisch, L. Havla, R. Eschbach, E. Baloch, B. Schwarz, M.F. Reiser, C.J. Bruns, K. Nikolaou; Munich/DE

Purpose: To investigate dynamic contrast-enhanced computed tomography (DCE-CT) for monitoring the effects of regorafenib on experimental colon carcinomas in rats by quantitative assessments of tumor microcirculation parameters with immunohistochemical validation.
Material and Methods: Colon carcinoma xenografts (HT-29) implanted subcutaneously in athymic rats (n=15) were imaged at baseline and after a 1-week treatment with regorafenib by DCE-CT (128-slice dual-source). The therapy group (n=7) received regorafenib daily (10 mg/kg bodyweight). Quantitative parameters of tumor microcirculation (plasma flow, mL/100mL/min), endothelial permeability (PS, mL/100mL/min), and tumor vascularity (plasma volume, %) were calculated using a 2-compartment uptake model. DCE-CT parameters were validated with immunohistochemical assessments of tumor microvascular density (CD-31), tumor cell apoptosis (TUNEL), and proliferation (Ki-67).
Results: Regorafenib significantly ($p<0.05$) suppressed tumor perfusion (12.8±2.3 to 8.8±2.9 mL/100 mL/min) and tumor vascularity (15.7±5.3 to 5.5±3.5%). Significantly lower microvascular density was observed in the therapy group (CD-31; 48±10 vs. 113±25, $p<0.05$). In regorafenib-treated tumors, significantly more apoptotic cells (TUNEL; 11,844±2,927 vs. 5,097±3,463, $p<0.05$) were observed. DCE-CT tumor perfusion and vascularity correlated significantly ($p<0.05$) with microvascular density (CD-31; $r=0.84$ and 0.66) and inversely with apoptosis (TUNEL; $r=-0.66$ and -0.71).
Conclusion: Regorafenib significantly suppressed tumor perfusion and vascularity quantified by DCE-CT in experimental colon carcinomas in rats with good to moderate correlations to an immunohistochemical gold standard. Tumor response biomarkers assessed by DCE-CT may be a promising future approach to a more personalized and targeted cancer therapy.

DOI: 10.1007/s13244-013-0254-8

SS 14.03

Is there a role for minimal preparation CT in bowel cancer screening?

D. Shetty, M. Strugnell, G.F. Maskell; Truro/UK

Purpose: The NHS Bowel Cancer Screening Programme (BCSP) offers screening every 2 years to all men and women in England aged 60– 69. An abnormal faecal occult blood test results in the patient undergoing colonoscopy. Patients unsuitable for colonoscopy or those with an incomplete colonoscopy are offered CT colonography (CTC). A small number of patients are considered unsuitable even for CTC, usually due to multiple co-morbidity or immobility. These have been referred for minimal preparation CT (MPCT) with oral contrast alone. These cases were retrospectively reviewed to determine what effect MPCT had on outcomes in this group of patients.

Material and Methods: Clinical, radiology and endoscopy records were reviewed for all patients referred for MPCT from the NHSBCSP in Cornwall, UK, from 2010 to 2012.

Results: 22 patients underwent MPCT. Indications were multiple co-morbidity in 11 (50%), severe immobility in 7 (32%) and mental incapacity in 4 (18%). Three patients (14%) had a positive result (suspected polyp or cancer). Only one patient (4.5%) had a polyp subsequently confirmed and treated by colonoscopy. One patient had a negative colonoscopy and one patient was considered unfit for further investigation.

Conclusion: The limited diagnostic value of MPCT makes it unsuitable for use in a screening programme. Patients in this group who are unfit for CTC are usually also unfit for subsequent therapeutic intervention even when pathology has been demonstrated.

SS 14.04

Role of perfusional MRI and DWI to predict pathological complete response to neoadjuvant chemoradiotherapy in rectal cancer

C.N. De Cecco[1], M. Ciolina[1], P. Lucchesi[2], M.M. Maceroni[2], F. Vecchietti[2], F. Iafrate[1], A. Laghi[2]; [1]Rome/IT, [2]Latina/IT

Purpose: To determine the ability of perfusional MRI (pMRI) and diffusion-weighted imaging (DWI) to predict pathological complete response (pCR) in patient treated with chemoradiotherapy.

Material and Methods: Eleven consecutive patients underwent pre-, during and post-treatment dynamic contrast-enhanced MRI performed at 3T. Gadolinium 0.1 mmol/kg was injected at a rate of 3 mL/s. Treatment protocol consisted of neoadjuvant chemoradiotherapy with oxaliplatin and 5-fluorouracile. Ktrans, Kep, Ve and IAUGC90 were calculated. Tumoral dimension and apparent diffusion coefficient (ADC) were analysed. Surgical specimens were the gold standard. For variable comparison, Spearman's rank correlation and Kruskal-Wallis test were used. $P<0.05$ was considered significant.

Results: Six patients showed cPR. Baseline Ktrans, IAUGC90 and Ve were significantly higher in non-responder (NR) patients (1.22±1.03 min^{-1}, 1.36±1.07 mM/s, 0.7±0.4) in comparison to cPR (0.92±0.91 min^{-1}, 0.69±0.6 mM/s, 0.37±0.15); Kep was significantly lower in NR (1.6±0.65 min^{-1} vs 2.93±2.71 min^{-1}). A significant reduction in Ktrans, IAUGC90 and Ve was observed in NR during (0.68±0.58, 0.62±0.33, 0.52±0.1) and after treatment (0.047±0.016, 0.052±0.025, 0.19±0.28); instead in cPR patient a significant increase in perfusional values was reported (1.24±1.15, 1.21±0.96, 0.63±0.26 and 1.13±1.36, 1.24±1.34, 0.59±0.34). No difference in baseline ADC value was observed between cPR (0.88±0.22x10^{-3} mm^2/s) and NR (0.85±0.09x$10^{-3}$$mm^2$/s). In cPR mean tumour ADC significantly increase during treatment comparing to NR (1.22±0.6x10^{-3} mm^2/s vs 0.98±0.12x10^{-3} mm^2/s). No correlation was found between ADC values and pMRI parameters.

Conclusion: pMRI and ADC values are two independent parameters to predict rectal tumour response to chemoradiotherapy.

SS 14.05

Acceptability of oral iodinated contrast media: a head to head comparison of 4 agents

A. Pollentine, E. Ngan-Soo, R. Hunt, P. McCoubrie; Bristol/UK

Purpose: Patient compliance in ingestion of oral contrast can be crucial in obtaining a technically adequate study. We assessed the palatability and preference of four iodinated oral contrast agents commonly used in abdominopelvic CT and CT colonography (CTC).

Material and Methods: 80 volunteers sampled four common contrast agents, Omnipaque, Telebrix, Gastromiro and Gastrografin in a computer-generated random order. Each agent was anonymised and diluted to a standard concentration of 30 mg iodine/ml, the dilution used for faecal tagging in our institution. A 100 mm visual analogue scale and a 7-point Likert scale were used to rate palatability. Willingness to drink 3 aliquots of 200 ml of each of the contrast agents over a 48 h period was also assessed, as per our institution's current bowel preparation protocol for CTC.

Results: Gastrografin was rated significantly less palatable than the remaining agents ($p<0.005$). Omnipaque and Telebrix were significantly more palatable than Gastromiro. No difference existed between Omnipaque and Telebrix. 39% of participants would refuse to consume the quantities of Gastrografin required for a CTC examination compared to Telebrix (7%) and Omnipaque (9%) ($p<0.05$).

Conclusion: Omnipaque and Telebrix are significantly more palatable than both Gastromiro and Gastrografin with participants more willing to ingest them in larger quantities, thereby reiterating the influence of palatability on patient compliance. We feel that this will directly influence the technical adequacy of CTC studies.

SS 14.06

CT colonography: clinical evaluation of novel software to automatically co-register polyps between follow-up surveillance studies

E. Helbren[1], H. Roth[1], T. Hampshire[1], P.J. Pickhardt[2], D. Hawkes[1], S. Halligan[1]; [1]London/UK, [2]Madison, WI/US

Purpose: To evaluate the software that aims to automatically identify and then register polyp location across sequential CTC acquisitions performed for polyp surveillance.

Material and Methods: We developed a registration algorithm to match endoluminal colonic surfaces between prone and supine CTC acquisitions. Haustral folds were automatically matched between scans to initialize a registration method that establishes correspondence over the entire colonic surface via non-rigid registration. Initial and follow-up CTC from 11 patients (14 polyps) undergoing surveillance were selected and the algorithm was tested via two methods: "Direct" (the algorithm used polyp co-ordinates from the initial prone and supine acquisitions to automatically predict polyp location on follow-up CTC) and "loop" (polyp co-ordinates from initial supine acquisition were used to predict polyp location on the initial prone acquisition, then follow-up prone, follow-up supine and back to initial supine, respectively). Registration accuracy was assessed by two observers via the Euclidean distance between true and predicted polyp locations.

Results: Successful polyp registration was achieved in all 11 cases for all 14 polyps using both loop and direct methods. Mean Euclidean registration error for individual polyps was 2.0 cm (range 0.1 to 9 cm) for "direct" method and 3.1 cm (range 0.3 to 8.5 cm) for "loop" method.

Conclusion: Our algorithm achieved automated registration of polyps across temporally separate CTC studies. This may facilitate rapid detection of known polyps in patients undergoing CTC surveillance.

DOI: 10.1007/s13244-013-0254-8

SS 14.07

True- and false-positive diagnosis of extracolonic cancers by CT colonography: discrete choice experiment

A. Plumb[1], S. Halligan[1], D. Boone[2], E. Helbren[1], S. Zhu[3], G.L. Yao[3], N. Bell[1], A. Ghanouni[1], C. Von Wagner[1], S.A. Taylor[1], S. Mallett[4], D. Altman[4], R. Lilford[3]; [1]London/UK, [2]Colchester/UK, [3]Birmingham/UK, [4]Oxford/UK

Purpose: To determine how healthcare professionals balance the potential benefits of detecting extracolonic cancer at screening CT colonography (CTC) versus risks of unnecessary investigations due to false-positives.

Material and Methods: 30 healthcare professionals underwent a discrete choice experiment. Participants chose between two hypothetical tests for colorectal cancer screening. One was unable to diagnose extracolonic cancer but generated no false positives (FP), whereas the other diagnosed a curable extracolonic cancer in 1 in 600 screenees, but generated FP. The FP rate was varied systematically to determine the "tipping point" at which the rate was deemed sufficient to outweigh the benefit of detecting cancer. FP leading to follow-up imaging and those precipitating invasive tests were presented separately.

Results: 14/30 (47%) participants were prepared to tolerate any rate of follow-up imaging to diagnose 1 extracolonic cancer in 600 screenees. Across all participants, the mean rate of further imaging deemed acceptable was 53.5%. Invasive tests were less acceptable: The mean "tipping point" was an invasive test rate of 9.7% to diagnose 1 in 600 screenees with a curable extracolonic cancer.

Conclusion: Healthcare professionals will tolerate numerous extracolonic FP by CTC if the consequence is simply further imaging. Tolerance for invasive tests is lower. The specificity of CTC for clinically significant extracolonic findings is likely to be highly acceptable to healthcare professionals, including surgeons, gastroenterologists and radiologists.

SS 14.08

Diverticular disease severity score based on computed tomographic colonography

N. Flor[1], P. Rigamonti[1], S. Romagnoli[1], A. Pisani Ceretti[1], F. Balestra[1], F. Sardanelli[1], G.P. Cornalba[1], P.J. Pickhardt[2]; [1]Milan/IT, [2]Madison, WI/US

Purpose: We propose a diverticular disease severity score (DDSS) based on CT colonography (CTC) findings.

Material and Methods: Seventy-nine patients (62±14.5 years; 39 females, 40 males) underwent CTC after acute diverticulitis. Two independent readers classified each case on 2D MPR using a 4-point DDSS, based on sigmoid colon wall thickness and lumen diameter: 1=wall thickness <3 mm, lumen diameter ≥15 mm; 2=wall thickness 3-8 mm, lumen diameter ≥15 mm; 3=wall thickness ≥8 mm, lumen diameter 5-15 mm; 4=wall thickness≥8 mm, lumen diameter <5 mm. Intra- and inter-observer reproducibility was evaluated. Of 79 patients, 32 (40%) underwent surgery after CTC; maximum sigmoid wall thickness was measured on pathologic specimen. Cohen κ, X2, Kruskall-Wallis, and Jonckheere-Terpstra tests.

Results: Intra- and inter-observer reproducibility of DDSS was almost perfect (k=0.84-0.90). DDSS significantly correlated with patient age (p=0.017) and with the probability of surgical treatment (p=0.001). Pathology for the 32 resected specimens revealed acute/chronic diverticular inflammation only in 29 and superimposed sigmoid cancer (n=2) or Crohn's disease (n=1) in three patients. All three patients with important coexisting pathology had a DDSS of 4. Maximum wall thickness at pathology correlated with DDSS (p=0.008).

Conclusion: DDSS is highly reproducible and correlates with pathologic wall thickness, as well as the probability of surgery. Nearly one of three patients with DDSS of 4 had important superimposed sigmoid pathology. CTC with DDSS can provide valuable information for surgeons.

SS 14.09

Accuracy of CT colonography in detecting colorectal cancer at our District General Hospital in North Wales

S. Sinha, C. Corr; Wrexham/UK

Purpose: To assess accuracy of CTC in diagnosing colorectal cancer (CRC) at our hospital with respect to nationally and internationally agreed standards.

Material and Methods: A retrospective study analysing all CTC's from November 2006 to May 2011 was performed. Radiology reports were reviewed and correlated with data of all patients with CRC diagnosed up to November 2012, which was obtained from pathology and cancer services. The following were recorded from radiology reports: demographics; cancer diagnosis; equivocal findings and extra-colonic cancers.

Results: 841 CTC's were performed of which 47 had confirmed CRC identified as cancer, suspicious for cancer, or suspicious polyp on CTC. Sensitivity and negative predictive value (NPV) were 100%. 40 cases were identified as definite CRC with no colonoscopy advised and 39 were proven to be cancer. Specificity was 97.5% for definitive CRC diagnosis. 16 cases were 'suspicious but uncertain' and colonoscopy advised – 6 of these were cancer. 18 cases diagnosed as benign were confirmed as benign. Combined specificity with CTC and colonoscopy for CRC diagnosis was 96%. 30 unexpected extracolonic malignancies were identified where 3 were concurrent with CRC.

Conclusion: CTC is very accurate for diagnosing CRC with high NPV and sensitivity. Specificity is also high and increases with the complementary use of colonoscopy in equivocal cases. CTC should be used as a first-line imaging investigation for diagnosis of CRC.

SS 14.10

Appendiceal length as an independent risk factor for acute appendicitis

P.J. Pickhardt, J. Suhonen, B.D. Pooler; Madison, WI/US

Purpose: To determine if appendiceal lengths differ among adults with proven acute appendicitis compared with normal adult controls.

Material and Methods: Preoperative MDCT in 321 consecutive adults with surgically proven appendicitis was compared with MDCT in 321 consecutive adult controls undergoing CTC screening. Appendiceal length at MDCT was obtained using curved reformatted images along the appendiceal long axis. For validation, MDCT length was compared with gross pathology length for the appendicitis group.

Results: Appendiceal length at MDCT correlated well with gross pathology (mean length, 6.76 vs 6.56 cm). Mean appendiceal length and standard deviation of length at MDCT were both significantly greater in controls compared with the acute appendicitis group (7.87±3.49 cm vs 6.76±1.94 cm; p<0.001). Appendicitis cases outnumbered controls at every 0.5-cm interval between 4.0 cm and 9.5 cm. The odds ratio (OR) for acute appendicitis within the 4.0-9.5 cm interval was 5.4 compared with controls, and increased to 37.9 for the 2.25-13.75 cm interval. 88.5% (284/321) of appendicitis cases fell within the 4.0-9.5 cm range, compared with only 56.1% (180/321) of controls (p<0.001).

Conclusion: Appendiceal length strongly correlates with the likelihood of acute appendicitis. Specifically, "intermediate" appendiceal lengths (4.0-9.5 cm) are more frequently complicated by acute appendicitis, whereas both "long" (>9.5 cm) and "short" (<4.0 cm) appendiceal lengths are more frequently seen in adult controls and may be more resistant to developing appendicitis.

DOI: 10.1007/s13244-013-0254-8

11:00 - 12:30 **Room H2**

Scientific Session 15

HCC: From diagnosis to treatment

SS 15.01

Incidence and predictive factors for HCC recurrence after liver transplantation

A. Pecchi, G. Besutti, M. De Santis, C. Del Giovane, S. Nosseir, G. Tarantino, F. Di Benedetto, P. Torricelli; Modena/IT

Purpose: To estimate incidence of HCC recurrence after liver transplantation (LT) and to identify clinical, pathologic and imaging predictive factors for HCC recurrence after LT.

Material and Methods: 165 patients who underwent LT for HCC between October 2004 and November 2011 and survived more than 2 months were included. Clinical data as liver damage etiology, alphafetoprotein (AFP) before LT and type of immunosuppressive therapy undertaken after LT were collected. Imaging findings were retrospectively evaluated on pretransplantation contrast-enhanced MDCT/RM performed within 75 days before LT. Histopathological findings were obtained by a review of the pathologic reports. Incidence of recurrence was evaluated. Predictive factors for recurrence were estimated by using univariate analysis and X^2 test.

Results: Recurrence was found in 24 (14.5%) patients. Univariate analysis revealed the following significant prognostic factors for recurrence($p<0.05$): presence of viable tumor, more than three viable nodules, >3 cm diameter of largest nodule and >5 cm overall viable tumor size on both pathology and imaging; bilobar distribution, pathologic grade >1, capsule contact, vascular invasion, microsatellitosis on pathology; liver resection undertaken before LT, AFP level >10 ng/mL and cyclosporine alone as immunosuppressive therapy undertaken after LT among clinical and theraputic data.

Conclusion: Incidence of HCC recurrence after LT was 14.5%. Different imaging, pathologic and clinical data were predictive factors for HCC recurrence after LT.

SS 15.02

Hepatocellular carcinoma: comparison of enhancement patterns with gadoxetate disodium versus gadobenate dimeglumine

T. Tirkes, A. Aisen, K. Sandrasegaran, F. Akisik; Indianapolis, IN/US

Purpose: To determine if there is any difference in enhancement properties of hepatocellular carcinoma (HCC) during contrast-enhanced magnetic resonance imaging utilizing gadoxetic acid (Gd-EOB-DTPA, Eovist®, Bayer) versus gadobenate dimeglumine (Gd-BOPTA, MultiHance®, Bracco).

Material and Methods: 118 patients with HCC were scanned; 80 patients with Gd-BOPTA and 38 with Gd-EOB-DTPA using a 1.5T scanner. Breath-hold volumetric fat-suppressed sequences were performed at precontrast, arterial (20 s), portal (1 min) and equilibrium (2 min) phases. The GD-EOB-DTPA was administered at a dose of 0.025 mmol/kg body weight and at a rate of 1 mL/s. Gd-BOPTA was administered at a dose of 0.1 mmol/kg body weight and at rate of 2 mL/s. Bolus triggering software was utilized for both patient groups to optimize the contrast enhancement during the arterial phase. The contrast-to-noise ratio (CNR) was calculated by $(SI_{lesion} - SI_{liver})/SD_{background}$ (SD=standard deviation, SI= signal intensity).

Results: HCCs demonstrated peak enhancement during the arterial phase and continuing washout when scanned with either Gd-EOB-DTPA or Gd-BOPTA. CNRs of Gd-EOB-DTPA and Gd-BOPTA were similar in arterial (p=0.67), portal (p=0.17) and equilibrium phases (p=0.53). HCCs demonstrated lower CNRs with Gd-EOB-DTPA compared to Gd-BOPTA in all three phases.**Conclusion:** 1. There was no statistically significant difference in CNRs of HCCs during arterial, portal and equilibrium phases scanned with Gd-EOB-DTPA compared to Gd-BOPTA. 2. Using approved doses of Gd-EOB-DTPA, there was overall lower CNRs compared to Gd-BOPTA.

SS 15.03

Qualitative analysis of small (≤2 cm) regenerative nodules, dysplastic nodules and well-differentiated HCCs with gadoxetic acid MRI

M. Di Martino, V.C. Lombardo, R. Di Miscio, C. Catalano; Rome/IT

Purpose: To evaluate radiological findings and diagnostic accuracy of gadoxetic acid magnetic resonance imaging (MRI) in the evaluation of small (≤2cm) regenerative nodules (RN), dysplastic nodules (DN) and well-differentiated hepatocellular carcinomas (HCCs).

Material and Methods: Forty-six cirrhotic patients, with 72 focal liver lesions were retrospectively recruited. The MRI study protocol included T1-weighted and T2-weighted pre-contrast sequences and 3D spoiled gradient-echo T1-weighted post-contrast sequences Gd-EOB-DTPA-enhanced obtained during the arterial, portal-venous and equilibrium phases 25 s, 60 s 180 s and after 20 m. All lesions (27 RN, 20 DN and 25 HCCs) were pathologically confirmed. One radiologist not involved in the datasets analysis reported the signal intensity characteristics of each lesion. Two radiologists blinded to clinical and pathological information evaluate radiological dataset images. Sensitivity, specificity and diagnostic accuracy were considered for statistical analysis.

Results: Regenerative nodules usually show enhancement during the arterial phase without wash-out sign during portal-venous and delayed phase. Dysplastic nodules tend to do not show enhancement during the arterial phase and present wash-out on delayed phase. Well-differentiated HCCs very often show typical vascular pattern and low signal intensity during the hepatobiliary phase. According to the AASLD radiological diagnosis the mean sensitivity, specificity and diagnostic accuracy in the diagnosis of HCC were, respectively (76.4%, 80%, 0.84).

Conclusion: Gadoxetic acid MR imaging is a reliable tool in the characterization of well-differentiated HCC from dysplastic and regenerative nodules.

SS 15.04

Dynamic enhancement pattern of Gd-EOB-DTPA compared to gadobutrol in patients with HCC

S. Kinner, C. Kloeters, T. Lauenstein, M. Forsting; Essen/DE

Purpose: The liver-specific contrast agent Gd-EOB-DTPA comprises high r1 and r2 values and seems to be well suited for dynamic MR imaging in addition to liver specific characteristics. Aim of this study was to compare Gd-EOB-DTPA to the extracellular agent gadobutrol at dynamic abdominal MRI.

Material and Methods: Dynamic contrast-enhanced liver imaging was performed in 42 patients with HCC with a T1-weighed volume interpolated breath hold examination. Gd-EOB-DTPA (0.25 mmol/ml) and gadobutrol (1 mmol/ml) were injected body weight adapted using care bolus technique at 2 ml/s on two consecutive days. SNR values of abdominal vessels and CNR values of HCC lesions during arterial phase were evaluated. For statistical evaluation, a Wilcoxon-signed-rank-test was used.

Results: SNR (aorta) with gadobutrol amounted to 106±15, with Gd-EOB-DTPA to 77±14 (p=0.12). The portal vein (pv) and vena cava (vc) exhibited similar SNR values in portalvenous/venous contrast phase (SNR(pv) gadobutrol= 68±6, SNR(pv) Gd-EOB-DTPA= 63±3; p=0.6; SNR(vc) gadobutrol= 59±4, SNR(vc) Gd-EOB-DTPA= 52±3; p=0.64). CNR values of HCC lesions amounted to 27±4 for Gd-EOB-DTPA, whereas with gadobutrol CNR = 41±6 (p=0.14).

Conclusion: Despite the higher r1 value of Gd-EOB-DTPA, SNR and CNR values for gadobutrol were higher. This might be due to the higher gadolinium concentration. To achieve best image quality, the agent used in liver MR should be adapted to the clinical question: gadobutrol should be used for vascular analysis, whereas Gd-EOB-DTPA should be used for lesion characterization.

DOI: 10.1007/s13244-013-0254-8

SS 15.05

Accuracy of contrast-enhanced imaging in the pretransplantation staging of HCC

A. Pecchi, G. Besutti, M. De Santis, C. Del Giovane, S. Nosseir, G. Tarantino, F. Di Benedetto, P. Torricelli; Modena/IT

Purpose: To assess the accuracy of imaging in HCC pretransplantation staging, with pathologic evaluation of the explanted liver as reference standard.
Material and Methods: 165 patients who underwent liver transplantation (LT) for HCC between October 2004 and November 2011 and survived more than 2 months were included, 146 of them (88.5%) having undergone pretransplantation treatment. Imaging findings were retrospectively evaluated on pretransplantation contrast-enhanced MDCT (n=130) or MR (n=35) performed within 75 days before LT. Histopathological findings were obtained by a review of the pathologic reports. Association between pretransplantation imaging and explanted liver pathology were estimated by using X^2 test. Sensitivity, specificity and accuracy of imaging, MDCT and MR in the detection of viable tumor were calculated and compared with histopathology by using McNemar test.
Results: A significant association was found between imaging and pathology in the assessment of the presence of viable tumor ($p \leq 0.001$, also in patients who had undergone pretransplantation treatment), number of nodules ($p \leq 0.001$), diameter of the largest ($p \leq 0.001$), overall tumor size ($p \leq 0.001$) and lobar distribution ($p=0.034$). Sensitivity, specificity and accuracy of imaging in the detection of viable tumor were 81.4%, 59.6% and 75% (82.3%, 55.9% and 75.4% for MDCT; 77.3%, 69.2% and 74.3% for MR), without significant difference between imaging and histopathology.
Conclusion: Contrast-enhanced imaging can be considered accurate in HCC pretransplantation staging, with a sensitivity of 81.4% and a specificity of 59.6% in the detection of viable tumor.

SS 15.06

Y-90 microspheres radioembolization of unresectable HCC: is this safe in cases of portal vein thrombosis?

F. Somma, R. D'Angelo, L. Aloj, S. Limone, F. Fiore; Naples/IT

Purpose: Assessment of safety and effectiveness of trans-arterial radioembolization (TARE) using Y-90 microspheres in cases of unresectable HCC not responsive to other loco-regional treatments.
Material and Methods: Between November 2005 and January 2013, 74 TARE were performed in 68 patients with unresectable HCC and bilirubin values up to 2.5 mg/dl, 19 with portal vein thrombosis (PVT). Every patient was studied with multislice computed tomography (MSCT) scans and angiography while just some of them underwent the embolization of the gastro-duodenal artery. In these cases, a previous study was performed with the injection of TC-99MAA through a 3F microcatheter. Proton-pump inhibitors (PPI) were administered to prevent gastritis and ulcers.
Results: The average dose administered was 1.7 GBq. After-treatment fevers and abdominal pain were found in 25 and 19 patients, respectively. No other side effect was observed. RECIST criteria were used to evaluate the response: at least a partial response was found in 71% of patient three months after the procedure and in 91% at 9 months. The mean survival of patients with PVT was similar to those without thrombosis. Moreover, a regression of PVT was registered in more than 50% of patients.
Conclusion: Among the loco-regional treatments of HCC, TARE using Y-90 microspheres is a safe and effective technique, even in patients with PVT. Furthermore, TARE showed to be useful in case of relapse after trans-arterial embolization or chemoembolization, improving the survival of these patients.

SS 15.07

Limits of CT scan in the evaluation of sarcopenia in cirrhotic patients

M. Giusto, M. Di Martino, R. Di Miscio, V.C. Lombardo, B. Lattanzi, M. Merli, C. Catalano; Rome/IT

Purpose: To evaluate the relationship between CT, dual-energy X-ray absorptiometry (DEXA) and anthropometry to assess sarcopenia in cirrhotic patients.
Material and Methods: Adult patients eligible for elective LT for whom CT was available were considered. Skeletal muscle cross-sectional area was measured by CT and sarcopenia was defined using previously published gender-specific cutoffs. Mid-arm muscle circumference (MAMC,cm) was calculated according to standard methods. Fat-Free Mass Index (FFMI, kg/m^2) and Appendicular Skeletal Muscle Index (ASMI, kg/m^2) were calculated using DEXA. Agreement was assessed through Kendall's tau statistic. We used multi-state-models to model survival taking into account the possible intermediate transplant event.
Results: Fifty-nine patients (78% males, median age 59 years, 56% post-viral, 41% with HCC) were included. Median MELD was 16 in patients without HCC and 12 in patients with HCC. CT sarcopenia was diagnosed in 45 patients (76%) with similar prevalence in males and females. A reduction of FFMI and ASMI was observed in 42-52% of the patients while 52% showed a MAMC≤10thpercentile. A significant but slight correlation between FFMI, ASMI and CT was observed while MAMC significantly correlate with CT only in males. Eight patients died before LT and 7 within 12 months after LT. CT sarcopenia did not correlate with mortality, while MAMC and FFMI (only in males) were associated with higher mortality ($p \leq 0.005$).
Conclusion: CT and others techniques of muscle evaluation are not good predictive modalities in the evaluation of mortality post-OLT.

SS 15.09

Withdrawn by the authors

SS 15.10

Radiofrequency ablation of HCC: impact of size of the lesion, Child-Pugh score and technical parameters on outcome

P. Shriduth, S. Moorthy, P.V. Ramachandran, K.P. Sreekumar, R. Rajesh Kannan; Kochi/IN

Purpose: To correlate the pre-procedural tumor morphology (size of the lesion on contrast imaging), Child-Pugh score and technical parameters with the outcome of radiofrequency ablation (successful ablation or local tumor progression).
Material and Methods: This prospective study involved 40 HCC patients treated over a period from June 2010 to June 2012. We used Cool-tip radiofrequency ablation system (Covidien). The patients were then followed up by contrast imaging. The modified RECIST (mRECIST) assessment for HCC was applied to define the treatment response to RFA and tumor progression. The median follow- up period was 5 months.
Results: (1) Overall complete response (CR) was noted in 72.5% of cases. Less than 3 cm tumors showed CR of 88.5%. Even >3 cm tumors also showed CR of 42.9%. (2) Overall local tumour progression (LTP) was seen in 27.5% of lesions. More than 3 cm tumors showed LTP of 57.1%. (3) The median recurrence free survival was 6 months. (4) The 1-year survival rate of Child-Pugh A and B patients was 61 and 50%, respectively.
Conclusion: (1) Preprocedural tumor morphology showed statistically significant association with the outcome. Less than 3 cm lesions showed good response; larger lesions require multiple needle placements, longer procedure time and reablation. (2) Child-Pugh score and technical parameters did not show any statistically significant association with the outcome.

DOI: 10.1007/s13244-013-0254-8


European Society
ESGAR
Gastrointestinal and Abdominal Radiology

DOI: 10.1007/s13244-013-0254-8

DOI: 10.1007/s13244-013-0254-8

M

N

O

P

Q

R

DOI: 10.1007/s13244-013-0254-8

S

T

U

V

W

Y

Z

DOI: 10.1007/s13244-013-0254-8

European Society
ESGAR
Gastrointestinal and Abdominal Radiology

ESGAR 2014

JUNE 18 - 21

SALZBURG
AUSTRIA

European
Society
of Gastrointestinal
and Abdominal
Radiology

www.esgar.org